

Probing the structure of *Escherichia coli* catalase HPII

by

Prashen V G B K Chelikani

A thesis

submitted to Faculty of Graduate Studies

in partial fulfillment of the requirements for the degree of

Doctor of Philosophy

Department of Microbiology

University of Manitoba

Winnipeg, Manitoba

© January, 2004

THE UNIVERSITY OF MANITOBA
FACULTY OF GRADUATE STUDIES

COPYRIGHT PERMISSION

Probing the structure of *Escherichia coli* catalase HPII

BY

Prashen V G B K Chelikani

A Thesis/Practicum submitted to the Faculty of Graduate Studies of The University of

Manitoba in partial fulfillment of the requirement of the degree

Of

DOCTOR OF PHILOSOPHY

Prashen V G B K Chelikani © 2004

Permission has been granted to the Library of the University of Manitoba to lend or sell copies of this thesis/practicum, to the National Library of Canada to microfilm this thesis and to lend or sell copies of the film, and to University Microfilms Inc. to publish an abstract of this thesis/practicum.

This reproduction or copy of this thesis has been made available by authority of the copyright owner solely for the purpose of private study and research, and may only be reproduced and copied as permitted by copyright laws or with express written authorization from the copyright owner.

ABSTRACT

Substrate H_2O_2 must gain access to the deeply buried active site of catalases through channels of 30 to 50 Å in length. The most prominent or main channel approaches the active site perpendicular to the plane of the heme and contains a number of residues that are conserved in all catalases. Changes in Val169, 8 Å from the heme in catalase HP II from *Escherichia coli*, introducing smaller, larger or polar side chains reduces the catalase activity. Changes in Asp181, 12 Å from the heme, reduces activity by up to 90% if the negatively charged side chain is removed when Ala, Gln, Ser, Asn or Ile are the substituted residues. Only the Asp181Glu variant retains wild type activity. Determination of the crystal structures of the Glu181, Ala181, Ser181 and Gln181 variants of HP II reveals lower water occupancy in the main channel of the less active variants, particularly at the position forming the sixth ligand to the heme iron and in the hydrophobic, constricted region adjacent to Val169. It is proposed that an electrical potential difference exists between the negatively charged aspartate (or glutamate) side chain at position 181 and the positively charged heme iron 12 Å distant. The potential field acts upon the electrical dipoles of water generating a common orientation that favors hydrogen bond formation and promotes interaction with the heme iron. Substrate H_2O_2 would be affected similarly and enter the active site oriented optimally for interaction with active site residues. To date most structure-function studies of the main channel have targeted residues in the lower part of the channel in and around the active site. The second part of this study focused on, Ser234 and Glu530, situated 16 Å and 20 Å respectively, from active site heme in the main channel of HP II. These are

not conserved residues and are present only in large subunit enzymes. A number of HP11 variants were constructed and characterized at positions Ser234 and Glu530. The observed K_m (H_2O_2 at $V_{max}/2$) for the non-polar S234A and S234I variants are two to three fold higher than wild type showing that these variants have reduced affinity for the substrate, suggesting a need for hydrogen bonding at position 234. Similarly, the non-polar variants E530A and E530I were less active and exhibited three fold higher observed K_m . Consistent with their lower activity, the non-polar variants contained heme b and attempt to convert it "invitro" into heme d were unsuccessful, suggesting that Glu530 might be influential in selecting hydrophilic molecules (like H_2O and H_2O_2) early in the channel. To elucidate the direction of flow of substrate through the channels in catalase, cysteine mutagenesis of some key residues was initiated to study the effect of reactive sulfhydryls and their modification in the channels of HP11. Several lines of evidence indicate that the prosthetic group in one of these cysteine variants, I274C, is covalently attached to the protein. Another major focus of the work presented here, is to elucidate the role of the additional domains in large subunit catalases. HP11 is the largest catalase so far characterized, existing as a homotetramer of 84 kDa subunits. Each subunit has a core structure that closely resembles small subunit catalases, supplemented with an extended N-terminal sequence and compact flavodoxin like C-terminal domain. Treatment of HP11 with trypsin, chymotrypsin, or proteinase K, under conditions of limited digestion, resulted in cleavage of 72-74 residues from the N-terminus of each subunit that created a homotetramer of 76 kDa subunits with 80% of wild-type activity. Longer treatment with proteinase K removed the C-terminal domain, producing a transient 59-kDa subunit, which was subsequently cleaved into two fragments, 26 and 32

kDa. The tetrameric structure was retained despite this fragmentation, with four intermediates being observed between the 336 kDa native form and the 236 kDa fully truncated form corresponding to tetramers with a decreasing complement of C-termini (4, 3, 2, and 1). The truncated tetramers retained 80% of wild-type activity. The T_m for loss of activity during heating was decreased from 85 to 77 °C by removal of the N-terminal sequence and to 59 °C by removal of the C-terminal domain, revealing the importance of the C-terminal domain in enzyme stability. The sites of cleavage were determined by N- and C-terminal sequencing, and two were located on the surface of the tetramer with a third being exposed by removal of the C-terminal domain. The truncated variants were purified on Superose12 FPLC column in amounts sufficient for crystallization trials. As expected, biochemical studies showed that the active site appears to be more accessible in N- & C-trunc variant than N-trunc and wild type HPII.

ACKNOWLEDGEMENTS

At the outset, I wish to express my deep sense of gratitude to Dr Peter Loewen, my advisor, for his benign disposition and encouragement throughout the period of my study in Canada. His wise counsel and concrete suggestions during the course of my doctoral program were *invaluable*. The guidance and encouragement from my advisory committee members, Dr Pavel Dibrov, Dr Barbara Triggs-Raine and especially, Dr Richard Sparling were of immense value. I am also thankful to Mr. Jacek Switala for his assistance and cooperation. The insights and suggestions I received from Drs Ivan Oresnik and Isamu Suzuki are gratefully acknowledged. I would also like to thank Dr Lynda Donald, Dr Maureen Spearman, Dr Linda Cameroon and Ms. Sharon Berg for their assistance. Our collaborators in Spain deserve special recognition, Prof. Ignacio Fita and his lab members, especially Xavi for teaching me how to set up crystallization trails. I am also thankful to the Loewen lab members Sherif, Taweewat, Ben, Rahul and the numerous project and summer students. A special thanks to my fellow graduate students in Microbiology including Ayush for his humor, George for the canoe trips, Patrick, Andrew, Reuben, Matt, Chris, Julius, Yong Quiang and all the others. The postgraduate Fellowship funding from Manitoba Health Research Council (MHRC) is also acknowledged. Without the loving support of my parents, brother, and my wife Renu, I could not have been what I am today.

TABLE OF CONTENTS

	Page
ABSTRACT	ii
ACKNOWLEDGEMENTS	v
TABLE OF CONTENTS	vi
LIST OF FIGURES	ix
LIST OF TABLES	xi
LIST OF ABBREVIATIONS	xii
1. GENERAL INTRODUCTION	
1.1. Oxygen: a boon and bane.....	1
1.1.1 Oxygen as stressor.....	1
1.1.2. Biology of reactive oxygen species.....	2
1.2. Antioxidant defense systems	6
1.2.1 Non-Enzymatic defenses	7
1.2.1.1 Hydrophilic scavengers	7
1.2.1.2 Hydrophobic scavengers	8
1.2.2. Enzymatic defenses	9
1.2.3. Antioxidant defenses in <i>E.coli</i>	11
1.3. Hydroperoxidases or catalases	12
1.4. Regulation of catalase gene expression	13
1.5. Heme catalases	20
1.5.1. Reaction mechanism	20
1.5.2. Phylogeny	20
1.5.3. Kinetic properties	21
1.5.4. Structural diversity among heme-catalases	22
1.5.4.1 Heme orientation	25
1.5.4.2 NADPH binding	26
1.6. Non-heme or Mn-containing catalases	27
1.6.1. Reaction mechanism	28
1.6.2. Structure of Mn catalases	29
1.7. Catalase-peroxidases	29
1.7.1. Reaction mechanism	29
1.7.2. Phylogeny	30
1.7.3. Structures of catalase-peroxidase	30
1.7.3.1 Covalent linkage joining Trp-Tyr-Met	32

1.8.	Channels in catalases	33
1.8.1.	Channel architecture in heme catalases	33
1.8.2.	Channel architecture in Mn catalases	37
1.8.3.	Channel architecture in catalase-peroxidases	37
1.9.	Object of the thesis	38
2.	MATERIALS AND METHODS	
2.1.	<i>Escherichia coli</i> strains, plasmids and bacteriophage	39
2.2.	Chemical and biochemical reagents	39
2.3.	Media, growth conditions and storage of cultures	41
2.4.	DNA manipulation	41
2.4.1.	Preparation of synthetic oligonucleotides	41
2.4.2.	DNA isolation and purification	42
2.4.3.	Restriction nuclease digestion	43
2.4.4.	Agarose gel electrophoresis	43
2.4.5.	Ligation	44
2.4.6.	Transformation.....	44
2.4.7.	DNA sequencing.....	45
2.4.8.	In vitro mutagenesis strategy.....	46
2.5.	Purification of HPII catalase.....	55
2.6.	Polyacrylamide gel electrophoresis.....	57
2.7.	Catalase assay and protein quantitation.....	58
2.8.	Absorption spectrophotometry.....	59
2.9.	Hemochromogen characterization.....	59
2.10.	Effect of inhibitors.....	60
2.11.	Determination of sulfhydryl groups.....	60
2.12.	Conditions of proteolysis.....	61
2.13.	ESI TOF mass spectrometry.....	61
2.14.	Conditions for crystal growth	62
3.	RESULTS	
3.1.	Construction and characterization of the main channel variants between 8Å and 12Å.....	63
3.1.1.	Introduction.....	63
3.1.2.	Effects of changes to Val169 situated 8Å from heme.....	65
3.1.3.	Effects of changes to Asp181 situated 12Å from heme.....	78
3.1.3.1.	Crystal structure of D181 variants.....	78
3.1.4.	Effect of changes to Arg180.....	79
3.2.	Construction and characterization of the main channel variants between 12 Å and 20 Å.....	90
3.2.1.	Introduction.....	90
3.2.2.	Effects of changes to Ser234 situated 16Å from heme.....	91
3.2.3.	Effect of changes to Glu530 situated 20Å from heme.....	91
3.3.	Construction and characterization of the cysteine variants in the channels of HPII.....	107
3.3.1.	Introduction.....	107

3.3.2.	Characterization of the cysteine variants.....	110
3.3.3.	Effect of 2-mercaptoethanol on cysteine variants.....	120
3.3.4.	Quantification of free sulfhydryl groups.....	120
3.4.	HPII exhibits enhanced resistance to proteolysis cleavage compared to other catalases	124
3.4.1.	Introduction.....	124
3.4.2.	Sensitivity of catalases to proteinase K, trypsin and chymotrypsin.....	125
3.4.3.	Time course of digestion of HPII.....	125
3.4.4.	N-and C-terminal sequence analysis of protease fragments.....	131
3.4.5.	Thermal stability of the truncated HPII variants.....	136
3.5.	Purification and characterization of truncated variants of HPII.....	141
3.5.1.	Introduction.....	141
3.5.2.	Purification of the truncated variants.....	141
3.5.3.	Catalatic and peroxidatic activities of the truncated variants.....	148
3.5.4.	Effect of inhibitors on the truncated variants of HPII.....	148
4.	DISCUSSION	
4.1.	Asp181 of HPII is important for catalysis.....	154
4.2.	An electrical potential in the access channel of catalases enhances catalysis.....	157
4.3.	Importance of hydrophilicity in the upper part of the access channel.....	160
4.4.	I274C: Covalently linked heme prosthetic group in catalases.....	161
4.4.1.	Cysteine mutagenesis of channel residues.....	162
4.5.	HPII exhibits enhanced resistance to proteolysis than other catalases.....	162
4.6.	Resistance of HPII to proteolytic cleavage provides insights into the enzymes thermal stability.....	164
4.7.	Truncated variants of HPII.....	166
4.8.	Future studies.....	167
5.	References	168

LIST OF FIGURES

1.1.	Dioxygen; a boon & bane.....	5
1.2.	Ribbon diagram for the comparison of the overall structures and sizes of heme-containing small and large subunit catalase, a catalase peroxidase and dimanganese catalase.....	24
1.3.	Structure of the channels providing access to the active sites in one subunit each of Cat F (A), HP11 (B), Bpkat G(C) and LTC (D).....	36
2.1.	Simplified restriction map of the cloned 3466bP chromosomal insert in PAML at E72.....	47
3.1.1.	Absorption spectra of wild type HP11 and various variants.....	69
3.1.2.	Elution profiles of heme extracted from HP11 (wild type), various variants bovine liver catalase (BLC) by C18 reverse phase HPLC chromatography.....	72
3.1.3.	Effect of H ₂ O ₂ concentration on enzyme velocity and HP11 and its variants.....	75
3.1.4.	SDS-polyacrylamide analysis of purified HP11 and variant catalase.....	77
3.1.5.	Stereo diagrams of the water distribution in the main channel of native HP11 (a), and D181A variant (b), the D181E variant (c), the D181Q variant (d), and the D181S variant (e).....	81
3.2.1.	SDS-polyacrylamide analysis of purified HP11 and variant catalase.....	94
3.2.2.	Absorption spectra of wild type HP11 and various variants.....	96
3.2.3.	Elution profiles of heme extracted from HP11 (wild type) and variants analyzed on C18 reverse phase HPLC chromatography.....	100
3.2.4.	Effect of H ₂ O ₂ concentration on enzyme velocity of HP11 and its variants..	103
3.2.5.	Crystals of S234I, E530A and E530D variants of HP11.....	106
3.3.1.	HP11 subunit showing the various cysteine(s).....	109
3.3.2.	SDS-polyacrylamide analysis of purified HP11 and variant catalases.....	112
3.3.3.	Absorption spectra of wild type HP11 and various variants.....	115
3.3.4.	Elution profiles of heme extracted from HP11 (wild type) and variants by C18 reverse phase HPLC chromatography.....	117
3.3.5.	Effect of H ₂ O ₂ concentration on enzyme velocity of HP11 and its variants..	119
3.3.6.	Comparison of the effects of 2-mercaptoethanol on HP11 and its cysteine containing variants.....	122
3.4.1.	Effect of treatment with proteinase K, trypsin and chymotrypsin on the activity of HP11 (A), BLC (B), and HPI (C).....	127
3.4.2.	Products of proteolytic cleavage of HP11 trypsin (A), chymotrypsin (B) and proteinase K (C).....	128
3.4.3.	Correlation of product size and activity during proteolytic cleavage of HP11 by proteinase K.....	130
3.4.4.	Non-denatured molecular weights of N-trunc and N-&C-trunc.....	133
3.4.5.	Mass analysis by nanospray ionization of HP11 protein before (A) and after (B) treatment with proteinase K	135
3.4.6.	Thermal stability of the truncated HP11 variants.....	137

3.4.7.	Conversion of HPII dimers to monomers.....	138
3.4.8.	Location of the three main locations on the HPII tetramer that are sensitive to proteolytic cleavage.....	140
3.5.1.	Elution profiles of truncated variants and wild type HPII purified by size exclusion chromatography on a Superose-12 FPLC column.....	143
3.5.2.	Effect of H ₂ O ₂ concentration on enzyme velocity of HPII and its truncated variants.....	147
3.5.3.	Comparison of the effects of sodium cyanide (NaCN) on wild type HPII N-trunc and N-&C-trunc variants	149
3.5.4.	Comparison of the effects of sodium azide (NaN ₃) on wild type HPII N-trunc and N-&C-trunc variants.....	150
3.5.5.	Comparison of the effects of Hydroxylamine [NH ₂ OH] (A) and <i>O</i> -Methyl hydroxylamine [O-Methyl HA] (B) on wild type HPII, N-trunc and N-&C- trunc variants.....	151
4.1.1	Schematic showing the distances among waters in the main channel of the D181E variant.....	156
4.2.1.	Schematic of the main channel illustrating the presence of a negative charge (in green) on the side chain of E181 and a positive charge (in green) on the heme iron	158
4.4.1	A proposed mechanism to explain the formation of Cys-heme covalent bond in HPII of <i>E. coli</i>	163

LIST OF TABLES

1.1.	Regulatory responses of catalases and catalase-peroxidases in bacteria and fungi.....	15
2.1.	Genotypes and sources of <i>Escherichia coli</i> strains, plasmids and bacteriophage used in this study.....	40
2.2.	Oligonucleotides and <i>katE</i> restriction fragments used in oligonucleotide-directed mutagenesis of <i>katE</i>	48
3.1.1.	Catalase activity in the crude extracts of cultures of <i>E. coli</i> UM255 producing variants of HP11, and specific activity of purified catalase protein	66
3.1.2.	Comparison of the calculated and observed kinetic parameters of Wild type and HP11 variant protein.....	67
3.1.3.	Water occupancy in the main or perpendicular channel of catalase HP11 subunits listed as B-factor (\AA^2).....	83
3.1.4.	Data collection and structural refinement statistics for Asp181 variants of HP11.....	86
3.2.1.	Catalase activity in crude extracts of cultures of <i>E. coli</i> UM255 producing variants of HP11, and specific activity of purified catalase protein.....	92
3.2.2.	Comparison of the calculated and observed kinetic parameters of wild type and HP11 variant proteins.....	93
3.3.1.	Catalase activity in crude extracts of cultures of <i>E. coli</i> UM255 producing variants of HP11, and specific activity of purified catalase protein.....	111
3.3.2.	Comparison of the calculated and observed kinetic parameters of wild type and HP11 variant proteins.....	113
3.3.2.	Quantitation of the free sulfhydryl groups of the cysteines variants with Ellmans reagent [5,5'-dithiobis-(2-nitrobenzoic acid)].....	121
3.4.1.	Sequences at protease cleavage sites in HP11.....	132
3.5.1.	Comparison of the specific activities of wild type HP11 and its purified truncated variant.....	144
3.5.2.	Comparison of the calculated and observed kinetic parameters of wild type and truncated HP11 variant proteins.....	145
3.5.3.	Sensitivity of wild type HP11 and truncated variants to various inhibitors...	152

LIST OF ABBREVIATIONS

A	Absorbance
ABTS	2,2, -azinobis (3-ethylbenzothiazolinesulfonic acid)
Amp ^r	Ampicillin resistant
ATP	Adenosine triphosphate
Bp	Base pair(s)
BSA	Bovine serum albumin
BLC	Bovine liver catalase
Ci	Curie
Da	Dalton
DAB	3,3'-diaminobenzidine
DEAE	Diethylaminoethyl
DMSO	Dimethylsulfoxide
DNA	Deoxyribonucleic acid
DTNB	5,5'-dithiobis- (2-nitrobenzoic acid)
EDTA	Ethylenediaminetetraacetic acid
ESI-TOF	Electrospray ionization time-of-flight
FPLC	Fast protein liquid chromatography
Fw _{mh}	Full width half maximum
HPI	<i>Escherichia coli</i> Hydroperoxidase I
HPII	<i>Escherichia coli</i> Hydroperoxidase II
HPLC	High performance liquid chromatography
HRP	Horseradish peroxidase
INH	Isonicotinic acid hydrazide (isoniazid)
k _{cat}	Turnover number
kDa	kiloDalton
K _m	Michaelis-Menten constant
NADH	Nicotinamide adenine dinucleotide (reduced)
NADP ⁺	Nicotinamide adenine dinucleotide phosphate (oxidized)
NADPH	Nicotinamide adenine dinucleotide phosphate (reduced)
OD	Optical density
PAGE	Polyacrylamide gel electrophoresis
PEG	Polyethylene glycol
PMSF	Phenylmethylsulfonyl fluoride
RNase	Ribonuclease
ROS	Reactive oxygen species
SDS	Sodium dodecyl sulfate
Tris	Tris (hydroxymethyl) aminomethane
V	Volts
V _{max}	Maximum velocity
w/v	Weight per unit volume
w/w	Weight per weight

1. General Introduction

1.1. Oxygen: a boon and bane

The history of life on earth may be presented as having gone through two eras: the first extending from the origins until oxygen (O_2) levels in the atmosphere reached 21% and the second era beginning then and extending until today with the same level of O_2 . If life originated 3.5 to 3.8 billion years ago, it evolved without O_2 . It is likely that O_2 began to appear at a later period and its levels began to increase until they reached the current level of 21%, approximately 780 million years ago. The transition from a completely anaerobic to an O_2 tolerant world must have been a gradual and slow process, during which all living forms used to anaerobiosis, began to confront O_2 . Several evolutionary events must have occurred. Those living forms endowed with a mechanism to use O_2 , or at least to defend themselves against the toxic effects caused by it or its derivatives, survived. They became oxygen-respirers (aerobes) or at least aerotolerant. Aerobic organisms have a more efficient metabolism as compared to that of most anaerobes; this advantage comes with a price, because both the chemical and metabolic reduction of O_2 result in the production of highly toxic and reactive oxygen species. Mechanisms had to evolve to cope with what today are known as toxic forms of oxygen, the reactive oxygen species (ROS).

1.1.1. Oxygen as stressor

A functional definition of stress is a situation caused by stressors. Stressors are agents of physical, chemical or biological nature, which represent a change in the environmental (intra or extra cellular) conditions for any life form. Excess of oxygen in a

cell might lead to a condition termed as oxidative stress (Farr and Kogoma, 1991). In a normal aerobic cell, accumulation of toxic O_2 species does not occur because there are mechanisms for their elimination. However, an imbalance of ROS production and elimination may happen, leading to ROS accumulation, which can cause oxidative stress, with ensuing damage to nucleic acids, lipids and proteins. Oxidative stress is in fact one of the leading mechanisms of aging and cell death (Horsburgh *et al.*, 2002; Sohal *et al.*, 2002).

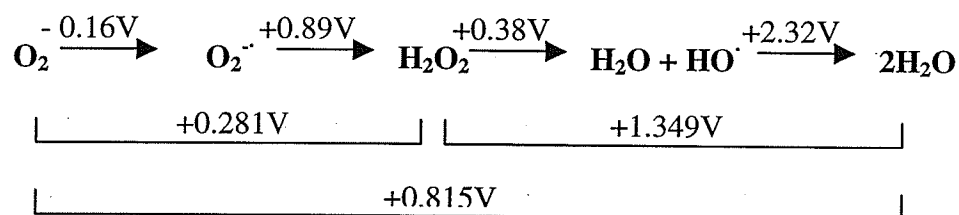
1.1.2. Biology of reactive oxygen species

Molecular oxygen or more appropriately dioxygen is an unusual chemical. Its thermodynamic potential as an oxidant (+ 0.85 Volts, O_2/H_2O redox couple) is remarkable (Woods, 1988). Aerotolerant organisms must have capitalized rapidly on the availability of such a useful oxidant as a thermodynamic sink, but the use of dioxygen in aerobic respiration is not without its difficulties. Saraste and Castresana suggested that dioxygen reducing centers evolved from nitric oxide-reactive sites (Saraste and Castresana, 1994). The molecular-orbital arrangement of electrons in dioxygen ensures that its potential can only be realized through transition-metal catalysts.

Dioxygen is a triplet species, with two spin-aligned, unpaired electrons. Consequently, potential electron donors that are singlet species (i.e., which have their electron spin paired) cannot form productive orbital overlaps with the half-filled orbitals of oxygen and therefore cannot concertedly transfer two electrons to it (Naqui and Chance, 1986). This kinetic inertness of dioxygen prevents the spontaneous combustion of biological molecules in aerobic environments. It was generally assumed that, dioxygen

being a small, uncharged molecule, could readily traverse biological membranes, and that no significant concentration gradient existed across respiring bacterial membranes (Unden *et al.*, 1995). On the contrary, recent work suggests that a metabolic advantage arises from expression of microbial globins (Khosla and Bailey, 1989; Tsai *et al.*, 1996), which may act, as in higher organisms (Wittenberg and Wittenberg, 1990) to facilitate transport or storage of dioxygen for aerobic respiration (Fig 1.1.).

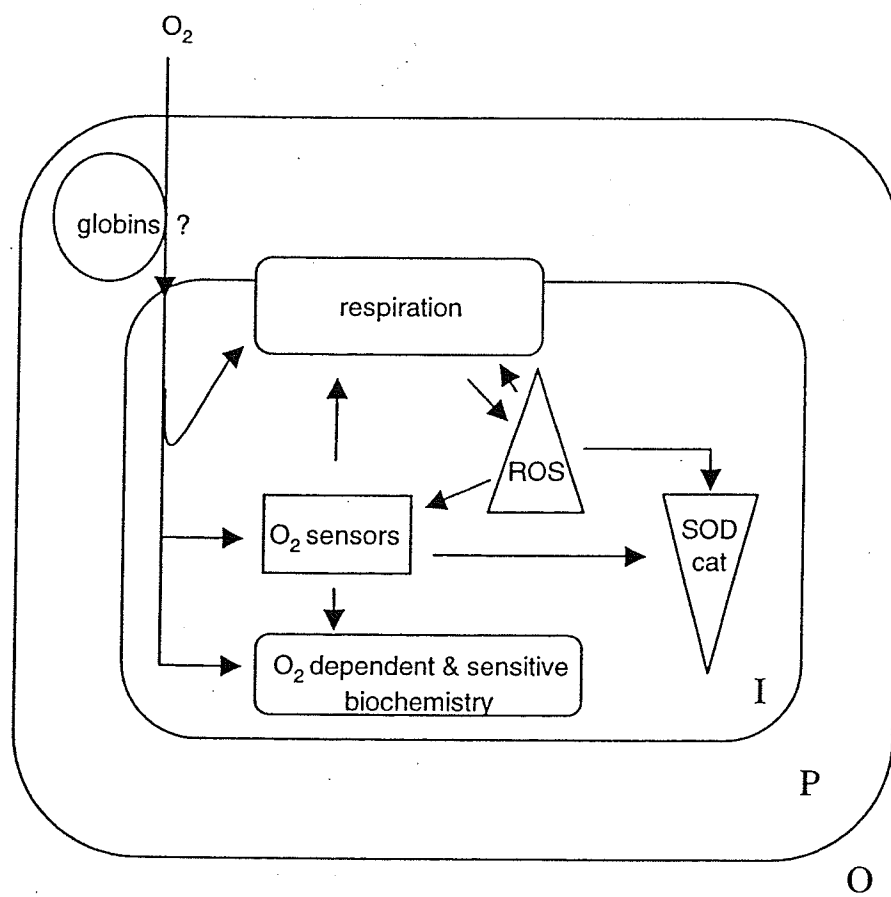
Only the four-electron reduction of dioxygen to water is 'safe', because intermediate reduction products are reactive toxic. The schematic below shows the potential diagram for the reduction of O_2 at pH 7 and the possible reactive intermediates.



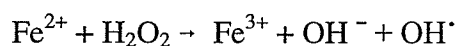
(Woods, 1988)

However, triplet species are not forbidden from participating in univalent electron- transfer reactions. The reduction of dioxygen to superoxide radical anion ($O_2^{\cdot-}$) has a lower redox potential than for H_2O_2 formation (Woods, 1987). However, only a single electron needs to be transferred. For this reason, $O_2^{\cdot-}$ formation is a characteristic of autoxidation. The autoxidation of hydroquinones, catecholamines (Misra and Fridovich, 1972), leukoflavins (Ballou *et al.*, 1969), thiols (Fridovich, 1978) and reduced ferredoxins (Misra and Fridovich, 1971) have all been shown to generate $O_2^{\cdot-}$. By contrast $O_2^{\cdot-}$ production by neutrophils is a deliberate act of biological warfare (Rossi, 1986), since the radical is used to attack engulfed bacteria.

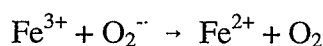
Figure 1.1. Dioxygen; a boon & bane. Dioxygen readily permeates from the outside (O) to the cell interior (I) through the outer and cytoplasmic bacterial membranes, and the intervening periplasm (P), although globins have been suggested to facilitate the process. Dioxygen is reduced primarily to water in respiration, but is also required for dioxygen dependent biochemistry such as oxygenase function. The respiratory chain is a source of ROS. Dioxygen is sensed by several global regulators (like Fnr), which control different cellular cascades including the antioxidant enzymes SOD, catalases.



The reduction of dioxygen to H₂O₂ is less energetically favorable than the complete reduction to water, but requires only two electrons in place of four. For this reason H₂O₂ is the product of O₂ reduction by many oxidases. In 1894, Fenton described the strong oxidizing properties of a mixture of H₂O₂ and Fe²⁺. The active species was shown by Haber & Weiss to be OH[·], formed by one electron transfer from Fe²⁺ (Haber and Weiss, 1934).



At pH 7, many iron complexes have a redox potential near 0 V (e.g. EDTA, +0.114; protoporphyrin-IX, -0.12 V) (Clark, 1960) making electron transfer to H₂O₂ a thermodynamically favorable reaction (Woods, 1988). In addition, the traces of unprotected iron (Fe³⁺) present in many biological systems can be sufficient, provided there is a means of regenerating the ferrous state (Cohen, 1985). This can be accomplished by one electron reduction of Fe³⁺ by O₂^{·-} (McCorel and Day, 1978).



1.2. Antioxidant defense systems

Biological antioxidants are natural molecules, which can prevent the uncontrolled formation of free radicals and activated oxygen species or inhibit their reactions with biological structures. The destruction of ROS and most free radicals relies on the oxidation of indigenous antioxidant molecules. Therefore redox recycling of such molecules increases their biological efficacy by decreasing the need for *de novo* synthesis or that of large uptakes of these antioxidant molecules (Chaudiere and Ferrari-iliou, 1999).

1.2.1. Non-Enzymatic defenses

Low molecular weight antioxidant molecules form the first line of defense in both prokaryotes and eukaryotes. Various small molecules frequently referred to as “antioxidant scavengers” act to neutralize free radicals (Halliwell *et al.*, 1999; Gilbert and Calton, 1999). Antioxidant scavengers are either physical quenchers of excited species such as singlet oxygen or chemical traps of oxidizing free radicals (Chaudiere and Ferrari-iliou, 1999). However from a biological point of view, it may be misleading to assume that superoxide ($O_2^{\cdot -}$), hydroxyl radical (OH^{\cdot}) and alkoxy (RO^{\cdot}) radicals are efficiently trapped by endogenous antioxidant scavengers. For example, the biological degradation of $O_2^{\cdot -}$, which is under exclusive control of superoxide dismutase (SOD) in most cells is not very efficient. It is dealt with in detail in a subsequent section (1.2.2). Non-enzymatic scavengers can be further categorized as either hydrophilic or hydrophobic scavengers.

1.2.1.1. Hydrophilic Scavengers

Hydrophilic scavengers are found in cytosolic, mitochondrial and nuclear aqueous compartments. Among these, ascorbate and glutathione (GSH) are the most important free radical scavengers. Their intracellular concentrations are typically between 1 and 10mM, much higher than other nucleophilic and reducing biomolecules (Bendich *et al.*, 1996; Gerard-Monnier and Chaudiere, 1996). GSH is a major low molecular weight thiol and is ubiquitous in nature. Free radical scavenging properties of GSH are due to its sulfhydryl group and because the pK_a (GSH/GS $^-$) of the thiol is ~ 9.2 (Jung *et al.*, 1972;

Huckerby *et al.*, 1985), only 1.2% of glutathione is in the thiolate form at pH 7.3 (Chaudiere and Ferrari-Iliou, 1999). The mercaptan acts as a scavenger of radicals such as OH \cdot , and also as an H atom donor. GSH in eucaryotic cells is a cofactor for the H₂O₂ destroying enzyme GSH peroxidase and it also supports the glutaredoxin pathway, which helps maintain proteins thiols in the cell (Grant, 2001; Carmel-Harel and Storz, 2000). More recently, ergothioneine a natural betaine is also shown to have antioxidant properties (Hartman, 1990; Akanmu *et al.*, 1991). Only fungi and mycobacteria synthesize ergothioneine. The ergothioneine content of mammalian cells is exclusively from vegetables in the food chain. Intracellular concentrations of ergothioneine are typically in the range of 0.1 to 1mM (Aruoma and Halliwell, 1987). Ergothioneine acts as a physical quencher of singlet oxygen (Rougee *et al.*, 1988), and scavenges hydroxyl radicals at very high rates (Asmus *et al.*, 1996).

1.2.1.2. Hydrophobic Scavengers

Hydrophobic scavengers are mostly found in the membranes and lipoproteins where they block the formation of hydroperoxides from singlet O₂ or prevent lipid peroxidation by destroying peroxy radicals (ROO \cdot) (Halliwell and Chirico, 1993). They include vitamin E (α -tocopherol), carotenoids and ubiquinol. α -tocopherol is the most efficient scavenger of peroxy radicals in phospholipid bilayers. It scavenges lipid peroxy radicals (LOO \cdot) through hydrogen atom transfer (Burton and Ingold, 1981). The role of ubiquinol as a membrane antioxidant *in vivo* is doubtful (Beyer, 1990). However it does act as a powerful antioxidant in *in vitro* models of lipoprotein oxidation (Kagan *et al.*, 1994; Tsuchiya *et al.*, 1994). The other common antioxidant scavengers embedded in

cell membranes are the carotenoids. These are unsaturated hydrocarbons which bear 10-12 conjugated double bonds (Krinsky, 1981). Carotenoid hydrocarbons, such as β -carotene and lycopene, are located within the hydrophobic membrane core where, like the more polar oxycarotenoids or xanthophyls, they occupy a membrane spanning orientation (Britton, 1995). Carotenoids act as physical quenchers of singlet oxygen (Sundquist *et al.*, 1994). *In vitro*, carotenoids also behave as scavengers of oxidizing free radicals and this may account for some of their antioxidant properties (Palozza and Krinsky, 1992; Rice-Evans *et al.*, 1997).

1.2.2. Enzymatic defenses

The advantage of using specific antioxidant enzymes is that the steady – state concentrations of peroxide or superoxide can be adapted to cellular requirements. Several of these enzymes can be induced, activated or inhibited. The induction of some key proteins in response to oxidative stress has been known for some time. For example, SOD activity increases in *E. coli* grown in high levels of oxygen or exposed to redox-cycling agents (Fridovich, 1995). These agents also induce glucose-6-phosphate dehydrogenase to replenish NADPH used up in the antioxidant reactions (eg. by GSH reductase) (Kao and Hassan, 1985). Exposure to H_2O_2 induces catalase activity in many organisms and increases GSH reductase levels in *E. coli* and *S. typhimurium* (Christman *et al.*, 1985). Enzymatic degradation of superoxide is catalyzed by SOD, while that of hydroperoxides is ensured by catalase, glutathione peroxidase (GPx) or ascorbate peroxidases. SOD and catalase are dismutases and therefore they do not consume cofactors and as such, the primary reactions catalyzed by these enzymes are not associated with any energetic cost.

Conversely, GPx and ascorbate peroxidases are reductases whose reducing coenzymes are regenerated by NADPH equivalent produced in metabolic pathways.

GPxs are absent in *E. coli*, but in animal cells, GPxs are selenoenzymes, which catalyze the reduction of hydroperoxides at the expense of GSH (Flohe *et al.*, 1989; Ursini *et al.*, 1995). The GPx active site contains selenium in the form of a selenocysteine residue (Flohe *et al.*, 1973; Stadtman, 1991). Selenium incorporation is found to be a cotranslational process and GPxs do not exist in the form of apoenzymes (Stadtman, 1991; Lee *et al.*, 1996). To date selenium dependent glutathione peroxidases have not been found in plant cells, where H₂O₂ is degraded by ascorbate peroxidases (Bunkelmann and Trelease, 1996; Smirnov, 1996). A similar activity has also been reported in insects (Mathews *et al.*, 1997).

SOD catalyzes the one-electron dismutation of superoxide into hydrogen peroxide and O₂ (Mc Cord and Fridovich, 1969; Steinman, 1982). Almost all aerobic organisms have at least one form of SOD or a small molecule equivalent (Fridovich *et al.*, 1995). On the contrary, with few exceptions (Seibert *et al.*, 1994) SOD and catalase genes are not generally present in anaerobes, as illustrated by their absence from most of the complete genome sequences now available for the anaerobic organisms (Bult *et al.*, 1996; Klenk *et al.*, 1997; Kawarabayasi *et al.*, 1998; Nelson *et al.*, 1999).

Very recently, the hyperthermophilic anaerobic *Pyrococcus furiosus* was shown to possess superoxide reductase (SOR) (Jenny *et al.*, 1999). Unlike SOD, SOR uses electrons from reduced NADP, by way of rubredoxin and an oxidoreductase to reduce O₂⁻ to H₂O₂ without the production of oxygen. *E. coli* has three isozymes of SOD, encoded by the *sodA*, *sodB*, and *sodC* genes (Imlay and Imlay, 1996). The products of

SodA and SodB are cytoplasmic, whereas SodC is periplasmic. The three SOD's of *E. coli* differ in the metals at their active sites: the SodA protein contains manganese; SodB contains iron; and SodC contains copper and zinc. *S. typhimurium* contains a second copper-zinc SOD in the periplasm, which is hypothesized to be important for virulence (Fang *et al.*, 1999).

1.2.3. Antioxidant defenses in *E. coli*

Yonei *et al.*, were the first to define the specific mechanism of protection exhibited by the enteric organism *E. coli* in terms of, predamage and postdamage systems (Yonei *et al.*, 1987). The postdamage system consists of DNA repair enzymes (Hagansee and Moses, 1989; Ahern, 1993). Some of the components of the enzymatic and non-enzymatic defenses described in the previous section (1.2), make up the predamage system of the organism that includes the thiol based antioxidant defenses. In *E. coli* the principal thiol present in the cytoplasm is glutathione (GSH) (Meister, 1988). GSH is capable of reducing the cellular components by itself or through the glutaredoxin (Grx) system (Prinz *et al.*, 1997). In order to maintain a pool of reduced GSH, *E. coli* has the enzyme glutathione reductase (Storz and Tartaglia, 1992). However, the organism lacks glutathione transferase and peroxidase two key enzymes involved in thiol based oxygen detoxification system (Lau *et al.*, 1980). Recently polyamines, the ubiquitous polycationic compounds, are implicated in protecting *E. coli* from toxic effects of O_2 , $O_2^{\cdot -}$ and H_2O_2 (Chattopadhyay *et al.*, 2003). Thiol independent enzymatic systems include SOD's and catalases or hydroperoxidases the latter dealt in the succeeding section (1.3).

1.3. Hydroperoxidases or catalases

Catalases or, more correctly, hydroperoxidases have been studied for more than a century, with the first report and naming of the enzyme appearing in 1901 (Loew, 1901). The originally described catalases are homotetramers, with each subunit containing a noncovalently bound heme prosthetic group characterized as protoferriheme (protoporphrin IX) (Baudhin and Deduve, 1973; Stern, 1936) in the high spin Fe (III) state (Maeda *et al.*, 1973). Subsequently other proteins exhibiting catalase reactivities were discovered. The overall reaction catalyzed by catalases is the degradation of two molecules of hydrogen peroxide to water and oxygen (reaction 1).



This deceptively simple overall reaction generally is broken down into two stages, but what is involved in each of the stages depends on the type of catalase. The mechanism relevant to a particular catalase will be addressed in the appropriate sections.

Three classes of proteins, unrelated on the basis of sequence and structure, exhibit significant catalase activity. The class that is most widespread in nature and which has been most extensively characterized is composed of monofunctional, heme-containing enzymes, subdivided based on having large (>75 kDa) or small (<60 kDa) subunits. Phylogenetic analyses have demonstrated the existence of two distinct clades or subgroupings of small subunit enzymes and one clade of large subunit enzymes among the mono-functional catalases [Von Ossowski *et al.*, 1994]. The second, less widespread, class is composed of bifunctional, heme-containing, catalase-peroxidases that are closely related by sequence and structure to plant peroxidases. The third class includes the non-heme catalases. There is also a diverse group of proteins, all heme-containing, such as

chloroperoxidase, plant peroxidases and myoglobin exhibit a very low level of catalase activity, attributable to the presence of heme which alone exhibits catalytic activity [Nicholls *et al.*, 2001].

1.4. Regulation of catalase gene expression

Cells usually modulate their stress response systems through regulatory proteins that sense the stressor or a messenger of the stressor and cause appropriate changes in transcription and occasionally, translation or proteolysis. However, bacterial gene function is regulated mainly at the transcriptional level. Cells have evolved transcriptional modulators that sense oxidative stress and respond by activating regulons. The earliest studies of catalase gene regulation were carried out in *E. coli* and these have been extensively reviewed (Loewen, 1997). OxyR is an H₂O₂ sensing transcriptional regulator controlling more than 36 genes in response to H₂O₂ in *E. coli*. HPI of *E. coli* is one of the genes activated by OxyR in log phase cultures (Christman *et al.*, 1989). As cells enter stationary phase a 10 to 20-fold increase in HPII levels are seen (Loewen *et al.*, 1985), this is the result of increasing levels of RpoS, a general stress response regulator. Recently, polyamines, including putrescine, spermidine and spermine were shown to protect *E. coli* cells from the toxic effect of oxygen (Chattopadhyay *et al.*, 2003), by up regulating both the OxyR and RpoS regulons in *E. coli* (Tkachenko *et al.*, 2001; Jung and Kim, 2003), but the mechanism remains unclear. The commonality of a reactive oxygen sensor and growth phase or σ -transcription factor control mechanism in catalase gene expression is illustrated in Table 1.1. Although in general there is no

consistency in the type of catalase, the type of regulator, or the sigma factor, the generality of the two control mechanisms is clear.

In *E. coli*, σ^S or KatF encoded by *rpoS* controls the expression of more than 50 genes as cells transition from exponential to stationary phase (Loewen *et al.*, 1998; Hengge-Aronis, 2002). The mechanism affecting the synthesis and accumulation of σ^S itself is controlled at the levels of transcription, translation, holoenzyme formation and proteolysis. Regulation by proteolysis is particularly important in stationary phase or non-growing cells. Proteolysis might be the only way to significantly reduce the level of proteins in non-growing cells because of the lack of dilution of components, as by cell division. Intracellular levels of σ^S are controlled by various cellular factors, which include the protease ClpXP, recognition factor RssB (Zhou *et al.*, 2001). Very recently, high levels of DNA supercoiling have been found to inhibit transcription by $E\sigma^S$ (Bordes *et al.*, 2003). Recently proteolysis is shown to be the single major factor controlling σ^S levels in stationary phase (Becker *et al.*, 1999).

OxyR is a redox-sensitive protein of the LysR family of DNA binding transcriptional modulators (Christman *et al.*, 1989). Physiological studies in aerobically growing *E. coli* indicated that the OxyR regulon is activated by as little as 100 nM intracellular H_2O_2 and growth is inhibited when internal levels reach 2 μM (Gonzalez-Flecha and Demple, 1997). As H_2O_2 decomposition is faster than diffusion across the cytoplasmic membrane, the addition of 10 μM external H_2O_2 is needed to achieve growth inhibiting levels inside the cell (Costa Seaver and Imlay, 2001).

Table 1.1. Regulatory responses of catalases and catalase-peroxidases in bacteria and fungi.

Organism	Catalase	Type ^a	Regulator	Additional response	Reference
<i>Agrobacterium tumefaciens</i>	KatA	CPx	OxyR		(Nakjarung <i>et al.</i> , 2003)
<i>Emericella nidulans</i>	CatA	3		Post-transcriptional control	(Navarro & Aguirre, 1998)
<i>Emericella nidulans</i>	CatB	2		Developmental, H ₂ O ₂	(Kawasaki <i>et al.</i> , 1997)
<i>Emericellas nidulans</i>	CatC	3		Stationary phase	(Kawasaki & Aguirre, 2001)
<i>Emericella nidulans</i>	CpeA	CPx	StuA		(Scherer <i>et al.</i> , 2002)
<i>Apergillus niger</i>	CatR	2		H ₂ O ₂	(Witteveen <i>et al.</i> , 1993)
<i>Bacillus firmus</i>	CatII	3		H ₂ O ₂ /Ascorbate	(Hicks, 1995)
<i>Bacillus firmus</i>	CatIII	2		Stationary phase	(Hicks, 1995)
<i>Bacillus subtilis</i>	KatA	3	PerR		(Bsat <i>et al.</i> , 1998)
<i>Bacillus subtilis</i>	KatE	2	σ ^B		(Engelmann <i>et al.</i> , 1995)
<i>Bacillus subtilis</i>	KatX	1	σ ^F		(Bagyan <i>et al.</i> , 1998)
<i>Bacteroides fragilis</i>	KatB	3	OxyR		(Rocha <i>et al.</i> , 2000)
<i>Brucella abortus</i>	KatE	3	OxyR		(Kim & Mayfield, 2000)
<i>Dinococcus radiodurans</i>	CatE	2		H ₂ O ₂	(Wang & Schellhorn, 1995)

<i>Escherichia coli</i>	HPI (KatG)	CPx	OxyR		(Christman <i>et al.</i> , 1989)
<i>Escherichia coli</i>	HPII (KatE)	2	σ^S		(Loewen <i>et al.</i> , 1985)
<i>Haemophilus influenzae</i>	HktE	3		H ₂ O ₂ /Ascorbate	(Bishai <i>et al.</i> , 1994)
<i>Helicobacter pylori</i>	KatA	3	Fur		(Odenbreit <i>et al.</i> , 1996)
<i>Mycobacterium smegmatis</i>	KatG	CPx	FurA		(Zahrt <i>et al.</i> , 2001)
<i>Mycobacterium tuberculosis</i>	KatG	CPx	FurA		(Pym <i>et al.</i> , 2001)
<i>Neisseria gonorrhoea</i>	Kat	3	OxyR		(Tseng <i>et al.</i> , 2003)
<i>Erinea carotovora</i>	HPII	2	σ^S		(Calcutt <i>et al.</i> , 1998)
<i>Pseudomonas aeruginosa</i>	KatA	3	Fur		(Hassett <i>et al.</i> , 1996)
<i>Pseudomonas aeruginosa</i>	KatB	1	OxyR		(Ochsner <i>et al.</i> , 2000)
<i>Pseudomonas putida</i>	CatA	3		Log phase	(Katsuwon & Anderson, 1989)
<i>Pseudomonas putida</i>	CatC	2		Stationary phase	(Katsuwon & Anderson, 1989)
<i>Pseudomonas syringae</i>	CatF	1		Stationary phase	(Klotz & Hutcheson, 1992)
<i>Pyrobaculum calidifontis</i>	Kat pc	Mn		aerobic conditions	(Amo <i>et al.</i> , 2002)
<i>Rhizobium etli</i>	KatG	CPx	OxyR		(Vargas <i>et al.</i> , 2003)
<i>Salmonella typhimurium</i>	KatM	Mn	σ^S		(Robbe-Saule <i>et al.</i> , 2001)

<i>Salmonella typhimurium</i>	HPI	CPx	OxyR		(Christman <i>et al.</i> , 1985)
<i>Salmonella typhimurium</i>	HPII	2	σ^S		(Fang <i>et al.</i> , 1992)
<i>Sinorhizobium leguminosarum</i>	Cat			Log phase	(Ohwada <i>et al.</i> , 1999)
<i>Sinorhizobium meliloti</i>	KatA	3		H ₂ O ₂	(Herouart <i>et al.</i> , 1996)
<i>Sinorhizobium meliloti</i>	KatC	2		Stationary phase	(Sigaud <i>et al.</i> , 1999)
<i>Staphylococcus simulans</i>	ACKI			Oxygen	(Fondren <i>et al.</i> , 1994)
<i>Staphylococcus aureus</i>	KatA	3	PerR, Fur		(Horsburgh <i>et al.</i> , 2001)
<i>Streptomyces coelicolor</i>	CatA	3	CatR		(Hahn <i>et al.</i> , 2000)
<i>Streptomyces coelicolor</i>	CatB	2	σ^B		(Cho <i>et al.</i> , 2000)
<i>Streptomyces coelicolor</i>	CatC	CPx	FurA		(Hahn <i>et al.</i> , 2000)
<i>Streptomyces reticuli</i>	CpeB	CPx	FurS		(Zou <i>et al.</i> , 1999)
<i>Vibrio fischeri</i>	KatA	3		Stationary phase, H ₂ O ₂	(Visick & Ruby <i>et al.</i> , 1998)
<i>Xanthomonas oryzae</i>	KatX	2	σ^S		(Mongkolsuk <i>et al.</i> , 1996)
<i>Xanthomonas campestris</i>	KatE	2	σ^S		(Vattanaviboon <i>et al.</i> , 2000)

^a 1, clade 1; 2 clade 2; 3, clade 3; CPx catalase-peroxidase; Mn, manganese-containing catalase

Storz and co-workers elegantly elucidated the structural and biochemical basis for the redox regulation of OxyR. The initial reaction of OxyR with H₂O₂ is postulated to occur at Cys-199, leading to the formation of an unstable Cys-sulphenic acid intermediate (Zheng *et al.*, 2001). Once oxidized, Cys-199 reacts with Cys-208 to form an intramolecular disulphide bond. As these two cysteine residues are separated by ~ 17 Å in the reduced state it is hypothesized that oxidation is necessarily accompanied by refolding of a central domain in the OxyR promoter (Choi *et al.*, 2001). However, the requirement of disulphide bond formation for redox regulation of OxyR was recently challenged (Kim *et al.*, 2002). They proposed that the modification of Cys199 to the sulphenic acid alone is sufficient to account for the observed *in vivo* regulation by peroxides. Moreover, they suggest that various modified forms of OxyR (S-OH, S-NO and S-glutathionylation) may have distinct biological roles. In light of the new development, it may not be surprising to note that OxyR, in addition to being a peroxide sensor, has been shown to respond to disulphide stress (Aslund *et al.*, 1999).

Regulators such as OxyR are widely distributed in most Gram-negative (both aerobes and anaerobes) and some Gram-positive bacteria. For example, *Mycobacterium tuberculosis* and *Mycobacterium smegmatis* are shown to lack a functional OxyR (Pym *et al.*, 2001; Zahrt *et al.*, 2001). In these Mycobacteria, FurA, a homologue of Fur (ferric uptake regulator) is hypothesized to act as a second regulator of oxidative stress, and is shown to act as a negative regulator of *katG* (Zahrt *et al.*, 2001). The Fur super family of metallo-regulatory proteins includes several small, dimeric DNA binding proteins that respond to metal ions including PerR (peroxide sensor), Zur (zinc sensor) and Fur itself

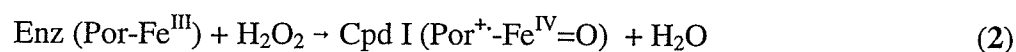
(iron sensor) (Bsat *et al.*, 1998; Gaballa and Helmann, 1998; Escolar *et al.*, 1999). *E. coli* Fur protein is a repressor governing a system of genes involved in iron uptake and the system is switched on when bacteria are grown in medium with limiting iron concentrations (Escolar *et al.*, 1999). The *B. subtilis* PerR regulon is shown to include *mrgA*, the gene for the major vegetative catalase (*katA*), the gene encoding the alkylhydroperoxide reductase (*ahpCF*), the heme biosynthesis operon (*hemAXCDBL*), *fur*, *perR* and a zinc uptake system (*zosA*) (Fuangthong *et al.*, 2002; Herbig and Helmann, 2002; Gaballa and Helmann, 2002). Like other Fur family members, PerR contains two metal binding sites per monomer (Faungthong and Helmann, 2003); one site binds Zn (II) and may play a largely structure role, whereas the second site binds the regulatory metal (Mongkolsuk and Helmann, 2002).

Heme synthesis must be sufficiently rapid to satisfy induced catalase synthesis rates. *E. coli* successfully increases the rate of heme synthesis to satisfy the demands in cells expressing plasmid-encoded catalases, but whether this is simply a response to heme demand or coordinate regulation of heme operons is not clear. In *Staphylococcal aureus*, *P. aeruginosa* and *B. subtilis*, there is coordinate control of oxidative stress proteins and iron storage and transport proteins (Horsburgh *et al.*, 2001; Ma *et al.*, 1999; Helmann *et al.*, 2003), but no link to the control of protoporphyrin synthesis has been demonstrated. There has been one report of iron deficient PMC being produced in *E. coli* during its rapid expression under the control of an inducible T7 promoter (Andreoletti *et al.*, 2003). During that study, the protoporphyrin was available for protein folding, but the availability or insertion rate of iron was limiting.

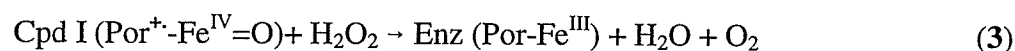
1.5. Heme Catalases

1.5.1. Reaction mechanism

Heme containing catalases or monofunctional catalases all have in common a two-stage mechanism for the degradation of H₂O₂. In the first step, one hydrogen peroxide molecule oxidizes the heme to an oxyferryl species in which one oxidation equivalent is removed from the iron and one from the porphyrin ring to generate a porphyrin cation radical [reaction 2].



The second hydrogen peroxide is utilized as a reductant of compound I to regenerate the resting state enzyme, water and oxygen [reaction 3].



Despite this common reaction, there are great differences in reactive capability among the members of this very large family of enzymes.

1.5.2. Phylogeny

Three reviews of catalase phylogeny have appeared, each succeeding review involving an increasing number of sequences from 20 in 1993 (Von Ossowski *et al.*, 1993) to 74 in 1997 (Klotz *et al.*, 1997) to 256 in 2003 (Klotz and Loewen, 2003). By 1997, the clear division of mono-functional catalases into 3 clades was obvious, arising from a minimum of two gene duplication events. The more exhaustive recent analysis confirms these conclusions, but integrates a larger picture including catalase-peroxidases and non-heme catalases into a universal tree of life. Clade 1 catalases are predominantly of plant origin, but with one algal representative and a subgroup of bacterial origin.

Clade 2 enzymes are all large subunit enzymes of bacterial and fungal origin. The one archaeobacterial clade 2 enzyme is postulated to have arisen in a horizontal transfer event from a *Bacillus* species. The clade 3 enzymes are all small subunit enzymes from bacteria, archaeobacteria, fungi, and other eukaryotes. The archetypal mono-functional catalase is probably a large subunit clade 2 enzyme from which an early gene duplication event, accompanied by loss of the sequence at the 5' and 3' ends gave rise to the clade 1 enzymes (Klotz and Loewen, 2003). Clade 3 enzymes are not present in older taxonomic groups suggesting that they arose much later in evolution as a result of a gene duplication in bacteria that then spread by horizontal and lateral transfers among bacteria, to archaeobacteria and eukaryotes.

1.5.3. Kinetic properties

Many catalases have been characterized over the century of study, but very few of the enzymes have been characterized in tandem. This has resulted in many independent reports of activities and properties, but no way to properly compare the results. Such a comparison of 16 common catalases, including eight for which the structures have been determined has revealed just how great a divergence in properties there is within the catalase family (Switala and Loewen, 2002). Catalases do not follow Michaelis-Menten kinetics except at very low substrate concentrations, and different enzymes are affected differently at higher substrate concentrations. Most small subunit enzymes begin to suffer inhibition at $[H_2O_2]$ above 300-500 mM and never reach the Michaelis-Menten V_{max} predicted by extrapolation from rates at low substrate concentrations. On the other hand, large subunit enzymes start to suffer inhibition only above 3 M $[H_2O_2]$, if at all, and

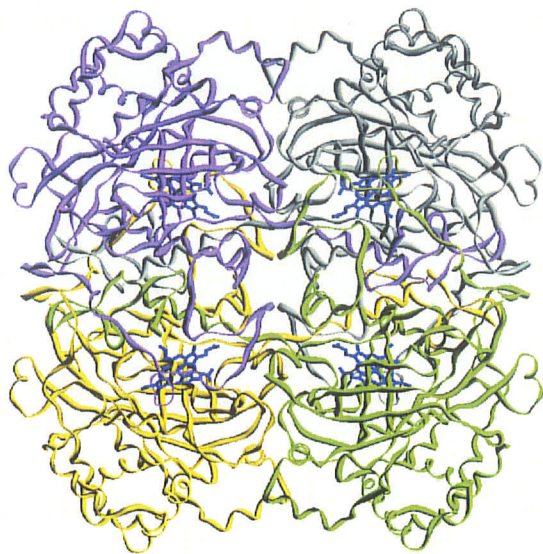
exceed the predicted Michaelis-Menten V_{\max} . Consequently, the presentation of observed data in terms of the typical constants K_m and V_{\max} is misleading because true Michaelis-Menten kinetics are not applicable. With this proviso in mind, the observed k_{cat} values ranged from 54,000 (*Pseudomonas aeruginosa* KatB) to 833,000 (*Proteus mirabilis*) sec^{-1} , and the $[\text{H}_2\text{O}_2]$ at $V_{\max}/2$ ranged from 38 to 599 mM (Switala and Loewen, 2002). Sequence differences among catalases must be responsible for the widely differing reaction rates and substrate affinities, but providing a rationale for how is not yet possible.

1.5.4. Structural diversity among heme-catalases

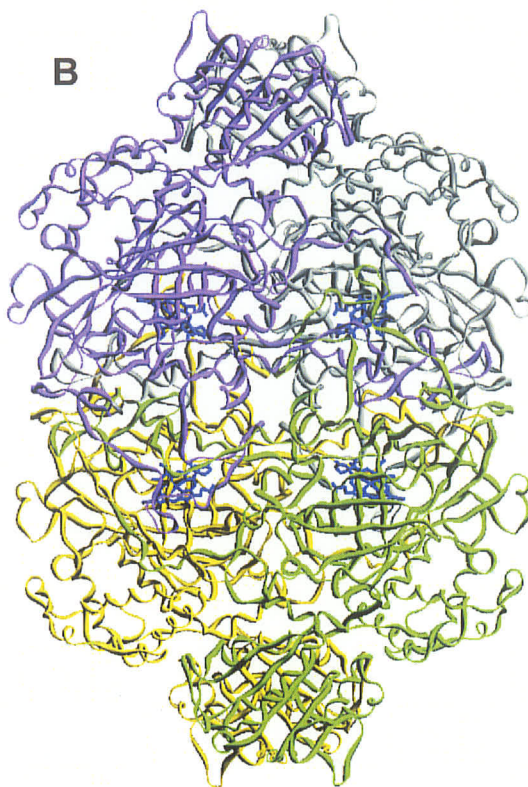
Heme-containing catalases consist of a scaffold, made up of a beta barrel inside which is the deeply buried heme active site. Eight heme-containing catalase structures have been reported. They include, the small subunit clade 3 enzymes from bovine liver (BLC) (Murthy *et al.*, 1981; Fita *et al.*, 1986), *Micrococcus luteus* (MLC) (Murshudov *et al.*, 1982), *Proteus mirabilis* (PMC) (Gouet *et al.*, 1995), *Saccharomyces cerevisiae* (CATA) (Berthet *et al.*, 1997; Mate *et al.*, 1999), and human erythrocytes (HEC) (Putnam *et al.*, 1999), and the large subunit clade 2 enzymes from *Penicillium vitale* (PVC) (Vainshtein *et al.*, 1981; Vainshtein *et al.*, 1986), *Escherichia coli* (HP11) (Bravo *et al.*, 1995; Bravo *et al.*, 1999] and CatF from *Pseudomonas syringae* (Carpena *et al.*, 2001; Carpena *et al.*, 2003). CatF provides the first look at a clade 1 catalase which presents an unexpected heme orientation and lacks NADPH. In addition, the presence of four subunits in the asymmetric unit of CatF makes possible an assessment of asymmetry, particularly in solvent location, among subunits and in comparison with other catalases (Carpena *et al.*, 2003).

Figure 1.2. Ribbon diagram for comparison of the overall structures and sizes of heme-containing small and large subunit catalases, a catalase-peroxidase and a dimanganese catalase. In panel, **(A)** a tetrameric small subunit, heme-containing catalase, CatF; **(B)** a tetrameric large subunit, heme-containing catalase, HP11; **(C)** a dimeric catalase-peroxidase, BpKatG; and **(D)** a hexameric dimanganese catalase, LTC are presented. All structures are presented at the same scale. The figure was prepared using SETOR (Evans, 1993).

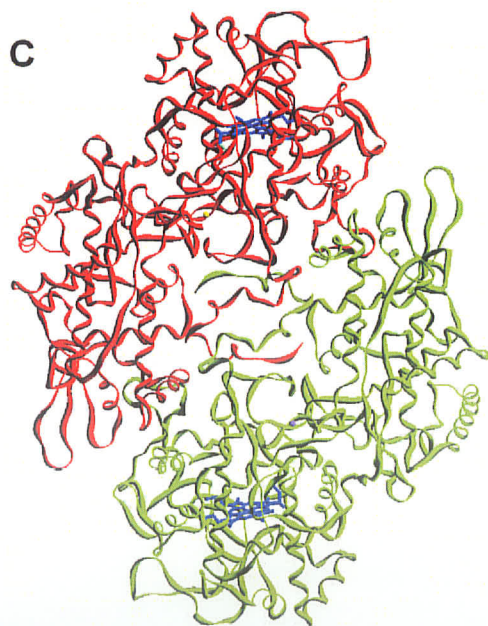
A



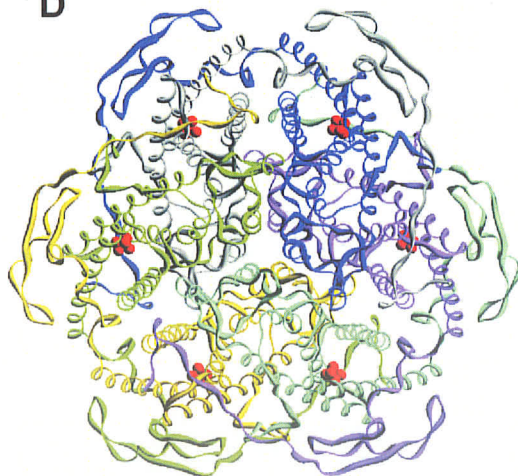
B



C



D



1.5.4.1. Heme orientation

The first catalase structures solved, BLC and MLC, had a common heme orientation in which the active site His was situated above ring III of the heme (referred to as the His-III orientation), leading to the conclusion that this was the normal orientation for heme in catalases. This was reinforced by the heme orientation found in PMC, CATA and HEC. The presence of the "flipped" orientation with the active site His located above ring IV of the heme (His-IV) in PVC and HP11, was assumed to be unique to large subunit enzymes. The fact that the hemes in PVC and HP11 were modified to heme d with a cis-hydroxyspirolactone group on ring III (Murshudov *et al.*, 1996) reinforced the idea that large subunit enzymes were unique. The CatF structure presented heme in the His-IV orientation suggesting that the "normal" and, in view of probable evolutionary development, original orientation of heme in catalases is His-IV. The residues making contact with the two methyl groups and two vinyl groups on rings I and II create a matrix of van der Waals interactions that favor the His-IV orientation in CatF, PVC and HP11, and would prevent any attempt to flip the heme to the His-III orientation. Similarly, the matrix of van der Waals interactions in the clade 3 catalases, BLC, MLC, PMC, HEC and CATA favor the His-III orientation and would prevent adoption of the His-IV orientation (Carpena *et al.*, 2003). A survey of 228 catalase sequences identified residues equivalent to 301 (Ala) and 350 (Leu) in CatF that are the key determinants in heme orientation, through their positions relative to the two vinyl groups on rings I and II. At position 301, 0% of clade 1 and clade 2 enzymes have Leu or Ile, but 80% of clade 3 enzymes do. The larger side chain prevents adoption of the His-IV orientation. At

position 350, 69% of clade 1 enzymes and 100% of clade 2 enzymes have Leu, whereas 0% of clade 3 enzymes do, and the location of the larger Leu side chain prevents adoption of the His-III orientation. Occupancy at the equivalent position in other catalases suggests that most clade 1 and all clade 2 enzymes will have the His-IV orientation, and that most clade 3 enzymes will have the His-III orientation. It will be interesting to determine if the apparent sequence exceptions conform to the clade majority, if there is a mixture of heme orientations or if there are small subsets of clade 1 and clade 3 enzymes with His-III and His-IV orientations, respectively.

1.5.4.2. NADPH binding

Since it was first noted almost 20 years ago (Kirkman and Gaetani, 1984), the presence of NADPH in catalases has presented the interesting problem to biochemists of explaining the purpose of the cofactor, and of determining its universality. The structures of the clade 3 enzymes BLC, HEC, PMC and CATA all contain NADPH in some fraction of their subunits, whereas the cofactor is not evident in the structures of the clade 2 enzymes, PVC and HPII. NADPH is not evident in the structure of CatF, and the potential binding site is modified compared to clade 3 binding sites to such an extent that NADPH binding should not be possible. The NADPH binding pockets of BLC, HEC, CATA and PMC contain a His, an Arg, a Val and a His (193, 202, 301 and 304, respectively using BLC numbering), which may be considered to be signatures for NADPH binding. In CatF, the equivalent residues are Arg196, Glu205, Ile304 and Asp307, each of which would interfere with NADPH binding either through electrostatic repulsion, direct steric interference or loss of favorable contacts. All clade 1 catalases,

lack the equivalent of Arg202 and His304 and most lack His193 and Val301 leading to the conclusion that most, if not all, clade 1 catalases do not bind NADPH. In the case of clade 2 enzymes, a portion of the extended C-terminal sequence protrudes into the NADPH binding site, precluding any possibility of NADPH binding in these enzymes. The conclusion seems to be that only clade 3 enzymes bind NADPH, but even in this clade, the coenzyme is not universal, based on the signature residues.

The widespread nature of the His-III orientation of heme in clade 3 enzymes suggests that this feature was adopted shortly after the separation of clade 3 from clade 1 enzymes. The more limited nature of NADPH binding among clade 3 enzymes suggests that it evolved independently and at a later date. Therefore, there would not appear to be a direct evolutionary link between the His-III orientation of the heme and NADPH binding as previously speculated (Carpena *et al.*, 2003). The role of NADPH and presumed reason for its binding site having evolved is to reduce inactive compound II back to the active native state (Kirkman and Gaetani, 1984) but the mechanism by which this is achieved remains unclear (Hillar and Nicholls, 1992; Olson and Bruice, 1995; Almarsson *et al.*, 1993, Kirkman *et al.*, 1999). Clade 2 enzymes do not form compound II, or, at least, it has not been possible to generate compound II in the laboratory (Sevinc, PhD thesis. 1997, University of Manitoba), making NADPH binding unnecessary. Similar attempts to generate compound II from a clade I catalase have not been reported.

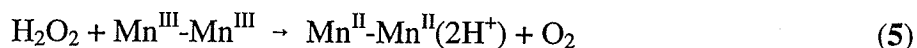
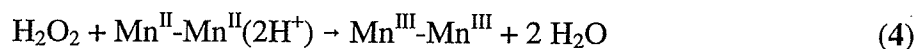
1.6. Non-heme or manganese-containing catalases

Non-heme catalases were initially referred to as pseudo-catalases because they did not contain heme (Kono and Fridovich, 1983) but other names including Mn-containing

(Allgood and Perry, 1986), non-heme (Nicholls *et al.*, 2001) and dimanganese catalase (Antonyuk *et al.*, 2000) to more accurately reflect their structure. The non-heme catalases are not as wide spread as the heme-containing catalases and so far have been identified only in bacteria. It is speculated that this type of enzyme may not have become as wide spread in nature because of its lower specific activity in relation to other catalases that were present in multiple forms in many bacteria (Klotz and Loewen, 2003).

1.6.1. Reaction mechanism

Like in heme-containing catalases, the reaction takes place in two stages, but here the similarity ends. The oxidation state of the dimanganese cluster is equally stable in either the **2,2** (Mn^{II}-Mn^{II}) or **3,3** (Mn^{III}-Mn^{III}) states resulting in the enzyme being isolated primarily as a mixture of these two states. Consequently, there is no temporal order to the oxidation and reduction stages, and either can occur first depending on the resting state of the enzyme. If the **2,2** state is encountered, the H₂O₂ is an oxidant (reaction 4) and if the **3,3** state is encountered, the H₂O₂ is a reductant [reaction 5].



Reactions 4 and 5 are presented as being analogous to reactions 2 and 3, but there is one overriding difference. Oxidation of the reaction center [reaction 4] involves removal of electrons from the active center, but a derivatized, reactive intermediate is not produced. As a result, the second stage does not involve reduction of a reactive intermediate, but a simple transfer of electrons to the dimanganese center generating oxygen. A nuance is

that both product waters are generated in reaction 4, unlike the heme catalases where one water is produced in each of reaction 2 and 3.

1.6.2. Structure of Mn catalases

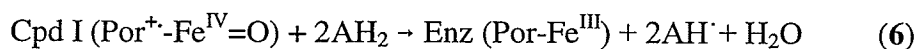
The crystal structures of the two non-heme catalases one from *Thermus thermophilus* (TTC) (Antonyuk *et al.*, 2000) and the second from *Lactobacillus plantarum* (LPC) (Barynin *et al.*, 2001) reveal that the catalytic center is a dimanganese group. The enzyme is a homo-hexameric structure of approximately 30 kDa monomers. The four-helix bundle motif of the individual monomers is highly conserved between the two enzymes with only the C-terminal tails differing. The dimanganese centers share a very similar environment. Direct coordination with the Mn atoms involves a virtually identical matrix of glutamate and histidine. The environments differ slightly in that one glutamate that normally interacts with Mn-associated waters in LPC is replaced by an arginine in TTC, and an arginine in LPC is absent in TTC.

1.7. Catalase-peroxidases

1.7.1. Reaction mechanism

Despite a very different sequence and tertiary/quaternary structure, the overall catalytic reaction of catalase-peroxidases takes place via the same two stages [reactions 2 and 3] as were described for the mono-functional catalases. In large part this is because both types of enzyme are heme containing, but it has the implication that the residues in the active site will have similar roles. The peroxidatic reaction presents another layer of

complexity involving the use of organic electron donors for the reduction of compound I to the resting state via two one-electron transfers [reaction 6].



In the presence of a suitable organic electron donor and low levels of H_2O_2 , the peoxidatic reaction becomes significant. Unfortunately, the *in vivo* peoxidatic substrate for the catalase-peroxidases has not been identified leaving the actual role of the peoxidatic reaction undefined (Carpena *et al.*, 2003).

1.7.2. Phylogeny of Catalase-peroxidases

The first review of KatG phylogeny appeared in 2000 and included 19 sequences (Faguy and Doolittle, 2000). The most recent report has included 58 sequences that have become available, the majority from bacteria but with 5 each from archaeobacteria and fungi (Klotz and Loewen, 2003). With the larger number of sequences in the data set, the tree is not as robust as the earlier tree and several interpretations of structure are possible. When integrated into a conceptual tree of life, it is apparent that the catalase-peroxidases evolved much later than the heme-containing mono-functional catalases, and a significant frequency of lateral gene transfer is evident. Very significantly, the data are consistent with the interpretation that sometime after a lateral gene transfer event from bacteria to the eukaryotic ancestor, the plant peroxidases evolved from the catalase-peroxidases.

1.7.3. Catalase-peroxidase structures

The first catalase-peroxidase HPI of *E. coli* was purified and characterized in 1979 (Claiborne and Fridovich, 1979), and the sequence of its encoding gene *katG*,

appeared in 1988 (Triggs-Raine *et al.*, 1988) providing the first catalase-peroxidase sequence and demonstrating the close phylogenetic link to plant peroxidases. It remained for the demonstration that KatG from *Mycobacterium tuberculosis* was responsible for the activation of the widely used anti-tubercular drug isoniazid (INH) (Zhang *et al.*, 1992) to bring the catalase-peroxidases into the spotlight. This led to extensive efforts around the world to crystallize the protein in order to characterize at the molecular level the interaction of the protein with the drug. Attempts to crystallize HPI from *E. coli* had commenced unsuccessfully in 1987, and success with the *M. tuberculosis* enzyme was no better. Persistence was finally rewarded in 2001 and 2002 with the preliminary reports of the crystallization of catalase-peroxidases from halophilic archaeobacterium *Haloarcula marismortui* (Yamada *et al.*, 2001), from the cyanobacterium *Synechococcus* (Wada *et al.*, 2002), the Gram negative bacterium *Burkholderia pseudomallei* (Carpena *et al.*, 2002) and the C-terminal domain of *E. coli* HPI (Carpena *et al.*, 2002). The structure of the *H. marismortui* enzyme (HmCPx) at 2.0 Å was reported first (Yamada *et al.*, 2002), followed by the structure of the *B. pseudomallei* enzyme (BpKatG) at 1.7 Å (Carpena *et al.*, 2003). There were obvious and clear similarities between the two enzymes, but the BpKatG structure presented a number of unusual features that provided potentially significant insights into the function of the enzyme.

The asymmetric unit for both catalase-peroxidases contains two subunits related by non-crystallographic two-fold symmetry, consistent with the predominant form of the enzyme in solution being a dimer. Each subunit is composed of 20 α -helical sections joined by linker regions and just three or four β -strand segments, making the structure very different from mono-functional catalases. It had previously been proposed that the

large gene size of *katG* had arisen through a gene duplication and fusion event (Welinder, 1991) resulting in a gene with two distinct sequence-related domains. Further support for this hypothesis was evident in the conservation of ten pseudo-symmetry related α -helical segments in the N- and C-terminal domains for which the r.m.s. deviation of 133 C α carbons following superimposition is just 2.19 Å in BpKatG. Superimposition of the N-terminal domain of BpKatG onto the structures of cytochrome c peroxidase, ascorbate peroxidase and horseradish peroxidase revealed r.m.s. deviations for the same 133 C α atoms in the 10 α -helical segments of 0.97 Å, 1.22 Å and 2.03 Å, respectively. Not surprisingly, the inactive C-terminal domain has suffered greater evolutionary drift with the corresponding 113 C α atoms in 10 α -helical segments having r.m.s. deviations of 3.62 Å, 3.75 Å and 4.06 Å when compared to cytochrome c peroxidase, ascorbate peroxidase and horseradish peroxidase (Carpena *et al.*, 2003). The high similarity between the HmCpx and BpKatG is illustrated by the r.m.s. deviation of 0.43 Å for the 133 C α atoms and 1.05 Å for the 685 C α atoms.

1.7.4. Covalent linkage joining Trp-Tyr-Met

The most striking and unusual feature in both catalase-peroxidase structures is a covalent structure involving the indole ring of the active site Trp (residue 111 in BpKatG) and the sulfur of a Met (264 in BpKatG) joined to the ortho positions of a Tyr ring (residue 238 in BpKatG). The structure is clearly evident in the electron density maps although the refined bond lengths are a bit longer than ideal for covalent bonds, and the bonds to the Tyr and Trp are not pure sp² in character, deviating somewhat from

planarity. Independent evidence for the existence of the covalent bonds was obtained from a mass spectrometry analysis of tryptic digests of BpkatG (Donald *et al.*, 2003).

The obvious question posed by such a covalent structure is what is its role? It had previously been shown that the active site Trp was essential for normal catalatic activity. Its replacement by Phe results in the loss of catalase activity and enhanced peroxidase activity in both HPI (Hillar *et al.*, 2000) and the *Synechocystis* KatG (Regelsberger *et al.*, 2000; Regelsberger *et al.*, 2001). Subsequent work has shown that replacement of either Met264 (Donald *et al.*, 2003) or Tyr238 (Jakopitsch *et al.*, 2003) has a similar effect in eliminating catalase activity with no effect or a positive effect on peroxidase activity. In other words the complete adduct is required for catalatic activity but not peroxidatic activity, providing a clear explanation for why the apparently closely related plant peroxidases have no, or only a vestige of catalase activity. Given that the adduct is required for catalase activity, electronic or steric roles, or a combination can be envisioned. A very precise and immovable positioning of the indole ring may be necessary for interaction with the reducing H_2O_2 in order that correct bond lengths leading to the transition state are realized. Alternatively or in addition, the adduct may alter the electronic environment on the indole enhancing the interaction with the substrate and facilitating the formation of the transition state. Determination of the structures of the variants individually lacking each of the Trp, Tyr and Met residues involved in the adduct will provide valuable evidence about the role of the adduct.

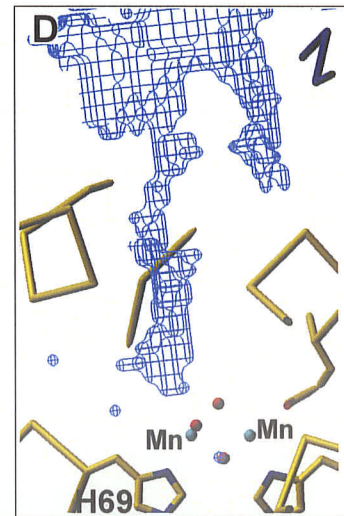
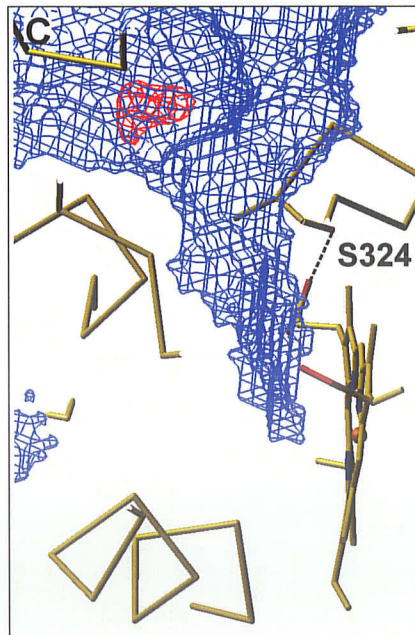
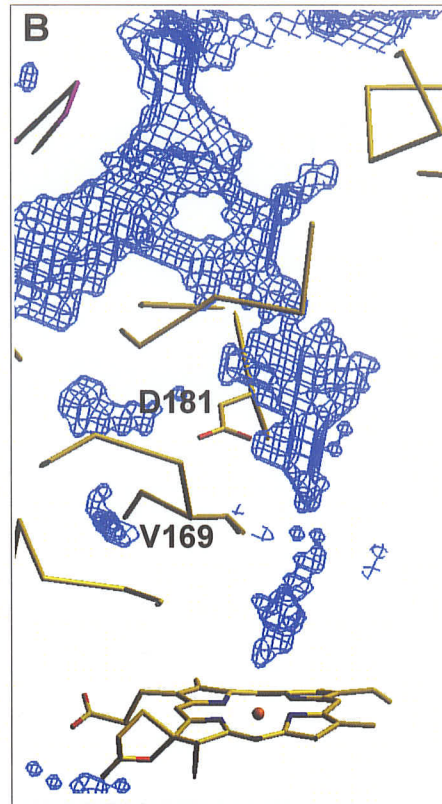
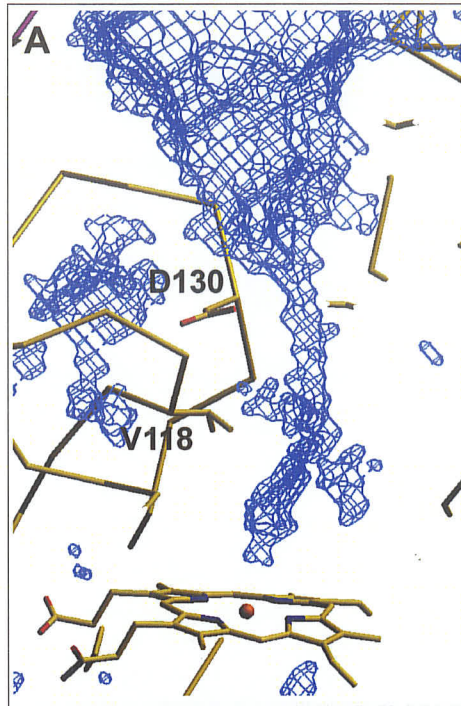
1.8. Channels in catalases

1.8.1. Channel architecture in heme catalases

The recently reported structures of CatF (Carpena *et al.*, 2003) and HP11 variants (Melik-Adamyan *et al.*, 2001) have provided significant insights into the channel architecture in catalases. Three obvious channels connect the heme-containing active site with the surface. The main channel, so named because it was the most obvious access route to the heme, approaches the heme perpendicular to its plane and has long been considered the primary access route for substrate H₂O₂ (Fig. 1.3), a concept supported by molecular dynamics modeling (Kalko *et al.*, 2001; Amara *et al.*, 2001). A second channel approaches the heme laterally, almost in the plane of the heme, and has been referred to as the minor or lateral channel. Limited evidence pointing to a role for the lateral channel in HP11 includes a 3-fold increase in specific activity resulting from an enlargement of the channel through removal of Arg260, part of Glu-Arg ionic pair situated in the channel. A third channel connects the heme with the central cavity, but no evidence for it having a role has been presented.

An extensive review of the waters occupying the main channels in each of the four subunits of CATF, HEC (+ CN and + peracetic acid), CATA + azide and HP11, and of the single subunits of MLC and PMC revealed a number of consistently occupied positions as well as a number of low occupancy sites (Carpena *et al.*, 2003). All enzymes contained a water interacting with the active site His and Asn, and some, including HP11, MLC and PMC contained a second water in the active site interacting with the heme iron and the active site His. Moving away from the heme in the channel, only one subunit of HP11 and inactive HEC contained waters in the hydrophobic region around the conserved Val169 (HP11 numbering). The lack of waters in hydrophobic portion of the channel between the conserved Asp (12 Å from the heme) and the active site His was interpreted

Figure 1.3. Structure of the channels providing access to the active sites in one subunit each of CatF (**A**), HPII (**B**), BpKatG (**C**) and LTC (**D**). The channel, as calculated by the program VOIDOO (Kleywegt and Jones, 1994), is presented as a blue chicken wire structure in a cross section slab of the enzyme. In **A** and **B**, the conserved valine (V118 & V169) and aspartate residues (D130 & D181) are shown. The active site heme is evident at the end of the channels in **A**, **B** and **C**. In **D**, the dimanganese cluster is presented as two blue balls (Mn) and four red balls (waters) and one of the coordinating histidines (His 69) is indicated for reference. All four channels are presented at the same scale for comparison. The figure was prepared using SETOR (Evans, 1993).



as a "molecular ruler" effect (Putnam *et al.*, 2000) arising from the lack of interaction sites on the protein and an distance that was inappropriate for the formation of a stable matrix of hydrogen bonded waters, but was appropriate for a matrix involving the slightly larger H_2O_2 .

1.8.2. Channel architecture in Mn catalases

Access to the dimanganese clusters is via a central channel that extends the full width of the hexamer, with branches into each subunit to the active center. The branch leading from the central channel into one of the dimanganese clusters is shown in Fig 1.3. and the similarity in length and narrowness of the channel to those of monofunctional catalases is quite striking. In all three cases, CatF, HP11, and LPC, the final 15 Å is uniformly narrow as compared to the funnel shape of the channel in catalase-peroxidases suggesting that restricted access to only substrate H_2O_2 is very important to the catalytic reaction. The absence of a glutamate and an arginine in the TTC active site creates larger cavity and a second access channel that allows in larger ions that cannot reach the LPC active site, but viewing this expanded channel will have to await the release of the TTC coordinates.

1.8.3. Channel architecture in catalase-peroxidases

The heme-containing active site is somewhat more deeply buried compared to peroxidases, but is accessed through a similar funnel shaped channel that approaches the heme laterally, rather than perpendicularly as in mono-functional catalases (Fig 1.3). Interpretation of possible substrate binding sites is complicated by the presence of a deep

crevasse on the side of the protein that could potentially be the binding site of a substrate, and the existence of a second channel approaching a small central cavity near the heme that also contains a single metal ion in BpKatG. Not knowing the natural peroxidatic substrate makes assigning roles to these features speculative at this point (Carpena *et al.*, 2003).

1.9 Object of the thesis

Long before any structural studies have been started on other types of protein channels (for example, aquaporins, porins, ion channels), structural studies carried out on catalases in the labs of Prof's Michael Rossmann and Boris Vanshtein (in the early 80's), showed that access to the deeply buried active site heme in catalases is through two or more channels that extend to the protein exterior. However, specific studies focusing on defining a role(s) for these channels in catalases have been very limited. Earlier structure-function studies done on HPII by Ingemar Von Ossowski (1993), Serdal Sevinc (1997) and others, focused on, residues around the active site, presumptive NADPH binding residues, and the C-terminal residues. The focus of the present study is two fold. The first objective was to elucidate the role of these channels in enzyme catalysis, and in the process, to address the direction of substrate flow in catalases by making substitution mutants along the channels. The second objective was to define the physiological functions of the extended N and C termini with specific emphasis on their contribution to stability of HPII.

2. Materials and Methods

2.1. *Escherichia coli* strains, plasmids and bacteriophage

E. coli strains, plasmids and bacteriophage used in this study are listed in Table 2.1. The *E. coli katE* gene, encoding HPII catalase, was originally cloned into a pKS+ (Stratagene Cloning Systems) to generate the plasmid pAMKatE72 (Von Ossowski *et al.*, 1991). Strain CJ236, harboring plasmid clone pAMKatE72 and subclass pKS⁺ H-E and pKS⁺ E-C of the *E. coli katE* gene (Fig 2.1) respectively, was used for generation of single stranded uracil-containing, DNA templates employed for site-directed mutagenesis. Helper phage R408 was used for infection of strain CJ236 to generate single stranded DNA. Strain NM522 was used as host for all plasmids and routine cloning. Strain JM109 was used for production of plasmid DNA for double stranded DNA sequencing. Strain UM255 was used for variant KatE expression and subsequent production of variant HPII proteins.

2.2. Chemical and biochemical reagents

Standard chemicals and biochemical reagents, used in the course of this study were usually obtained from either Sigma Chemical Co. (St.Louis, Mo.), or from Fischer Scientific Ltd. (Mississauga, Ont.). Restriction nucleases, endopeptidases, polynucleotide Kinases, DNA ligase and Klenow fragment of DNA polymerase were obtained from Invitrogen (Burlington, Ontario). Media used for growth of cell cultures were usually obtained from DIFCO (U.S.A). Unless otherwise stated, solutions were prepared using reverse osmosis distilled water.

Table 2.1. Genotypes and sources of *Escherichia coli* strains, plasmids and bacteriophage used in this study.

Genotype		Source
Strains		
CJ236	<i>dut1 ung1 thi-1 relA1/pCj105/cam^rF'</i>	Kunkel <i>et al.</i> , 1987
NM522	<i>supE</i> Δ (<i>lac-proAB</i>) <i>hsd-5</i> [F' <i>proAB lacI^r lacZ</i> Δ 15]	Mead <i>et al.</i> , 1985
UM255	<i>pro leu rps1 hsdM hsdR endI</i> <i>lacy katG2 katE12:: Tn10 recA</i>	Mulvey <i>et al.</i> , 1988
JM109	<i>recA1 supE44 endA1 hsdR17 gyrA96</i> <i>relA1 thi</i> Δ(<i>lac-proAB</i>)	Yanisch-Perron <i>et al.</i> , 1985
Plasmids		
pAMkatE72 (pKS ⁺ P-C, <i>katE</i> clone)	Amp ^r	von Ossowski <i>et al.</i> , 1991
pKS ⁻ E-H (subclone II)	Amp ^r	von Ossowski <i>et al.</i> , 1991
pKS ⁺ E-C (subclone III)	Amp ^r	von Ossowski <i>et al.</i> , 1991
Bacteriophage		
R408 (helper phage)		Stratagene Cloning Systems

2.3. Media, growth conditions and storage of cultures

E. coli cultures were routinely grown in LB (Luria-Bertani) medium containing 10 g/L tryptone, 5 g/L yeast extract, 5 g/L NaCl. Solid media contained 14 g/L agar. Ampicillin was added to 250 µg/ml for the liquid medium to select for Amp^r plasmid harboring cells. Chloramphenicol was added to 40 µg/ml in order to maintain the presence of the F' episome for the growth of strain CJ236. *E. coli* strains in both liquid and solid medium were grown at 37°C or 28°C. Liquid cultures were grown with vigorous aeration in shake flasks. Long term storage of stock cultures was in 24% dimethylsulfoxide at -60° C. Bacteriophage R408 was maintained at 4°C in LB culture supernatant.

2.4. DNA manipulation

2.4.1. Preparation of synthetic oligonucleotides

Oligonucleotides used for mutagenesis were purchased commercially from Invitrogen (Burlington, Ontario) in non-phosphorylated form. The concentration of oligonucleotide DNA was determined spectrophotometrically at 260 nm, where 1 absorbance unit = 40 µg/ml single stranded DNA (Sambrook *et al.*, 1989).

Oligonucleotides used for site-directed mutagenesis were phosphorylated at the 5' end using T₄ kinase (Invitrogen) according to Ausubel *et al.* (1989). Approximately 100 ng of oligonucleotide DNA in a volume of 25 µl containing 1 mM ATP and 10 units of kinase were incubated in appropriately diluted buffer supplied by the manufacturer at 37°C for 30 min. The reaction was terminated by heat inactivation at 65°C for 5 min.

2.4.2. DNA isolation and purification

Isolation of plasmid DNA was according to Sambrook *et al.* (1989). Plasmid harboring cells were grown in tubes containing 5 ml LB medium to stationary phase and were then pelleted by centrifugation and resuspended in 200 μ l Tris-glucose-EDTA buffer (25 mM Tris-HCl, pH 8.0, 1% glucose, 10 mM Na-EDTA). Resuspended cells were lysed by addition of 0.4 ml 1% SDS (w/v), 0.2M NaOH solution and gentle mixing. This was then neutralized by addition of 300 μ l 6.2 M ammonium acetate, pH 6.2. After 10 min incubation on ice, the mixture was centrifuged twice to remove all precipitates. Plasmid DNA was then precipitated by addition of 550 μ l isopropanol to the remaining supernatant followed by 15 min incubation at room temperature. Plasmid DNA was pelleted by centrifugation, washed twice with 1000 μ l of 70%(v/v) ice-cold ethanol, and then dried under vacuum. The DNA pellet was either stored in this condition at -20°C or was resuspended in HPLC grade distilled water or TE buffer (10 mM Tris, pH 8.0, 1 mM Na-EDTA) prior to being stored at -20°C until further use.

Preparation of single stranded template DNA for site-directed mutagenesis was carried out according to Vieira and Messing (1987). Plasmid harboring cells in a 5 ml LB culture in early exponential phase were infected with 10-50 μ l of helper phage R408 (10^{11} - 10^{12} PFU per ml) and grown overnight. After centrifuging 1.5 ml of culture in order to remove cells and debris, a solution of 300 μ l of 1.2 M NaCl, 20% PEG 6000 was added per ml of medium supernatant and mixed. This mixture was incubated for 15 min at room temperature and then centrifuged to pellet the phage particles. The pellet was then resuspended in TE buffer on ice and extracted first with an equal volume of buffer-

saturated phenol, followed by extraction with an equal volume of water- saturated chloroform. Single-stranded DNA was precipitated by addition of an equal volume of 7.5 M ammonium acetate, pH 7.5 and 4 volumes of ice-cold 95% ethanol followed by incubation at -20°C for 20 min. Single- stranded DNA was recovered by centrifugation and the pellet washed once with 95% (v/v) ethanol and 2 times with 70% (v/v) ethanol. The dried pellet was stored at -20°C until further use.

2.4.3. Restriction nuclease digestion

All restriction endonucleases and buffers used in this study were products of Invitrogen. Restriction digestions were carried out at 37°C for 2-5 hrs in total volumes of 10 µl, containing 1 µg RNase, 1 µl of 10X appropriate buffer provided by the supplier, ~ 1-5 µg DNA, and 0.5-1 µl (50 – 2,000 Units) of endonuclease. The 5'-phosphate groups of vector DNA obtained from single restriction digests were removed by 12.5-25 units of calf intestinal alkaline phosphate (Invitrogen) added during the cleavage reaction.

2.4.4. Agarose gel electrophoresis

Electrophoresis of restriction endonuclease digested DNA was performed according to Sambrook *et al.* (1989). Agarose gels prepared in TAE buffer (40 mM Tris-acetate and 1 mM EDTA, pH 8.0), containing 1% (w/v) agarose, and 0.1 µg/ml ethidium bromide was cast in Bio-Rad Mini Sub Cell plexiglass horizontal electrophoresis trays (6.5 cm x 10 cm). Samples of 10 µl volumes are mixed with 2 µL Stop buffer (40%[v/v] glycerol, 10mM EDTA pH 8.0, 0.25% [w/v] bromophenol blue). 1 kb DNA Ladder or 1 kb Plus DNA Ladder (Invitrogen) were used as molecular weight size standards.

Electrophoresis was carried out at 50-60 mA constant current in TAE buffer, usually until the bromophenol blue dye front had migrated two-thirds of the length of the gel.

Following electrophoresis, DNA bands were visualized with ultraviolet light using a (Bio-Rad) Gel Doc 1000.

2.4.5. Ligation

DNA fragments to be ligated were excised from agarose gels and purified using the Gene clean DNA extraction kit (M Bio.) according to the instructions supplied by the manufacturer. Ligation of insert DNA was carried out according to Sambrook *et al.* (1989). Purified DNA was mixed in a ratio of 2-3 of insert to vector in 10 μ l volumes, containing 1 unit of T4 DNA ligase (Invitrogen), and the manufacturer's supplied buffer. Ligation mixtures were incubated overnight at 15°C. A sample with no insert DNA added was used as the control.

2.4.6. Transformation

Transformation of *E. coli* cells with the various plasmids was performed according to Chung *et al.* (1989). Cells grown in tubes containing 5 ml LB medium to exponential phase (2-4 hr) were harvested by centrifugation and made competent by resuspension in 500 μ l ice-cold 0.1M CaCl₂ for 30 min on ice. 2-10 μ g DNA was usually added to 100 μ l of this cell suspension, followed by a further 30 min incubation on ice, and a 90 s heat shock at 42°C. LB medium (0.9 ml) was then added to the cell suspension and incubated at 37°C for 60-90 min without aeration. The mixture was then either spread-plated, or (in the case of ligation mixture transformations) mixed with 3 ml molten

(50°C) R-Top agar (0.125 g yeast extract, 1.25 g tryptone, 1g NaCl, 1g agar per 125 ml volume with 0.25 ml 1M CaCl₂ and 0.42 ml 30% glucose sterile solutions added for autoclaving) and poured onto ampicillin-containing LB plates.

2.4.7. DNA sequencing

DNA sequencing was carried out according to Sanger *et al.* (1977). Sequencing was carried out manually with double stranded DNA templates using primers shown in Table 2.2. To prepare a double stranded DNA template, 5 µg plasmid DNA was resuspended and denatured in a 40 µl volume of 2 M freshly prepared NaOH. This mixture was incubated for 10 min at 37°C, and then reprecipitated by addition of 10 µl 3 M sodium acetate, pH 4.8 and 140 µl ice-cold 95% ethanol. Following incubation at -20°C for 30 min, the DNA pellet recovered by centrifugation, washed once with 1 ml 95% ice-cold ethanol, and once with 0.2 ml 70% ice-cold ethanol, and then evaporated to dryness under vacuum. Annealing and sequencing reactions were carried out using a T7 sequencing kit (USB Corporation, USA) according to the specifications of the supplier and using 5-15 µCi [³⁵S] dATP (NEN-Dupont). Reaction mixtures were separated and resolved on 8% (w/v) polyacrylamide vertical slab gels containing 7 M urea, 0.13 M Tris, 0.13 M boric acid, and 10 mM EDTA. Electrophoresis was carried out at 18-24 mA constant current in TBE buffer (90 mM Tris, 89 mM borate, 2.2 mM EDTA) for 1.5-5 h as required. Dried gels were exposed to X-ray film (Kodak X-OMAT AR) overnight, in order to visualize the DNA bands.

2.4.8. In vitro mutagenesis strategy

Site-directed mutagenesis of *E. coli katE* was done according to the methodology described by the Kunkel *et al.* (1987). A simplified restriction map of *E. coli katE* that indicates the location of individual subclone fragments is shown in Fig 2.1. The subclones rather than the whole gene were mutagenized to limit the amount of sequencing needed for mutant characterization. Target codons for mutagenesis were selected from the DNA sequence of *katE* shown in Fig 2.2. The DNA sequences of the oligonucleotides used for mutagenesis are listed in Table 2.2. Mutagenesis was performed by annealing the phosphorylated oligonucleotides encoding the desired base modification to uracil-containing single-stranded DNA templates obtained from the appropriate Bluescript phagemid subclone, propagated on the *dut⁻ ung⁻* CJ236 strain. The complementary DNA strand was then synthesized *in vitro* by unmodified T7 DNA polymers (New England Biolabs) using the annealed oligonucleotide as the primer. The 3' and 5' ends of the completed complementary strand were ligated by adding T4 DNA ligase (Invitrogen) in the reaction mixture. The double-stranded DNA was then transformed into NM522 strain so that the uracil-containing DNA strand was degraded. Plasmid DNA recovered from this strain was used to screen for the desired mutation in the plasmid subclone by DNA sequencing. Once the desired mutation was identified, the complete sequence of the subclone was ascertained to ensure that no other base changes had been introduced. The mutated subclone was then used to construct the entire *katE* gene, which was transformed into UM255 for determination of enzyme activity and

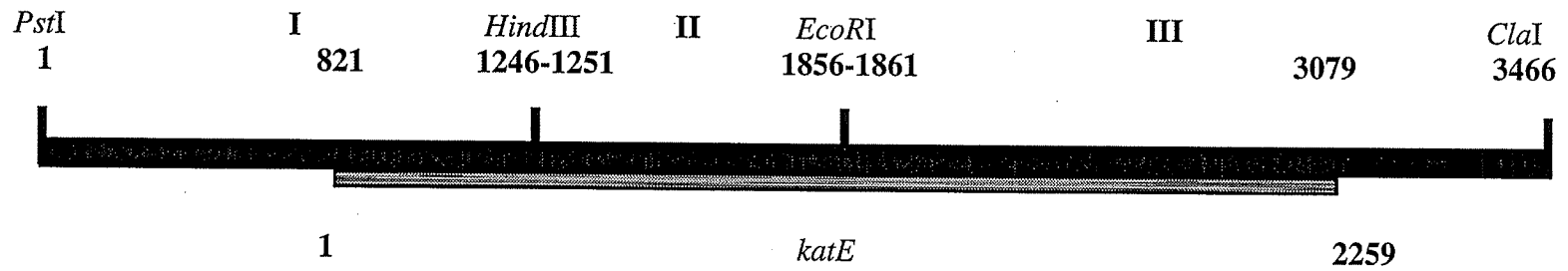


Figure 2.1. Simplified restriction map of the cloned 3466 bp chromosomal insert in pAMKatE72. The 2259 nucleotide long *katE* open reading frame (▨) is shown as part of the chromosomal insert (■) as are the three subclones (I, II, III) employed in site directed mutagenesis. (redrawn from von Ossowski *et al.*, 1991).

Table 2.2. Oligonucleotides and *katE* restriction fragments used in oligonucleotide-directed mutagenesis of *katE*.

Mutant	Sequence Change	Oligonucleotide ^a	Restriction fragment
V169I	(GTT→ATT)	TTCTCTACCATTCAGGGTGGT	HindIII-EcoRI (1246-1856)
V169F	(GTT→TTT)	TTCTCTACCTTTCAGGGTGGT	HindIII-EcoRI (1246-1856)
VI69W	(GTT→TGG)	TTCTCTACCTGGCAGGGTGGT	HindIII-EcoRI (1246-1856)
R180A	(CGT→GCT)	GATACCGTGGCTGATATCCGT	HindIII-EcoRI (1246-1856)
R180K	(CGT→AAA)	GATACCGTGAAAGATATCCGT	HindIII-EcoRI (1246-1856)
D181A	(GAT→GCT)	ACCGTGCGTGCTATCCGTGGC	HindIII-EcoRI (1246-1856)
D181S	(GAT→TCT)	ACCGTGCGTTCTATCCGTGGC	HindIII-EcoRI (1246-1856)
D181E	(GAT→GAA)	ACCGTGCGTGAAATCCGTGGC	HindIII-EcoRI (1246-1856)
D181Q	(GAT→CAA)	ACCGTGCGTCAAATCCGTGGC	HindIII-EcoRI (1246-1856)
D181N	(GAT→AAT)	ACCGTGCGTAATATCCGTGGC	HindIII-EcoRI (1246-1856)
D181I	(GAT→ATT)	ACCGTGCGTATTATCCGTGGC	HindIII-EcoRI (1246-1856)
D181W	(GAT→TGG)	ACCGTGCGTTGGATCCGTGGC	HindIII-EcoRI (1246-1856)
H128N/ D181A	(CAT→AAT, GAT→GCT)	CGTATTGTTAATGCACGCGGA ACCGTGCGTGCTATCCGTGGC	PstI-HindIII (1-1246) HindIII-EcoRI (1246-1856)

S234A	(AGT→GCT)	CAAGGGCAAG CT GCCCACGAT	HindIII-EcoRI (1246-1856)
S234D	(AGT→GAT)	CAAGGGCAAG AT GCCCACGAT	HindIII-EcoRI (1246-1856)
S234N	(AGT→AAT)	CAAGGGCA AA ATGCCCACGAT	HindIII-EcoRI (1246-1856)
S234I	(AGT→ATT)	CAAGGGCA AA TTGCCCACGAT	HindIII-EcoRI (1246-1856)
E530A	(GAG→GCT)	TTCAGTTTT GCT TTAAGCAAA	EcoRI-ClaI (1856-3466)
E530I	(GAG→ATT)	TTCAGTTTT A TTTTAAGCAAA	EcoRI-ClaI (1856-3466)
E530D	(GAG→GAT)	TTCAGTTTT GAT TTAAGCAAA	EcoRI-ClaI (1856-3466)
E530Q	(GAG→CAG)	TTCAGTTTT CAG TTAAGCAAA	EcoRI-ClaI (1856-3466)
D181C	(GAT→TGC)	ACCGTGC GT TGCATCCGTGGC	HindIII-EcoRI (1246-1856)
S234C	(AGT→TGC)	CAAGGGCA ATG CGCCCACGAT	HindIII-EcoRI (1246-1856)
R260C	(CGC→TGC)	ATGTC GGAT TGCGGCATCCCC	HindIII-EcoRI (1246-1856)
I274C	(ATT→TGC)	GGCTTC GGT TGCCACACCTTC	HindIII-EcoRI (1246-1856)
S421C	(AGT→TGC)	ACACAA ATCTG CCGTCTTGGT	EcoRI-ClaI (1856-3466)

^a The sequence in bold is the codon that has been modified.

Figure 2.2. The DNA sequence and corresponding amino acid sequence of *E. coli katE* showing the restriction sites and the target codons selected for mutagenesis in this study. The sequencing primers used are also shown (in alphabetical order). (Sequence from von Ossowski *et al.*, 1991).

Escherichia coli katE (HPII or KatE)

CTGCAGCCTTTCTTTAAAAGAGTCGAAAGCCAGGCTTTTAATATTTAAATCACCATAATT GACGTCGAAAGAAAATTTCTCAGCTTTTCGGTCCGAAAATTATAAATTTAGTGGTATTAA <i>Pst</i> I	60
ACTCTGTATTAAGTTTTGTAGAAAACATCTCCCGCCTCATATTGTTAACAAAATTATTATC TGAGACATAATTCAAACATCTTTTGTAGAGGGCGGAGTATAACAATTGTTTTAATAATAG	120
TCATTTAAATCTAAGTCATTTACAATATAAGTTTTAAGAGCGACGCCACAGGATGAACTAT AGTAAATTTAGATTCAGTAAATGTTATATTCAAATTCCTCGCTGCGGTGTCTACTTGATA	180
CAAAAATAGCTCATCATGATTAGCAAACTTAACCATTTTTAAATAAATAACAATTTAAA GTTTTTATCGAGTAGTACTAATCGTTTTGAATTGGTAAAATTTTATTTATTTGTTAATTT	240
GAAAAAAGATCACTTATTTATAGCAATAGATCGTCAAAGGCAGCTTTTTGTTACAGGTGG CTTTTTCTAGTGAATAAATATCGTTATCTAGCAGTTTTCCGTGAAAAACAATGTCCACC	300
TTTGAATGAATGTAGCAACGAAATACAGAATTTCAAGGTCATGTAACCTCCGGCAAACCGG AAACTTACTTACATCGTTGCTTTATGTCTTAAACTCCAGTACATTGAGGGCCGTTTGGCC	360
GAGGTATGTAATCCTTACTCAGTCACTTCCCCTTCTGGCGGATCTGATTTGCCCAACGT CTCCATACATTAGGAATGAGTCAGTGAAGGGGAAGGACCGCCTAGACTAAACGGGTTGCA	420
TGGGCAGATTCAGGCACAGTAAACGCCGGTGAGCGCAGAAATGACTCTCCCATCAGTACA ACCCGTCTAAGTCCGTGTCATTTGCGGCCACTCGCGTCTTTACTGAGAGGGTAGTCATGT	480
AACGCAACATATTTGCCACGCAGCATCCAGACATCACGAAACGAATCCATCTTTATCGCA TTGCGTTGTATAAACGGTGCCTGCTAGGTCTGTAGTGCTTTGCTTAGGTAGAAATAGCGT	540
TGTTCTGGCGGCGCGGGTTCCGTGCGTGGGACATAGCTAATAATCTGGCGGTTTTGCTGG ACAAGACCGCCGCGCCAAAGGCACGCACCCTGTATCGATTATTAGACCGCCAAAACGACC	600
CGGAGCGGTTTTCTTCATTACTGGCTTCACTAAACGCATATTA AAAATCAGAAAACTGTA GCCTCGCCAAAGAAGTAATGACCGAAGTGATTTGCGTATAATTTTTAGTCTTTTTGACAT A→	660
GTTTAGCCGATTTAGCCCCTGTACGTCCCGCTTTGCGTGTATTTATAACACCGTTTTCCA CAAATCGGCTAAATCGGGGACATGCAGGGCGAAACGCACATAAAGTATTGTGGCAAAGGT 1→ (1A?)	720
GAATAGTCTCCGAAGCGGGATCTGGCTGGTGGTCTATAGTTAGAGAGTTTTTTGACCAA CTTATCAGAGGCTTCGCCCTAGACCGACCACCAGATATCAATCTCTCAAAAACTGGTTT	780
ACAGCGGCCCTTTCAGTAATAAATTAAGGAGACGAGTTCAATGTCGCAACATAACGAAAA M S Q H N E K (7)	840

-----AAA-----R180K→

K F Y T E E G I F D L V G N N T P I F F (207)
 CAAGTTCTATAACCGAAGAGGGTATTTTTGACCTCGTTGGCAATAACACGCCAATCTTCTT 1440
 GTTCAAGATATGGCTTCTCCATAAAAACTGGAGCAACCGTTATTGTGCGGTTAGAAGAA

I Q D A H K F P D F V H A V K P E P H W (227)
 TATCCAGGATGCGCATAAATTCCTCCGATTTTGTTCATGCGGTAAAACCAGAACC GCACTG 1500
 ATAGGTCCTACGCGTATTTAAGGGGCTAAAACAAGTACGCCATTTTGGTCTTGGCGTGAC
 D2→

A I P Q G Q S A H D T F W D Y V S L Q P (247)
 GGCAATTCACAAGGGCAAAGTGGCCACGATACTTTCTGGGATTATGTTTCTCTGCAACC 1560
 CCGTTAAGGTGTTCCCGTTTTACGGGTGCTATGAAAGACCCTAATAACAAAGAGACGTTGG

-----GCT-----S234A→

-----GAT-----S234D→

-----AAT-----S234N→

-----ATT-----S234I→

-----TGG-----S234W→

E T L H N V M W A M S D R G I P R S Y R (267)
 TGAAACTCTGCACAACGTGATGTGGGCGATGTCGGATCGCGGCATCCCCCGCAGTTACCG 1620
 ACTTTGAGACGTGTTGCACTACACCCGCTACAGCCTAGCGCCGTAGGGGGCGTCAATGGC

E→

-----TGC-----R260C→

T M E G F G I H T F R L I N A E G K A T (287)
 CACCATGGAAGGCTTCGGTATTCACACCTTCGCGCTGATTAATGCCGAAGGGAAGGCAAC 1680
 GTGGTACCTCCGAAGCCATAAGTGTGGAAGGCGGACTAATTACGGCTTCCCTTCCGTTG
 -----TGC-----I274C→

F V R F H W K P L A G K A S L V W D E A (307)
 GTTTGTACGTTTCCACTGGAAACCACTGGCAGGTAAAGCCTCACTCGTTTGGGATGAAGC 1740
 CAAACATGCAAAGGTGACCTTTGGTGACCGTCCATTTGGAGTGAGCAAACCCTACTTCG

Q K L T G R D P D F H R R E L W E A I E (327)
 ACAAAAACCTCACCGGACGTGACCCGGACTTCCACCGCCGCGAGTTGTGGGAAGCCATTGA 1800
 TGTTTTTGAGTGGCCTGCACTGGGCTGAAGGTGGCGGCGCTCAACACCCTTCGGTAACT

A G D F P E Y E L G F Q L I P E E D E F (347)
 AGCAGGCGATTTTCCGGAATACGAACTGGGCTTCCAGTTGATTCCTGAAGAAGATGAATT 1860
 TCGTCCGCTAAAAGGCCTTATGCTTGACCCGAAGGTCAACTAAGGACTTCTTCTACTTAA

EcoRI

K F D F D L L D P T K L I P E E L V P V (367)
 CAAGTTCGACTTTCGATCTTCTCGATCCAACCAAACCTTATCCCGGAAGAAGTGGTGCCCGT 1920
 GTTCAAGCTGAAGCTAGAAGAGCTAGGTTGGTTTGAATAGGGCCTTCTTGACCACGGGCA

F→

Q R V G K M V L N R N P D N F F A E N E (387)
 TCAGCGTGTCCGGCAAAATGGTGCTCAATCGCAACCCGGATAACTTCTTTGCTGAAAACGA 1980
 AGTCGCACAGCCGTTTTACCACGAGTTAGCGTTGGGCCTATTGAAGAAACGACTTTTGT

Q A A F H P G H I V P G L D F T N D P L (407)
 ACAGGCGGCTTTCCATCCTGGGCATATCGTGCCGGGACTGGACTTCACCAACGATCCGCT 2040
 TGTCCGCCGAAAGGTAGGACCCGTATAGCACGGCCCTGACCTGAAGTGTTGCTAGGCGA

L Q G R L F S Y T D T Q I S R L G G P N (427)
 GTTGCGAGGGACGTTTGTCTCCTATACCGATACACAAATCAGTCGTCTTGGTGGGCCGAA 2100
 CAACGTCCCTGCAAACAAGAGGATATGGCTATGTGTTTAGTCAGCAGAACCACCCGGCTT
 -----TGC-----S421C→

F H E I P I N R P T C P Y H N F Q R D G (447)
 TTTCCATGAGATTCCGATTAACCGTCCGACCTGCCCTTACCATAATTTCCAGCGTGACGG 2160
 AAAGGTACTCTAAGGCTAATTGGCAGGCTGGACGGGAATGGTATTAAGGTGCGACTGCC
 G→ -----GCC-----C438A→

M H R M G I D T N P A N Y E P N S I N D (467)
 CATGCATCGCATGGGGATCGACACTAACCCGGCGAATTACGAACCGAACTCGATTAACGA 2220
 GTACGTAGCGTACCCCTAGCTGTGATTGGGCCGCTTAATGCTTGGCTTGAGCTAATTGCT
SphI

N W P R E T P P G P K R G G F E S Y Q E (487)
 TAACTGGCCGCGCGAAACACCGCCGGGGCCGAAACGCGGCGGTTTTGAATCATACCAGGA 2280
 ATTGACCGGCGCGCTTTGTGGCGGCCCGGCTTTGCGCCGCCAAAACCTTAGTATGGTCCT

R V E G N K V R E R S P S F G E Y Y S H (507)
 GCGCGTGAAGGCAATAAAGTTCGCGAGCGCAGCCATCGTTTGGCGAATATTATCCCA 2340
 CGCGCACCTTCCGTTATTTCAAGCGCTCGCGTCGGGTAGCAAACCGCTTATAATAAGGGT

P R L F W L S Q T P F E Q R H I V D G F (527)
 TCCGCGTCTGTTCTGGCTAAGTCAGACGCCATTTGAGCAGCGCCATATTGTCGATGGTTT 2400
 AGGCGCAGACAAGACCGATTCAAGTCTGCGGTAAACTCGTCGCGGTATAACAGCTACCAAA
 H→

S F E L S K V V R P Y I R E R V V D Q L (547)
 CAGTTTTGAGTTAAGCAAAGTCGTTCCGTCATATTCGTGAGCGCGTTGTTGACCAGCT 2460
 GTCAAAACTCAATTGCTTTTCAGCAAGCAGGCATATAAGCACTCGCGCAACAACCTGGTCTGA
 -----GCT-----E530A→
 -----GAT-----E530D→
 -----ATT-----E530I→
 -----CAG-----E530Q

A H I D L T L A Q A V A K N L G I E L T (567)
 GGCGCATATTGATCTCACTCTGGCCAGGCGGTGGCGAAAAATCTCGGTATCGAACTGAC 2520
 CCGCGTAACTAGAGTGAGACCGGGTCCGCCACCGCTTTTTAGAGCCATAGCTTGACTG

D D Q L N I T P P P D V N G L K K D P S (587)
 TGACGACCAGCTGAATATACCCACCTCCGGACGTCAACGGTCTGAAAAGGATCCATC 2580
 ACTGCTGGTCTGACTTATAGTGGGGTGGAGGCCTGCAGTTGCCAGACTTTTTCTAGGTAG

L S L Y A I P D G D V K G R V V A I L L (607)

CTTAAGTTTGTACGCCATTCCCTGACGGTGATGTGAAAGGTCGCGTGGTAGCGATTTTACT 2640
GAATTCAAACATGCGGTAAGGACTGCCACTACACTTCCAGCGCACCATCGCTAAAATGA
I→

N D E V R S A D L L A I L K A L K A K G (627)
TAATGATGAAGTGAGATCGGCAGACCTTCTGGCCATTCTCAAGGCGCTGAAGGCCAAAGG 2700
ATTACTACTTCACTCTAGCCGTCTGGAAGACCGGTAAGAGTTCGCGGACTTCCGGTTTCC

V H A K L L Y S R M G E V T A D D G T V (647)
CGTTCATGCCAAACTGCTCTACTCCCGAATGGGTGAAGTGACTGCGGATGACGGAACGGT 2760
GCAAGTACGGTTTGACGAGATGAGGGCTTACCCACTTCACTGACGCCTACTGCCAAGCCA

L P I A A T F A G A P S L T V D A V I V (667)
GTTGCCATAGCCGCTACCTTTGCCGGTGACCTTCGCTGACGGTCGATGCGGTCATTGT 2820
CAACGGATATCGGCATGGAACGGCCACGTGGAAGCGACTGCCAGCTACGCCAGTAACA

P C G N I A D I A D N G D A N Y Y L M E (687)
CCCTTGCGGCAATATCGCGGATATCGCTGACAACGGCGATGCCAACTACTACCTGATGGA 2880
GGGAACGCCGTTATAGCGCTATAGCGACTGTTGCCGCTACGGTTGATGATGGACTACCT
----GCC-----C669A→

A Y K H L K P I A L A G D A R K F K A T (707)
AGCCTACAAACACCTTAAACCGATTGCGCTGGCGGGTGACGCGCGCAAGTTTAAAGCAAC 2940
TCGGATGTTTGTGGAATTTGGCTAACGCGACCGCCCACTGCGCGGTTCAAATTTCTGGT
J→

I K I A D Q G E E G I V E A D S A D G S (727)
AATCAAGATCGCTGACCAGGGTGAAGAAGGGATTGTGGAAGCTGACAGCGCTGACGGTAG 3000
TTAGTTCTAGCGACTGGTCCCACTTCTTCCCTAACACCTTCGACTGTCGCGACTGCCATC

F M D E L L T L M A A H R V W S R I P K (747)
TTTTATGGATGAACTGCTAACGCTGATGGCAGCACACCGCGTGTGGTCACGCATTCTTAA 3060
AAAATACCTACTTGACGATTGCGACTACCGTCGTGTGGCGCACACCAAGTGCGTAAGGATT

I D K I P A * (753)
GATTGACAAAATTCCTGCCTGATGGGAGCGCGCAATTGCGCCGCCTCAATGATTTACATA 3120
CTAACTGTTTTAAGGACGGACTACCCTCGCGGTTAACGCGGCGGAGTTACTAAATGTAT

GTGCGCTTTGTTTATGCCGGATGCGCGTGAACGCCTTATCCGGCCTACAAAATGTGCAA 3180
CACGCGAAACAAATACGGCCTACGCGCACTTGCGGAATAGGCCGGATGTTTTGACACGTT

ATTCAATATATTGCAGGAAACACGTAGGCCTGATAAGCGAAGCCATCAGGCAGTTTTGCG 3240
TAAGTTATATAACGTCCTTTGTGCATCCGGACTATTTCGCTTCGGTAGTCCGTCAAACGC

TTTGTGAGCAGTCTCAAGCGGCGGAGTTACGCCGCTTTGTAGGAATTAATCGCCGGAT 3300
AAACAGTCGTGAGAGTTCGCCGCGTCAATGCGGCGGAAACATCCTTAATTAGCGGCCTA

GCAAGGTTACGCGGATCTGGCAAACATCCTCACTTACACATCCCGATAACTCCCCAACCC 3360
CGTTCCAAGTGC GGCTAGACCGTTTGTAGGAGTGAATGTGTAGGGCTATTGAGGGGTTGG

GATAACCACGCTGAGCGATAGCACCTTTCAACGACGCTGATGTCAACACATCCAGCTCCG 3420
CTATTGGTGC GACTCGCTATCGTGGAAAGTTGCTGCGACTACAGTTGTGTAGGTCGAGGC

TTAAGCGTGGGAAACAGTAAGCACTCTGACGGATAGTATTATCGAT 3466
AATTCGCACCTTTGTCATTTCGTGAGACTGCCTATCATAATAGCTA

visualization of protein in whole cells by SDS-PAGE. Variants expressing HP11-like protein were then grown in large scale batches (4 -7 liters) for purification and characterization.

2.5. Purification of HP11 catalase

For whole cell assay used in determination of relative levels of protein expression and catalase activity, plasmid containing cells were grown in 30 ml of LB medium in 125 ml shaker flasks at 37°C and 28°C for 16-20 hrs. Whole cell cultures were used for enzyme assay and protein visualization was carried out by electrophoresis on sodium dodecyl sulfate polyacrylamide gels (SDS-PAGE).

For large scale preparations, UM255 cells over expressing the desired protein from the appropriate plasmid borne gene were grown in 4-6 liters of LB medium, in 2 liter shake flasks (500 ml LB per flask) supplemented with 100 µg/ml ampicillin for 20-22 hrs at 28°C or 16-20 hrs at 37°C with good aeration. Isolation of HP11 proteins was done according to Loewen and Switala (1986) with modification.

Cells were harvested from the growth medium by centrifugation and the cell pellet was kept at -60°C overnight. The cell pellet was then resuspended in 150-250 ml of 50 mM potassium phosphate buffer, pH 7.0, containing 5 mM EDTA. The cells were disrupted by passing through a French pressure cell at 20,000 psi. The unbroken cells and debris were removed by centrifugation, and to this crude extract was added streptomycin sulfate to a final concentration of 2.5% (w/v). The resulting precipitates were removed by centrifugation and discarded, solid ammonium sulfate was then added with gentle stirring

to precipitate the desired protein. HP11 and most of its variants were found to precipitate in ammonium sulfate at 50-60% saturation. The pellets from 50 and 60% precipitations were combined together and the mixture was heat treated at 55°C for 15 min and dialyzed against 2 L of 50 mM of potassium phosphate buffer, pH 7.0 (Buffer A) overnight. The dialyzed sample was then centrifuged and loaded on to a 2.5 cm x 23 cm column of DEAE-cellulose A-500 (cellufine, Amicon) equilibrated with buffer A until the OD₂₈₀ of the eluting solution was below 0.05. The protein of interest was then eluted with 0-500 mM NaCl linear gradient in buffer A, usually in a final volume of 1 L, 80 drop fractions were collected throughout and then the appropriate fractions were pooled and concentrated under nitrogen using a protein concentrator (Model 8050, Amicon), using a YM-30 (Amicon) membrane to a volume of 5 ml. The concentrated sample was then dialyzed against 1L of buffer A overnight. The purity of catalase was estimated spectrophotometrically A₄₀₇/A₂₈₀ ratio (heme/protein) and by SDS-PAGE. If the ratio was found to be below 0.8, the protein was loaded on to a 2.5 cm x 15 cm hydroxyapatite column (Bio-Rad) equilibrated with buffer A. Protein was eluted with 50-400 mM potassium phosphate buffer, pH 7.0, from the column using 50 drop fractions throughout. Selected fractions were then pooled and concentrated as before. If the purity of the protein recovered from this HTP column still fell below 0.8, the protein was dialyzed in 100 volumes of 50 mM Tris, pH 7.0 (buffer C), overnight. Approximately, 5 mg of the above protein was loaded for a single run on a Superose-12 column (Pharmacia) equilibrated with 50 mM Tris, pH 7.0, 0.1 M NaCl (buffer D) and mounted on an FPLC (Bio-Rad). The protein was eluted using an isocratic flow of buffer D at a rate of 0.2 ml/min. Additional runs were done and eluted fractions from each run were pooled and

concentrated as before. The purified protein, as determined from its heme/protein ratio and visualized on a SDS-PAGE, was dialyzed against buffer A or buffer C, overnight. Dialyzed samples were stored frozen in small aliquots of 0.5-1 ml volumes at -60°C.

2.6. Polyacrylamide gel electrophoresis

Denaturing SDS-PAGE was carried out according to Weber *et al.* (1972).

Polyacrylamide gels were cast as vertical slabs of dimensions 10 cm x 10 cm and 0.5 mm thickness (mini gels) and consisted of 4% stacking and 8% separating gels. Samples loaded usually contained about 10-20 µg protein for crude extracts or 2-4 µg of purified protein. Protein samples were mixed with an equal volume of sample buffer (3.4 mg/ml NaH₂PO₄, 10.2 mg/ml Na₂HPO₄, 10 mg/ml SDS, 1.28 M 2-mercaptoethanol, 0.36 g/ml urea and 0.15% bromophenol blue) and boiled for 3 min before loading. Samples were run at 150 V constant voltage in a BIO-RAD Mini-Protean II electrophoresis system, using a running buffer containing 14 g glycine, 3 g Tris base, and 1 g SDS per liter. Gels were stained for 1 hr in staining solution containing 0.5 g/L Coomassie Brilliant Blue R-250, 30% ethanol and 10% acetic acid and destained with repeated changes of destaining solution containing 15% methanol and 7% acetic acid, until the background was clear. Gels were soaked in a final destaining solution of 7% acetic acid and 1% glycerol, for a few minutes. Gels were then mounted on a 3 mm Whatman paper, covered with a clear plastic film and dried at 80°C for 1 hr on a slant gel dryer under vacuum (Savant).

Non-denaturing PAGE was carried out according to Davis (1964) with minor modifications. Gels were cast as described for SDS-PAGE, but without the SDS component in the mixtures. In order to visualize enzyme activity, samples

corresponding to 1 unit of catalase activity were loaded. Samples were mixed with equal volumes of 2x sample buffer containing 10% (w/v) glycerol and 0.15% bromophenol blue and were loaded without boiling. The running buffer for non-denaturing PAGE contained 14 g glycine, 3 g Tris base per liter. The method of Hedrick and Smith (Hedrick and Smith, 1968) was used to determine the non-denatured molecular weights of the truncated variants of HPII on different acrylamide gel concentrations of 7, 8 and 9%. Electrophoresis conditions were same as described for SDS-PAGE.

Gels were stained for catalase activity according to the method of Clare *et al.*, (1984) with minor modifications. Gels were soaked in a solution of 50 $\mu\text{g/ml}$ horseradish peroxidase (Sigma) in 50 mM potassium phosphate, pH 7.0 for 45 min, then briefly rinsed with water, incubated in 20 mM H_2O_2 for 10 min, and finally soaked in a solution of 40 mg 3, 3'- diaminobenzidine (DAB) in 80 ml water containing 1ml glycerol. Catalase activity was visualized as zones of clearing on a brown background. Color development was usually complete within 30-60 min.

2.7. Catalase assay and protein quantitation

Catalase activity was determined by the method of Rørth and Jensen (1967) in a Gilson oxygraph equipped with a Clark electrode. One unit of catalase is defined as the amount of enzyme that decomposes 1 μmol H_2O_2 in 1 min in 60 mM H_2O_2 at 37°C, pH 7.0, 1.8 ml of 50mM potassium phosphate buffer, pH 7.0 was added to the reactor chamber followed by addition of 50 μl H_2O_2 to a final concentration of 60 mM, incubated for 0.5-1 min, at 37°C, then appropriately diluted enzyme samples or cell cultures were added. Catalase activity as units/ml was determined from the slope of the plot

representing oxygen evolution. Specific catalase activity was expressed as units/ml per mg purified protein or units/ml per mg dry cell weight. Protein concentration (mg/ml) was estimated spectrophotometrically based on A_{280}/A_{260} ratios (Layne, 1957). Specific activities were always determined as the average of a minimum of two or more individual determinations.

2.8. Absorption spectrophotometry

Absorption spectra were performed on a Pharmacia Ultrospec 4000 or a Milton Roy MR3000 spectrophotometer. Spectra were obtained at ambient temperature in 1 ml quartz, semi micro cuvettes. Protein samples were in 50 mM potassium phosphate buffer, pH 7.0 or 50 mM Tris pH 7.0; the same buffer was used as a reference. Data was then transferred to Sigma Plot computer software for preparation of spectra.

2.9. Hemochromogen characterization

Heme extraction and characterization were carried out according to Loewen *et al.* (1993). 50 μ l of protein sample (~1 mg) is treated with 1 ml acetone-HCl (10 ml acetone, 13 μ l concentrated HCl) for 1 min at room temperature. The sample was centrifuged and supernatant was transferred to a fresh tube and neutralized by adding 8 μ l 1M Na_2CO_3 , mixed and centrifuged. The supernatant was lyophilized in a speed vacuum (Savant). Lyophilized samples were stored at -20°C until ready for use. For HPLC analysis, samples were redissolved in 50 μ l of Buffer B (containing 48% methanol, 48% acetonitrile and 4% acetic acid), then 50 μ l of HPLC grade water was added, mixed, centrifuged and supernatant transferred into the tubes made for automatic sample

injection (Waters Corporation, MA, USA). Samples were loaded on a 4.6 x 250 mm column packed with Whatman 5 μ M ODS-3 (C18 coated, Altech HPLC column) and eluted with a gradient of 24: 24: 4: 48 to 48: 48: 4: 0 methanol / acetonitrile / acetic acid / water in a Waters HPLC system with detection at 390 nm. For preparation of elution profiles, data collected were transferred to Sigma Plot computer software.

2.10. Effect of inhibitors

The effects of NaCN and NaN₃ on the catalase activity of the truncated variants of HPII were studied. In the case of activity assays various concentrations of NaCN and NaN₃ were incubated with the enzyme for 1 min in the reaction chamber, prior to initiation of the reaction by addition of H₂O₂ into the reaction cell. The cysteine variants were subjected to inhibition studies by the thiol reagent, β -mercaptoethanol (MSH). For this assay the variants were incubated with the MSH at 37°C for various time intervals before assay. The concentration of MSH in the reaction chamber for all assays was kept constant at 5 mM. To test the reversibility of inhibition, the variants that were incubated for various time intervals and then dialyzed against 1 liter of 50 mM potassium phosphate buffer, pH 7.0, with two changes of the dialysis buffer every 3 hrs, before re-assaying.

2.11. Determination of sulfhydryl groups

The number of sulfhydryl groups in HPII catalase was determined spectrophotometrically using 5, 5'- dithiobis - (2-nitrobenzic acid) [DTNB] (Ellman, 1959). Sulfhydryl groups as non-denatured protein were quantitated using 5-10 mM protein in 1 ml of 50 mM potassium phosphate, pH 8.0 to which was added 20 ml of 10

mM DTNB solution. The A_{412} values were determined after 5-10 min at room temperature. The amount of sulfhydryl group was calculated using an extinction coefficient of $13,600 \text{ M}^{-1} \text{ cm}^{-1}$ for DTNB product. The ratio of sulfhydryl groups to subunits was then determined by using a molecular weight of 84,000 per HPII subunit. For determining the sulfhydryl groups on denatured protein (Wardell, 1974), 5-10 mM protein was treated with 20 ml of 0.5N NaOH, incubated at room temperature for 3 hrs and the mixture neutralized with an equal volume of 0.5 N HCl prior to assay.

2.12. Conditions of proteolysis

Limited digestions of HPII, BLC and HPI were performed at 37°C in 50 mM potassium phosphate, pH 7.0, for various times with trypsin, chymotrypsin and proteinase K. The ratio of catalase to protease (w/w) is described for each experiment. Proteolysis was stopped by the addition of phenylmethylsulfonyl fluoride (1 mM).

2.13. Electrospray ionization time-of-flight mass spectrometry (ESI-TOF-MS)

Mass spectrometric analysis of HPII was kindly carried out by Dr. LG Donald. Pure catalase protein was dialyzed into 100 mM ammonium acetate (Aldrich 99.999%) by ultrafiltration in a Centricon 50 (Amicon). To determine the mass of the subunit, an aliquot of protein was denatured by diluting to about $10 \mu\text{M}$ in 2% acetic acid and 50% methanol and analyzed by electrospray ionization with a declustering voltage of 150 V and nitrogen as the curtain gas. To examine the intact complex, a further aliquot of the protein was diluted to $5 \mu\text{M}$ subunit in 100 mM ammonium acetate. After proteolysis, samples were again dialyzed into 100 mM ammonium acetate, using a Centricon 50 to

remove the protease and the phosphate buffer. These samples were diluted in the same manner as the intact protein. For each sample, a new New Objective PicoTip was cut to the required length, rinsed with a small amount of sample, and then loaded with 3 μL of sample. Spectra were acquired with SF₆ as the curtain gas, and the declustering voltage that controls the kinetic energy of the ions in the interface, was varied from 100 to 400 V in order to assess the stability of the complexes.

2.14. Conditions for crystal growth

Crystals of HP11 and its variants were obtained at room temperature (approximately 22°C) by the vapor diffusion hanging drop method, at a protein concentration of 10 to 15 mg/ml over a reservoir containing 10-17% PEG 3350 (Carbowax), 1.2-1.8% LiCl (Fischer) and 0.1M Tris-HCl pH 9.0.

3. RESULTS

3.1. Construction and characterization of the main channel variants between 8 Å and 12 Å

3.1.1. Introduction

In the active center of catalase HPII from *E. coli*, three of the highly conserved residues that are important for catalysis include a histidine (His128) and an asparagine (Asn201), both on the distal side of the heme, and a tyrosine (Tyr415) on the proximal side, all deeply buried within a β -barrel core. HPII is also unique among catalases in having two post-translational modifications in the vicinity of the active center, an oxidized heme, in the form of a *cis* spirolactone, termed heme d (also found in other large subunit catalases (Murshudov *et al.*, 1996)), and a covalent bond between the N^δ of His392 and the C^β of Tyr415, the proximal side fifth ligand of the heme (Bravo *et al.*, 1997). Both modifications are generated self-catalytically by the catalase, and seem to require some degree of catalytic activity (Bravo *et al.*, 1999).

A large number of catalase HPII variants have been constructed, incorporating changes into the catalytic residues, His128 and Asn201, as well as a diverse group of other residues. The properties and structures of these variants have provided much information about the catalytic mechanisms operative in the enzyme, and about the pathways by which substrate and reaction products access and leave the active site cavity. For example, replacement of His128 with any one of a number of residues results in variants with no detectable activity or in variants that are defective in folding, such that no protein accumulates (Loewen *et al.*, 1993). The addition of substrate H₂O₂ to such

variants resulted in significant changes in the solvent matrix in the main channel leading to the active site (oriented perpendicular to the heme) and to the localization of H₂O₂ molecules at three locations in the channel (Melik-Adamyanyan *et al.*, 2001).

The presence of H₂O₂ in the main channel and the relatively direct route provided by the main channel to the heme suggests that it is the primary route for substrate movement to the heme-containing active site. The situation in HPII is complicated by the elongation and possible bifurcation of the main channel caused by the C-terminal domain and by evidence suggesting that a second channel, oriented laterally to the heme, may play a role (Sevinc *et al.*, 1999). These complications notwithstanding, the main or perpendicular channel remains the most likely route for substrate ingress and this is supported by theoretical calculations of solute flow in the enzyme (Kalko *et al.*, 2001; Amara *et al.*, 2001).

The essential histidine is located within 4 Å of the heme on its distal side. Progressing along the main channel away from the heme, there are two other residues that are conserved among all catalases, a valine and an aspartate (Val169 and Asp181 using HPII numbering). Val169 is about 8 Å from the heme in the narrowest section of the channel and D181 is another 4 Å further along the channel. The importance of the valine to enzyme activity was investigated in yeast CATA revealing that replacement with alanine reduced the catalytic activity but increased the peroxidatic activity (Zamocky *et al.*, 1995). This suggested that the dimensions of the channel are important for controlling access of H₂O₂ to the heme pocket. This concept was expanded upon in the study of human catalase, which suggested that it was the length of the hydrophobic region around the valine that selected for preferential H₂O₂ entry (Putnam *et al.*, 2000).

Residues in the channel further from the heme than the valine have not been investigated, so site-directed mutagenesis of the conserved residues D181 and R180 situated, in and around the “Molecular ruler” are done, to determine, whether they play any role in catalysis.

3.1.2. Effects of changes to Val 169 situated 8 Å from heme

A conserved valine is situated in the main channel of all catalases about 8 Å from heme. Its side chain causes a constriction or narrowing of the channel to a diameter of about 3 Å that prevents any molecules much larger than H₂O₂ from gaining access to the active site heme. Changing this valine to alanine in yeast catalase CATA allowed an increase in peroxidatic activity consistent with the concept that valine restricted access to the active site. Counter intuitively, the valine to alanine change in both CATA and HP11 also caused a decrease in catalytic activity, leading to the conclusion that dimensions of the channel were critical in determining the rate of H₂O₂ movement into the active site (Mate *et al.*, 1999). To investigate the effect of larger side chains at this location in HP11, *katE* was mutated to express the variants V169I, V169F and V169W. Purification and characterization of variants V169I and V169F revealed activities that are 10-15% of wild type (Table 3.1.1), even lower than those of the V169A and V169S (Mate *et al.*, 1999). The calculated turnover (k_{cat}/K_m) values of the variant are less than that of the wild type by an order of magnitude (Table 3.1.2) consistent with the larger side chains interfering with substrate access to the active site. The absorption spectra of the variants revealed incomplete heme conversion from heme b to heme d (Fig 3.1.1), which was also confirmed by HPLC analysis of the extracted heme(s) (Fig. 3.1.2). The V169W variant did not accumulate protein, presumably because the larger side chain adversely affected

Table 3.1.1. Catalase activity in crude extracts of cultures of *E.coli* UM255 producing variants of HPII, and specific activity of purified catalase protein.

Variant	Crude extract activity (Units/mg dry cell weight)		Purified enzyme activity (Units/mg)
	28°C ^a	37°C ^a	
Wild type	320 ± 50	440 ± 45	19,100 ± 900
V169I	98 ± 20	170 ± 25	3,730 ± 400
V169F	60 ± 7	75 ± 10	1,470 ± 120
V169W	<0.1	<0.1	ND
R180A*	146 ± 45	90 ± 38	11,200 ± 1,150
R180K*	223 ± 40	68 ± 9	22,700 ± 1,650
D181A	14 ± 5	19 ± 6	810 ± 60
D181S	44 ± 13	98 ± 7	2,550 ± 190
D181E*	300 ± 70	188 ± 10	21,900 ± 700
D181Q*	28 ± 6	20 ± 3	1,770 ± 70
D181N	18 ± 7	57 ± 8	2,800 ± 400
D181I*	12 ± 4	33 ± 8	2,330 ± 350
D181W	<0.1	<0.1	ND
H128N/D181A	<0.1	<0.1	70 ± 20

^a Denotes the temperatures at which the cultures were grown for 16 - 20 hr prior to catalase assay.

* Large scale cultures for these proteins grown at 28°C.

ND Not determined.

Table 3.1.2. Comparison of the calculated and observed kinetic parameters of wild type and HPII variant proteins.

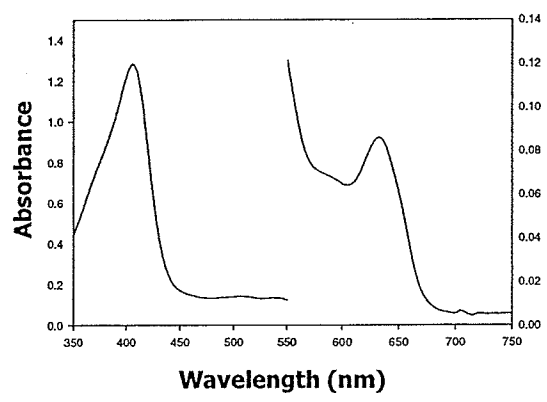
Variant	Observed		Calculated ^a		
	V_{\max}^b	$[\text{H}_2\text{O}_2]@V_{\max}/2, \text{mM}$	V_{\max}^b	$K_m \text{ (mM)}$	$k_{\text{cat}}/K_m \text{ s}^{-1}\text{M}^{-1}$
Wild Type	100,780	221	54,020	47	1.14×10^6
V169I	29,000	576	7,970	51	1.56×10^5
V169F	12,460	370	4,470	81	5.51×10^4
R180A	40,600	85	42,340	88	4.81×10^5
R180K	102,000	98	132,580	157	0.85×10^6
D181A	19,000	1440	5,000	154	3.24×10^4
D181S	25,700	395	7,880	62	1.27×10^5
D181Q	30,700	474	24,810	355	6.98×10^4
D181N	32,000	637	11,910	51	2.33×10^5
D181E	125,000	373	67,820	85	0.80×10^6
D181I	3,100	200	1,478	2	7.39×10^5

^a Calculated for $\text{H}_2\text{O}_2 < 100 \text{ mM}$.

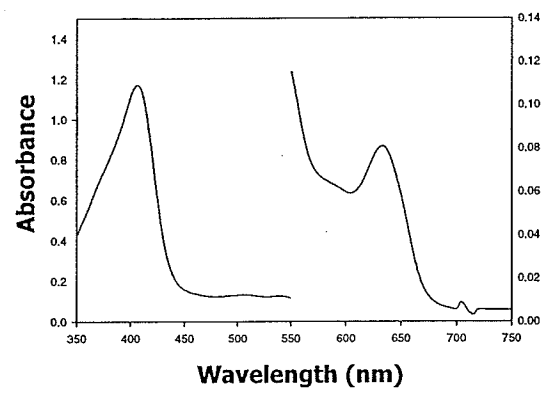
^b Units of V_{\max} are $\mu\text{mol H}_2\text{O}_2 \mu\text{mol heme}^{-1} \text{ s}^{-1}$.

Figure 3.1.1. Absorption spectra of wild type HPII and various variants. The left axis is for the range from 350 to 550nm while the right axis is for the range from 550 to 750 nm.

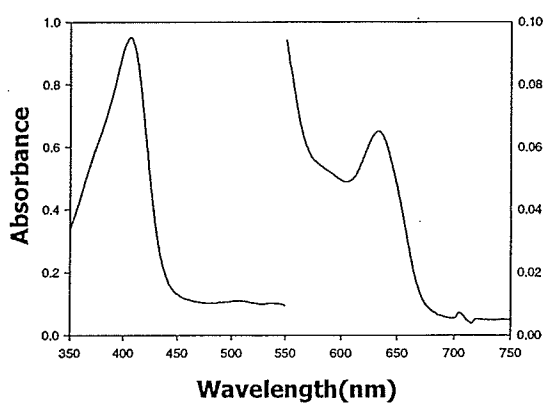
D181A



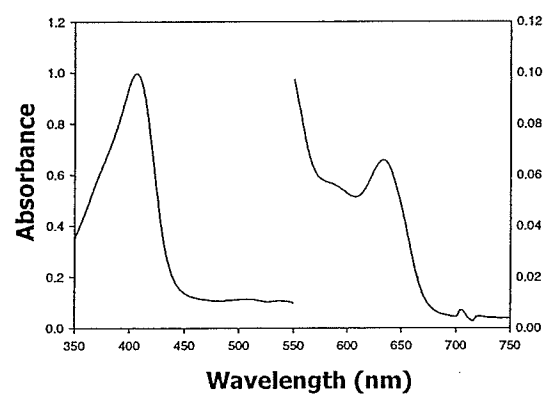
D181S



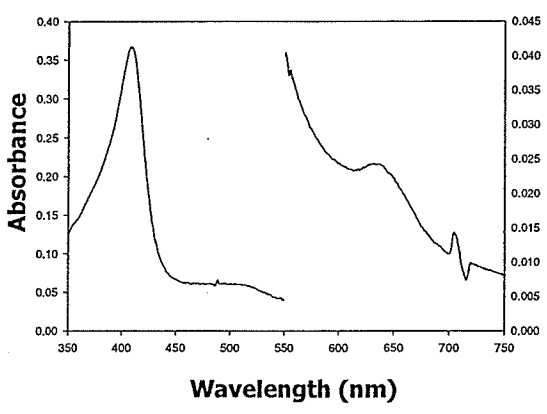
D181Q



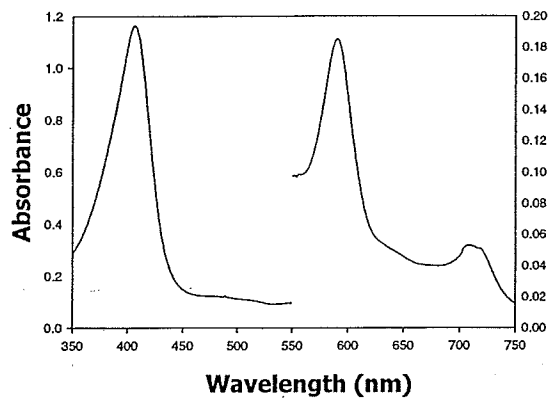
D181N



D181I



D181E



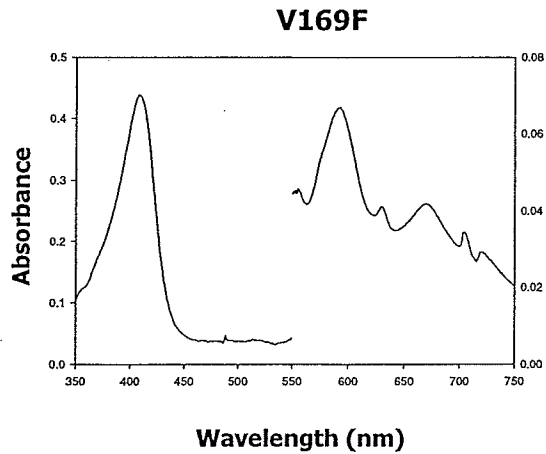
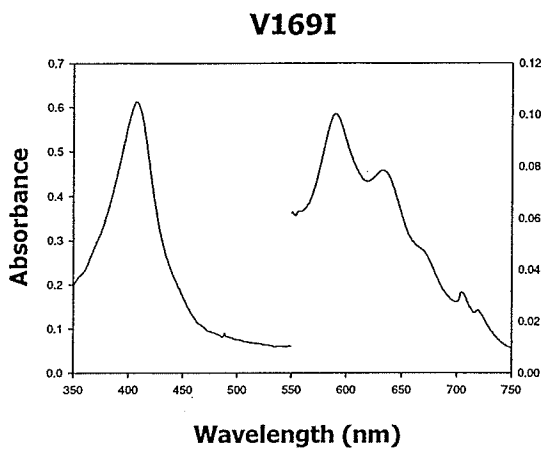
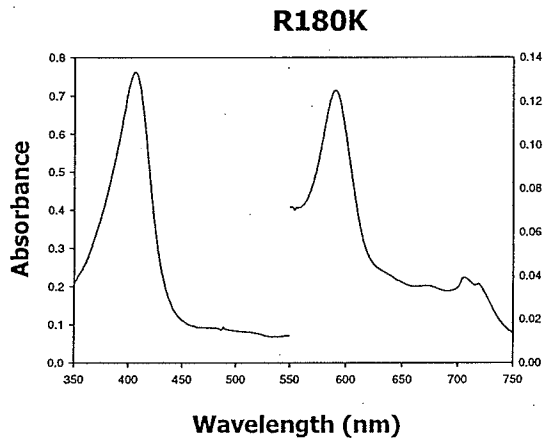
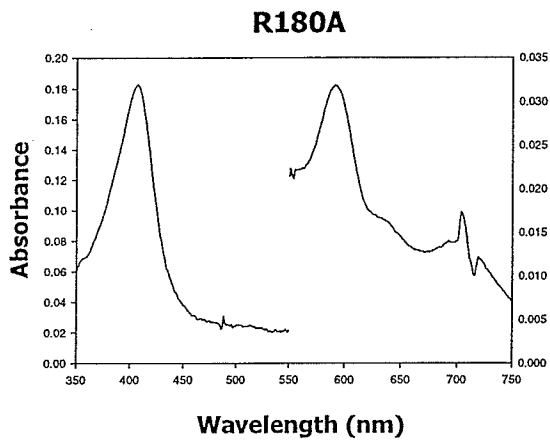
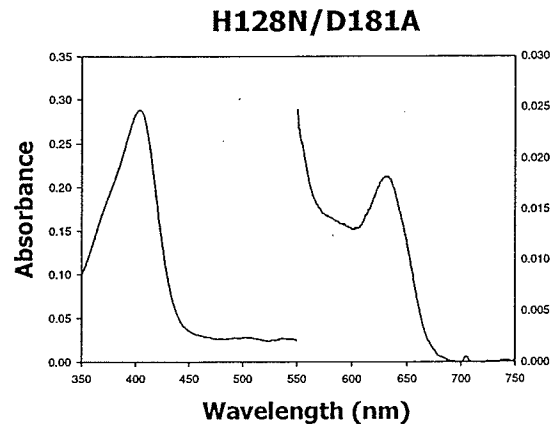
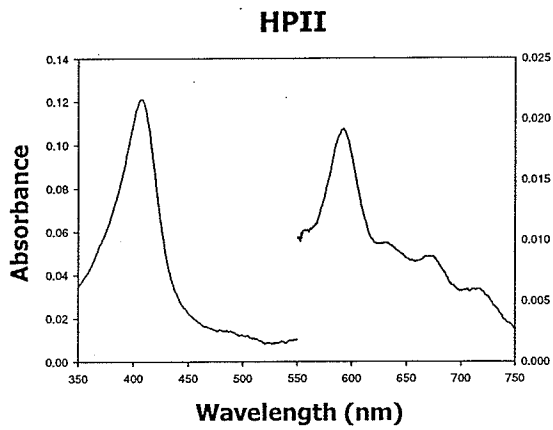
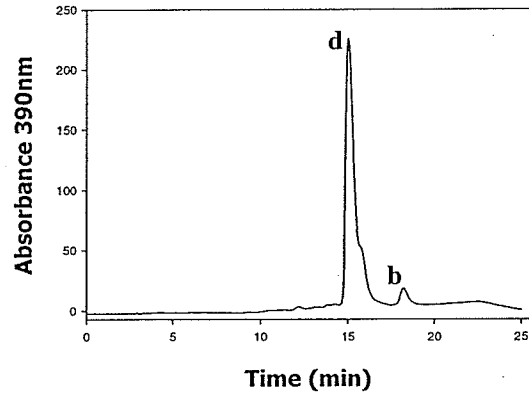
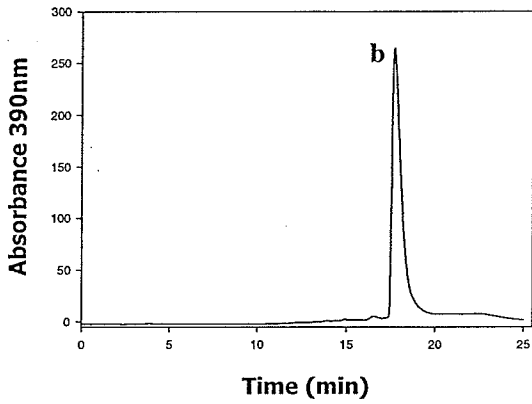


Figure 3.1.2. Elution profiles of heme extracted from HPII (wild type), various variants and bovine liver catalase (BLC) by C18 reverse phase HPLC chromatography. Letters b and d denote heme b and heme d respectively.

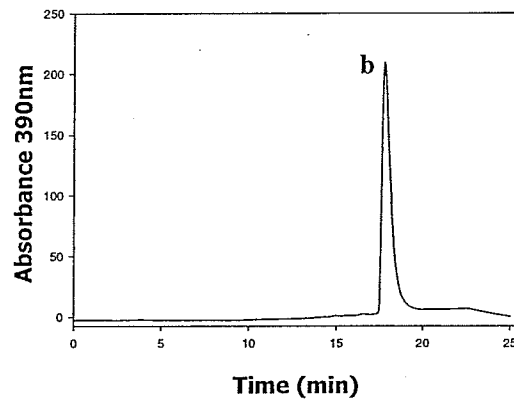
HPII



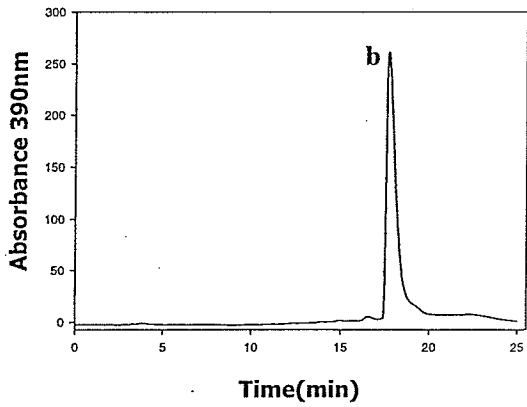
D181A



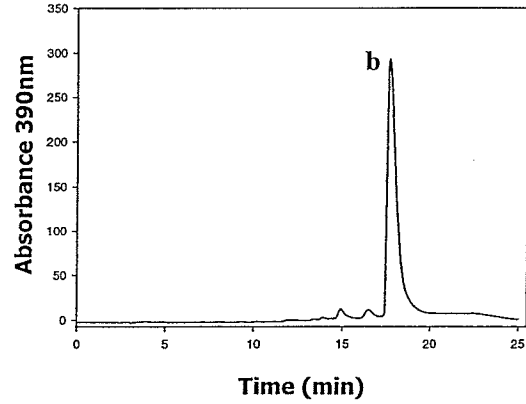
D181S



D181Q



D181N



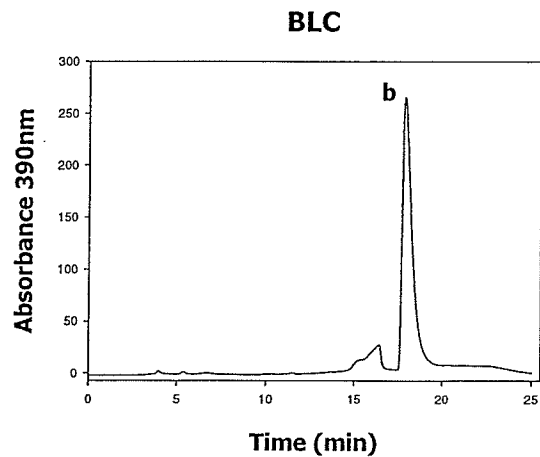
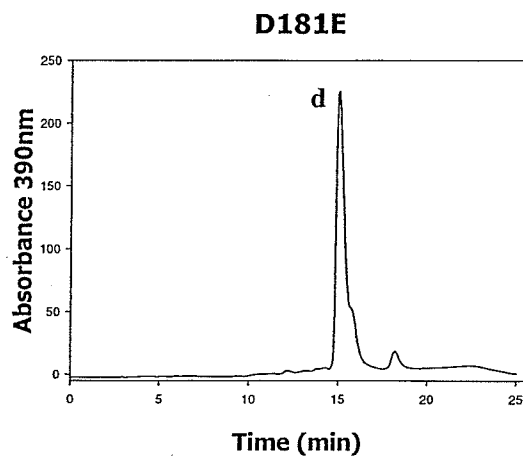
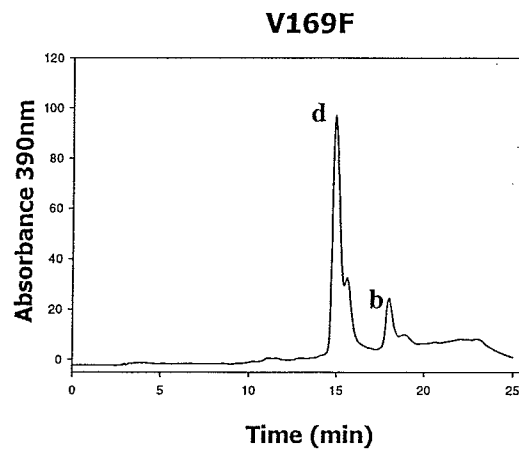
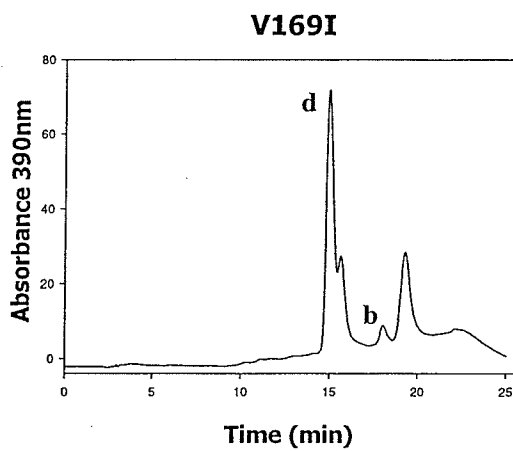
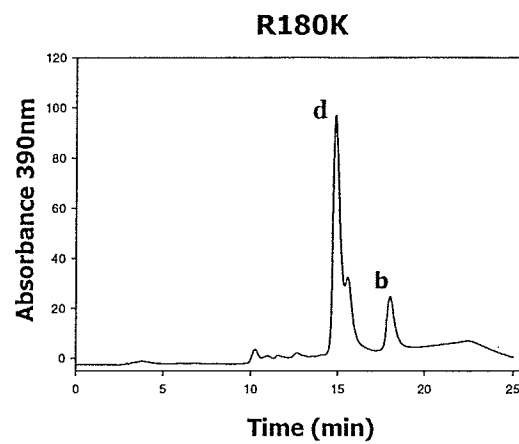
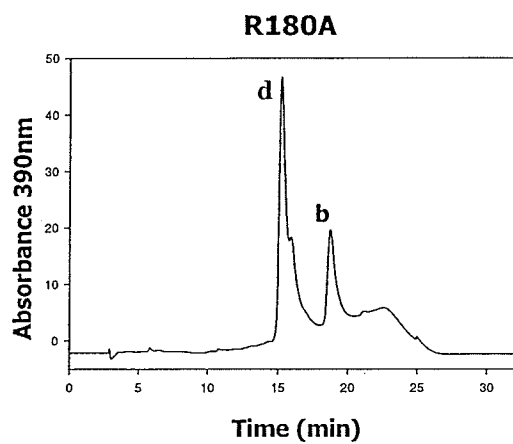
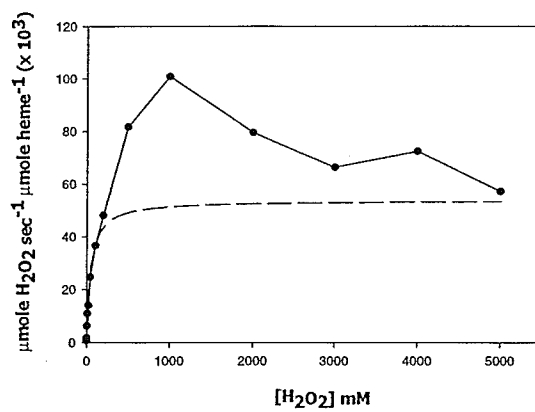
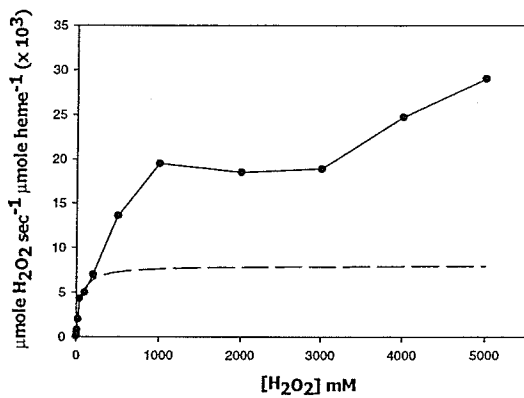


Figure 3.1.3. Effect of H_2O_2 concentration on enzyme velocity of HPII and its variants. In all panels the solid line represents the observed data and the dashed line represents the theoretical Michaelis-Menten curve calculated from constants determined at low H_2O_2 concentration (Table 3.1.2.). Note the differences in the scales of the velocity axis (i.e. y-axis).

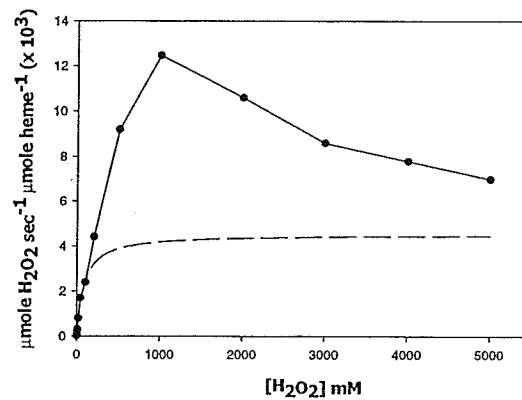
HPII



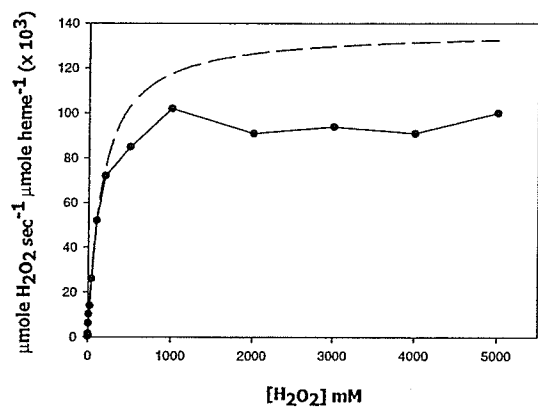
V169I



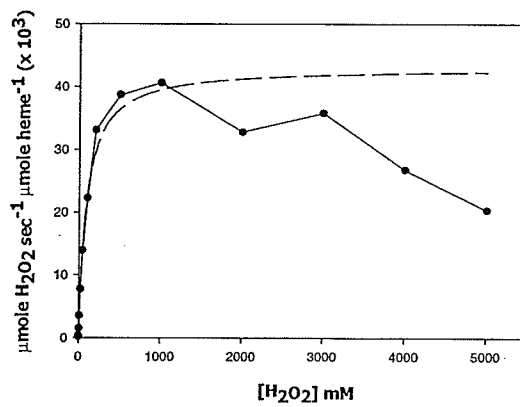
V169F



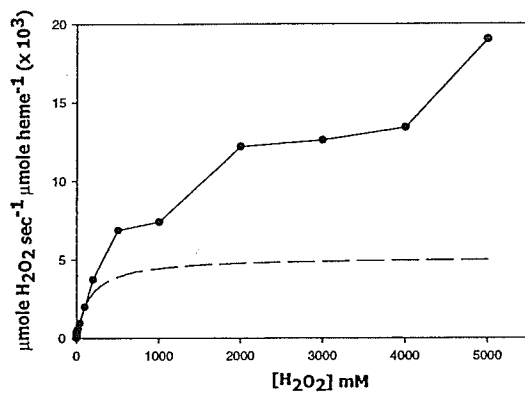
R180K



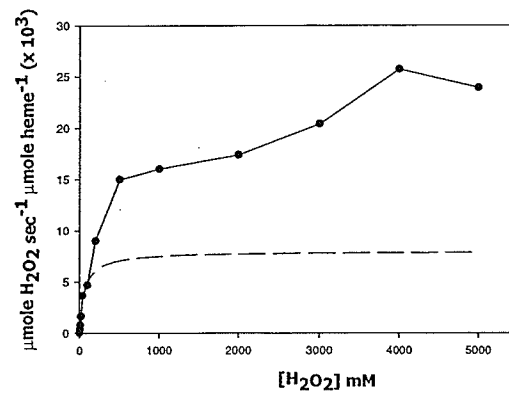
R180A



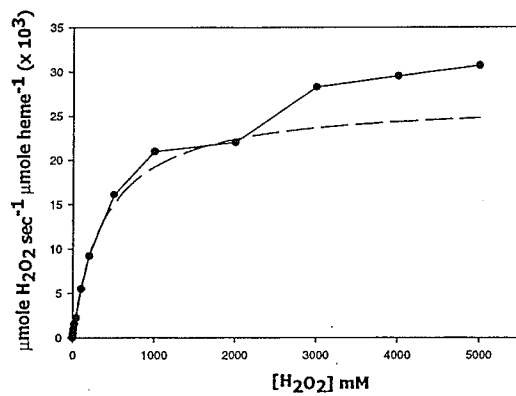
D181A



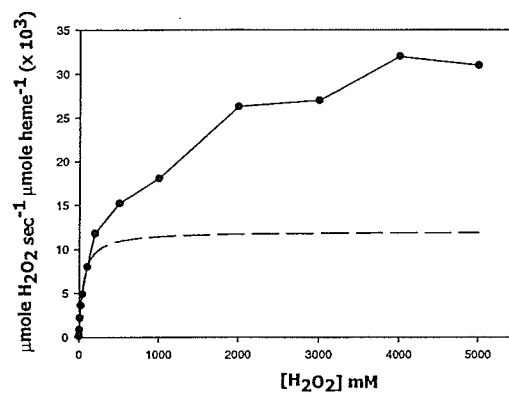
D181S



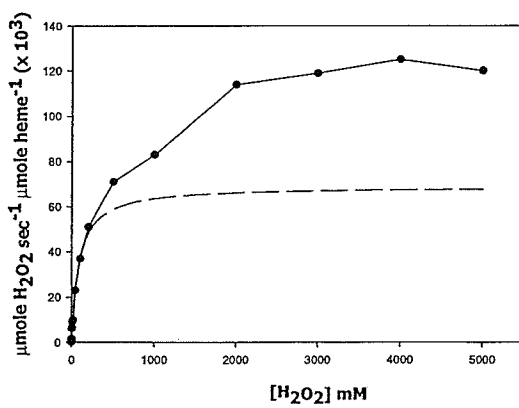
D181Q



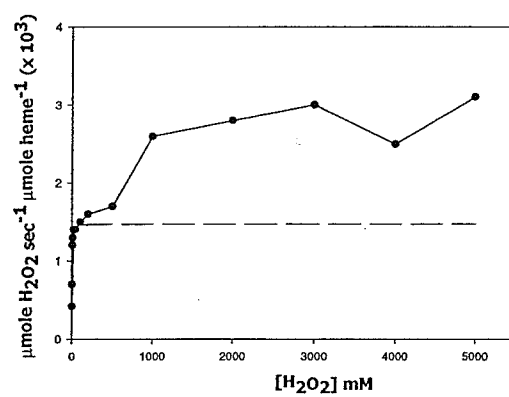
D181N



D181E



D181I



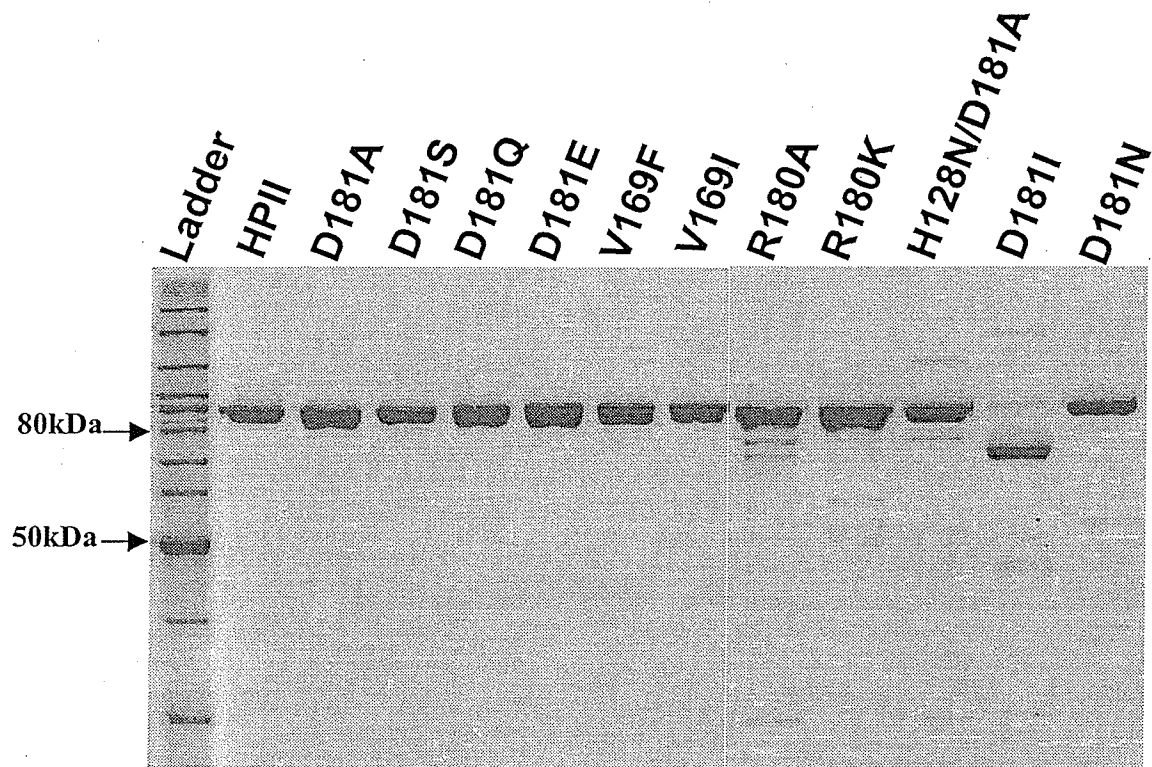


Figure 3.1.4. SDS-polyacrylamide analysis of purified HPII and variant catalases. Approximately 2 μ g of samples were run on an 8% polyacrylamide gel and stained with Coomassie brilliant blue.

protein folding, and the misfolded protein was probably proteolyzed.

3.1.3. Effects of changes to Asp181 situated 12 Å from heme

Proceeding up the channel, Asp181 is present at a distance of ~ 4 Å from the Val169 and 12 Å from the heme prosthetic group. Asp181 is highly conserved in the catalase sequences and is present with its side chain protruding into the channel directly perpendicular to the heme iron. Initial mutagenesis of this residue to alanine resulted in a variant exhibiting less than 5% of wild type activity. In order to investigate further the role of Asp181, an extensive mutagenesis of this residue was carried out (Table 3.1.1, Fig 3.1.4). Variants D181S, D181Q, D181N, D181I exhibited only 10-15% of activity whereas the D181E variant retained wild type levels of activity, suggesting that a negatively charged side chain is essential at this position. Assay of crude extracts showed that no HP11-like protein accumulated for the D181W variant (Table 3.1.1), indicating that protein folding was defective demonstrating the narrowness of the channel in this region. Visible absorption spectra and HPLC profiles of the extracted heme showed that, except for D181E, the D181 variants contained heme b (Figs 3.1.1, 3.1.2). The specific activity, observed V_{\max} and calculated k_{cat} / K_m are very low for these variants, with only the D181E retaining wild type activity and turnover rates (Table 3.1.2, Fig 3.1.3)

3.1.3.1. Crystal structure of D181 variants

In order to understand why a negative charge situated at 12 Å from the active site heme is essential for the enzyme activity, the three-dimensional structures of the D181 variants were determined at 2.2 Å to 1.65 Å resolutions. The starting model was the structure of native HP11, from which the substituted residue and neighboring solvent

molecules were omitted. The refinement data and statistics are summarized in Table 3.1.4.

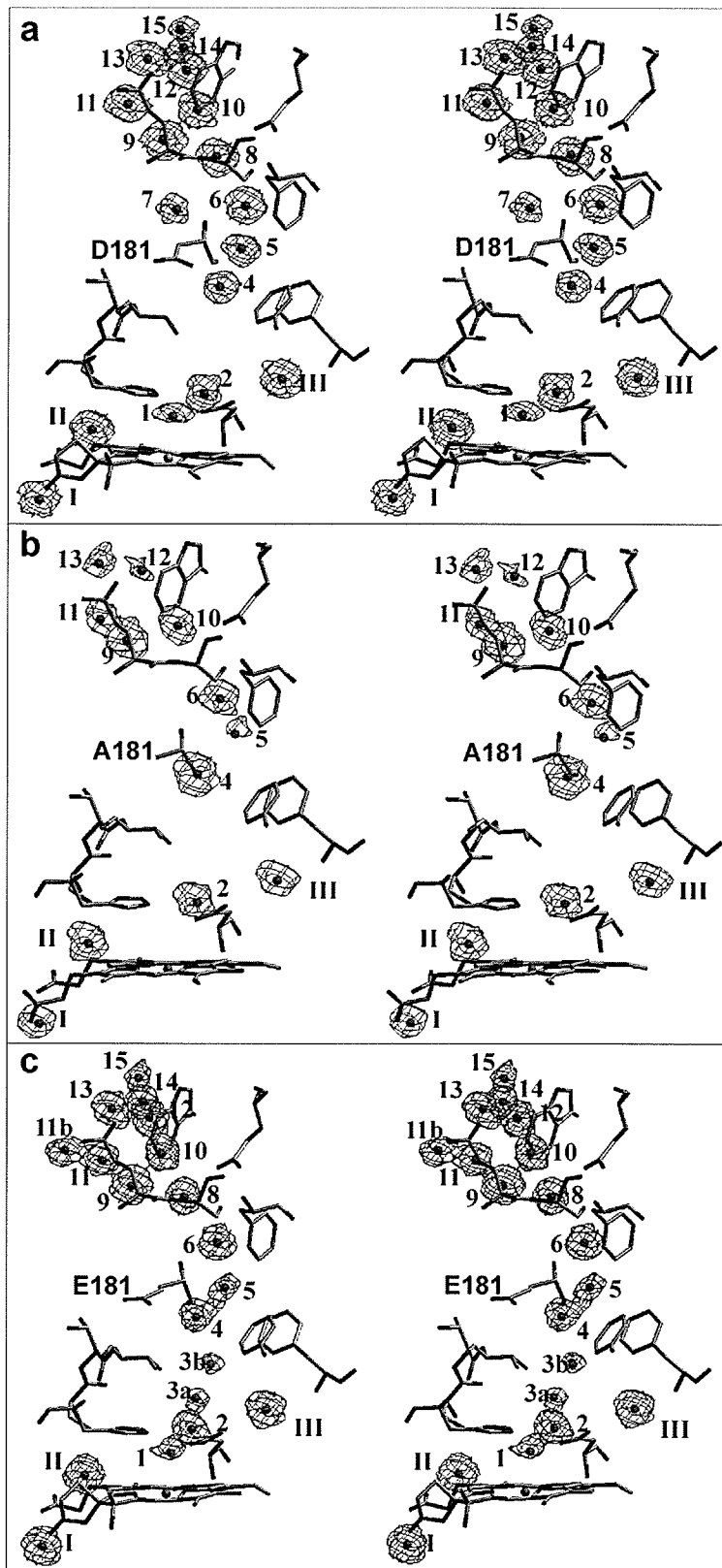
The primary structural change in the D181A, S and Q variants is in solvent occupancy in the perpendicular channel. In native HPII, water 1 at the distal sixth ligand is situated at a distance of about 2.5 Å from heme iron but it is absent in the variants. In addition, the solvent matrix in the upper part of the channel varies among the variants (Fig 3.1.5.B and Table 3.1.3).

D181E retains wild type levels of activity showing that a negatively charged residue is important at this position and the most interesting changes in this variant lie in the vicinity of the Val 169 that forms the most hydrophobic section of the channel (Fig 3.1.5.C) and in the presence of water 1 in all 4 subunits. The side chain of Val 169 is located at the narrowest part of the main channel and only one subunit of wild type HPII has a water (3b) in this region. The variant has two waters 3a and 3b in this hydrophobic section, establishing a continuous chain of hydrogen bonded solvent molecules throughout the entire channel leading to water 1 (Table 3.1.3).

3.1.4. Effect of changes to Arg180

Arg180 is another highly conserved residue in catalases, and even though it is adjacent to Asp181, its side chain is oriented away from the channel and is situated almost 20 Å from the heme. To determine whether the influence of residues in this part of the channel is general or specific, *katE* was mutated to express variants R180A and R180K. Both presented wild type activities and turnover rates (Table 3.1.1 and 3.1.2). HPLC profiles of the extracted heme also showed heme d, indicating that other residues in the vicinity of D181 did not exert as great an influence on catalysis.

Figure 3.1.5. Stereo diagrams of the water distribution in the main channel of native HPII (a), the D181A variant (b), the D181E variant (c), the D181Q variant (d), and the D181S variant (e). The $2F_o-F_c$ electron density corresponding to the individual water molecules is modeled at 1σ and shown as a blue wire mesh. The map for native HPII was derived from PDB submission 1GGE and its associated structure factors. The numbering scheme for the waters is the same as in Table 3.1.3 where the occupancy or B factors for the various waters are listed.



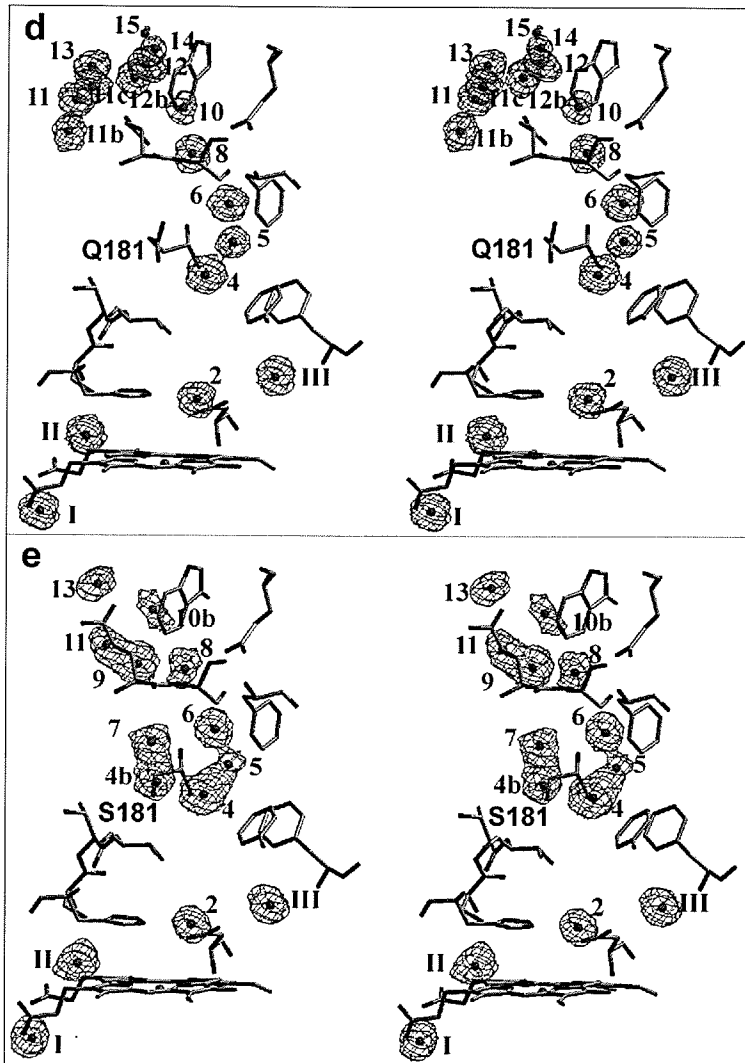


Table 3.1.3. Water occupancy in the main or perpendicular channel of catalase HP11 subunits listed as B-factor (\AA^2). The positions associated with the water numbering are shown in Fig 3.1.5.

Water #	Subunit			
	A	B	C	D
(a) HP11	(1.9 \AA ; IGGE)	Av.B factor;	9.2 (protein);	17.7 (water)
1	40.0	28.1	42.7	-
2	15.3	17.4	16.3	12.9
3	-	-	32.3	-
4	24.0	20.5	22.5	29.9
5	30.7	41.2	29.0	27.9
6	10.7	11.6	14.8	10.4
7	28.0	31.1	33.3	24.1
8	7.7	10.9	18.6	6.6
9	7.1	9.4	12.0	4.7
10	15.3	17.1	14.8	13.4
11	16.7	18.8	23.7	10.9
12	8.8	19.5	14.8	13.8
13	19.3	35.5	-	17.5
14	33.6	31.3	-	25.3
15	30.1	-	30.1	-
I	3.7	7.1	4.8	6.2
II	5.1	6.1	5.0	7.1
III	4.0	8.9	6.4	8.1
(b) D181A	(2.4 \AA)	Av.B factor	26.2(protein)	31.9 (water)
2	16.7	20.0	22.1	21.6
4	6.1	8.1	15.1	11.5
5	44.1	28.8	31.3	31.4
6	25.4	34.3	28.0	32.5
9	21.8	18.5	25.4	20.0
10	37.0	25.0	22.4	39.0
11	43.0	-	-	-
12	48.9	34.1	33.4	35.0
13	39.9	45.8	47.8	44.3
15	-	-	38.0	-
I	19.3	21.2	13.3	13.5
II	17.8	19.9	18.8	12.2
III	15.5	15.5	17.1	17.2

(c) D181E	(1.8 Å)	Av.Bfactor:	16.7(protein)	26.2(water)
1	35.1	43.4	44.2	46.1
2	26.5	23.9	28.4	29.4
3a	44.6	69.6	39.5	43.7
3b	34.0	30.2	32.1	25.4
4	35.0	47.5	42.3	41.7
5	37.8	36.7	37.7	32.7
6	16.0	17.0	20.1	16.5
8	20.7	22.8	37.3	17.4
9	12.6	15.8	18.1	14.9
10	26.6	33.6	28.9	24.1
11	24.8	28.2	33.7	20.4
11b	30.1	35.8	-	-
12	19.2	20.9	21.3	23.7
13	27.5	-	-	30.9
14	36.2	37.4	48.9	28.4
15	34.4	-	48.9	-
I	10.4	10.3	9.7	14.1
II	9.0	11.5	14.0	7.9
III	11.7	13.6	10.7	13.3

(d) D181Q	(1.65 Å)	Av.B factor:	18.8(protein)	31.2 (water)
2	14.1	17.9	18.1	14.6
4	18.0	20.9	24.4	20.6
5	22.8	27.4	27.0	24.9
6	18.1	21.2	18.9	18.2
8	23.5	24.3	27.4	22.3
10	37.1	35.3	39.1	39.6
11	19.4	22.4	21.4	18.7
11b	23.0	-	23.4	22.9
11c	22.9	21.8	25.1	20.2
12	19.6	25.9	24.0	24.5
12b	30.3	22.9	27.4	31.2
13	25.9	26.8	23.5	26.6
14	34.4	-	31.6	-
15	56.2	-	38.6	-
I	13.5	15.3	12.9	11.9
II	11.3	11.5	14.2	13.7
III	14.3	14.2	14.6	13.2

(e) D181S	(2.2 Å)	Av.B factor:	22.5 (protein)	29.6 (water)
2	22.9	18.8	20.6	16.0
4	13.9	14.2	21.3	13.9
4b	25.1	23.2	26.6	25.6
5	39.0	47.5	53.9	54.9
6	25.3	27.2	33.9	19.7
8	33.2	32.2	37.0	32.1
9	16.5	13.7	16.1	-
10b	44.8	40.8	38.4	-
11	34.7	31.3	-	40.1
12	-	-	44.1	37.3
13	43.8	46.8	-	-
14	-	-	44.1	-
I	12.0	13.6	13.8	12.5
II	10.7	16.4	15.5	11.2
III	11.7	10.7	11.5	13.5

Table 3.1.4. Data collection and structural refinement statistics for Asp181 variants of HP11

A. Data collection statistics

	D181A	D181S	D181Q	D181E
Space group	P2 ₁	P2 ₁	P2 ₁	P2 ₁
Cell: a (Å)	93.11	93.34	93.76	93.38
b (Å)	132.50	132.88	133.13	132.86
c (Å)	121.49	121.45	122.50	122.04
β°	109.5	109.4	109.5	109.5
Resolution range (Å)	29.8-2.4(2.49-2.4) ^a	29.8-2.2(2.27-2.2)	29.8-1.65(1.71-1.65)	29.9-1.8 (1.86-1.8)
Unique reflections	105,578 (7,994)	138,759 (11,109)	323,591(23,749)	251,911(20,645)
Completeness (%)	96.9 (93.8)	99.1 (94.6)	95.1 (79.0)	98.7 (93.6)
<I /σ (I)>	10.6 (35.7)	7.7 (21.4)	5.0 (46.5)	7.2 (36.7)
R _{sym} (%) ^b	9			

B. Refinement statistics

Working set	100,246 (7,579)	131,677 (10,519)	307,191 (22,578)	239,324 (19,579)
-------------	-----------------	------------------	------------------	------------------

Free reflections	5,332 (415)	6,965 (590)	16,400 (1,171)	12,587 (1,066)
$R_{\text{cryst}} (\%)^{\circ}$	14.4 (18.7)	15.2 (17.4)	17.4 (23.3)	17.7(23.2)
$R_{\text{free}} (\%)$	22.5 (27.8)	21.6 (25.2)	20.6 (26.7)	21.8 (26.5)
<i>No. of non-hydrogen atoms</i>				
Protein	22,972	22,976	22,988	22,988
Water	2,767	2,733	3,221	3,072
Heme	172	172	172	176
<i>Rmsd from ideality</i>				
Bond lengths (Å)	0.012	0.012	0.008	0.011
Bond lengths (deg.)	2.4	2.0	1.6	1.6
Planarity (Å) (peptide)	0.024	0.023	0.020	0.022
(aromatic)	0.012	0.012	0.007	0.010
Est. coordinate error (Luzzati) (Å)	0.20	0.18	0.17	0.18
<i>Averaged B factor (Å²)</i>				
Main chain	26.2	22.2	18.2	16.3
Side chain	26.2	22.7	19.5	17.1

Water	31.9	29.6	31.2	26.2
-------	------	------	------	------

^a Values in parentheses correspond to the highest resolution shell

$$^b R_{\text{sym}} = \frac{\sum_{hkl} \sum_j |I_{hklj} - \langle I_{hkl} \rangle|}{\sum_{hkl} \langle I_{hkl} \rangle}$$

^c $R_{\text{cryst}} = \frac{\sum ||F_{\text{obs}}| - |F_{\text{calc}}||}{\sum |F_{\text{obs}}|}$. R_{free} is as for R_{cryst} but calculated for a test set comprising reflections not used in refinement (5%).

The double variant H128N/D181A has been constructed to verify whether the negative charge at D181 is essential for the presence of water 1 and for solvent occupancy in the channel compared to the H128N variant (Melik Adamyan *et al.*, 2001), which exhibits high solvent occupancy in this region. Not surprisingly the double variant, was completely inactive (Table 3.1.1).

3.2. Construction and characterization of the main channel variants between 12 Å and 20 Å

3.2.1. Introduction

In catalase HP11, the interaction of subunits along the R axis, specifically the wrapping of the C-terminal domain around the β -barrel core of the adjacent subunit, increases the effective length of the main channel to ~ 50 Å, from 25 Å to 30 Å in small subunit catalases. For example, in *Saccharomyces cerevesiae* catalase, *Proteus mirabilis* catalase and *Pseudomonas syringae* catalase, the channel is ~ 30 Å in length (Mate *et al.*, 1999; Gouet *et al.*, 1995; Carpena *et al.*, 2003), and in human erythrocyte catalase it is ~ 25 Å in length (Putnam *et al.*, 2000). The channel is lined with hydrophilic groups over most of its length except for the final 12 Å leading to the heme where hydrophobic residues predominate (Fita and Rossmann 1985).

The conservation of a relatively narrow and hydrophobic portion of the channel just above the heme, seems to be related to or may actually affect the enzymatic efficiency of catalases. To date most structure-function studies of the main channel have targeted residues in the lower part of the channel, in and around the active site. Further more molecular dynamic calculations have showed the external part of the main channel to be the most flexible part in the protein (Kalko *et al.*, 2001). In order to study the role of residues bordering the channel more distant from the heme, a number of HP11 variants were constructed and characterized.

3.2.2. Effects of changes to Ser234 situated 16 Å from heme

Ser234 is situated about 4 Å above the conserved Asp181 or about 16 Å from the heme. In wild type HPII, the CH₂-OH of Ser234 is hydrogen bonded to waters 6 and 8 (Fig 3.1.5.a), suggesting that it may be important in stabilizing the solvent matrix in this part of the channel. Replacing serine with the non-polar alanine (S234A) decreased activity by 50%, while replacement with polar residues such as Asp or Asn reduced activity only 20-30% compared to wild type (Table 3.2.1). Introduction of the bulkier tryptophan at this position (S234W) resulted in barely detectable levels of activity (Table 3.2.1) and no significant protein band corresponding to catalase on SDS-PAGE gels from crude extract (data not shown). The SDS-PAGE gel of the purified variants is shown in figure 3.2.1. The S234I variant did accumulate protein and showed 20% of wild type activity. The visible absorption spectra of this variant was consistent with the presence of heme b, whereas the other S234 variants all contained heme d (Fig 3.2.2), a fact confirmed by HPLC analysis of the extracted heme(s) (Fig 3.2.3).

The observed kinetic parameters of the S234A, S234D and S234N variants are similar to the wild type, whereas the S234A variant exhibited a lower observed k_{cat} value (Table 3.2.2.). The S234I variant differed in having higher observed and calculated k_m and V_{max} (Fig. 3.2.4.). The initial crystallization scans on the S234I variant are promising with good quality crystals available for X-ray diffraction (Fig. 3.2.5.).

Table 3.2.1. Catalase activity in crude extracts of cultures of *E. coli* UM255 producing variants of HPII, and specific activity of purified catalase protein.

Variant	Crude extract activity (Units/mg dry cell weight)		Purified enzyme activity (Units/mg)
	28°C ^a	37°C ^a	
Wild type	320 ± 50	440 ± 45	19,100 ± 900
S234A	180 ± 15	160 ± 15	10,800 ± 440
S234D*	130 ± 20	40 ± 15	13,750 ± 850
S234I	60 ± 25	100 ± 10	2,810 ± 400
S234N	210 ± 30	160 ± 40	16,000 ± 700
S234W	5 ± 4	10 ± 2	ND
E530A	185 ± 15	245 ± 65	11,290 ± 1200
E530D	145 ± 40	200 ± 50	10,100 ± 880
E530I*	145 ± 10	40 ± 15	6,900 ± 400
E530Q	180 ± 45	240 ± 50	7,420 ± 700

^a Denotes the temperatures at which the cultures were grown for 16 - 20 hr prior to catalase assay.

* Large scale cultures for these proteins grown at 28°C.

ND Not determined.

Table 3.2.2. Comparison of the calculated and observed kinetic parameters of wild type and HPII variant proteins.

Variant	Observed		Calculated ^a		
	V_{\max}^b	$[\text{H}_2\text{O}_2]@V_{\max}/2, \text{mM}$	V_{\max}^b	$K_m \text{ (mM)}$	$k_{\text{cat}}/K_m \text{ s}^{-1}\text{M}^{-1}$
Wild Type	100,780	221	54,020	47	1.14×10^6
S234A	88,800	460	25,560	33	7.74×10^5
S234D	100,500	370	54,620	102	5.35×10^5
S234I	162,700	680	127,333	1,286	9.90×10^4
S234N	84,900	265	45,560	74	6.15×10^5
E530A	182,000	675	90,233	188	4.79×10^5
E530D	71,200	166	43,720	47	0.94×10^6
E530I	96,500	577	33,250	138	2.40×10^5
E530Q	75,000	560	29,733	68	4.37×10^5

^a Calculated for $\text{H}_2\text{O}_2 < 100 \text{ mM}$.

^b Units of V_{\max} are $\mu\text{mol H}_2\text{O}_2 \mu\text{mol heme}^{-1} \text{ s}^{-1}$.

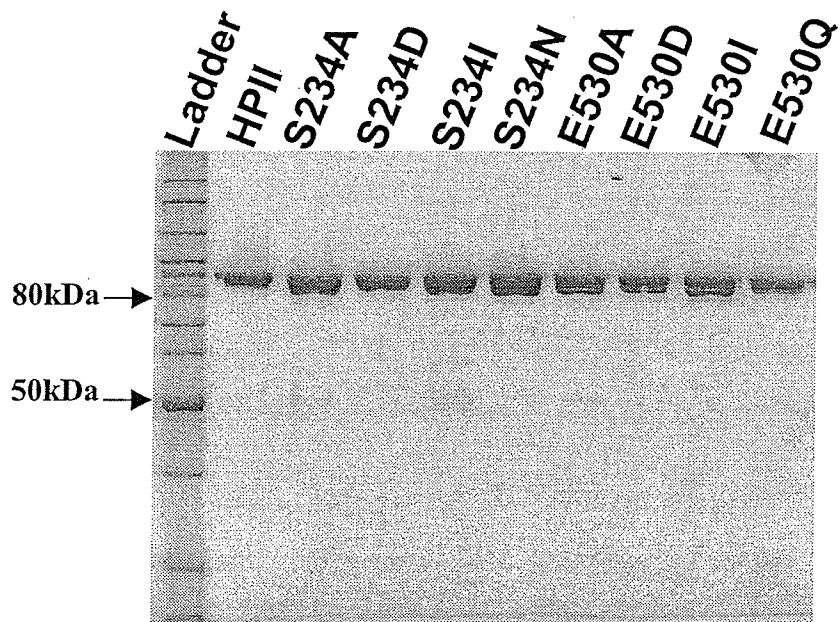
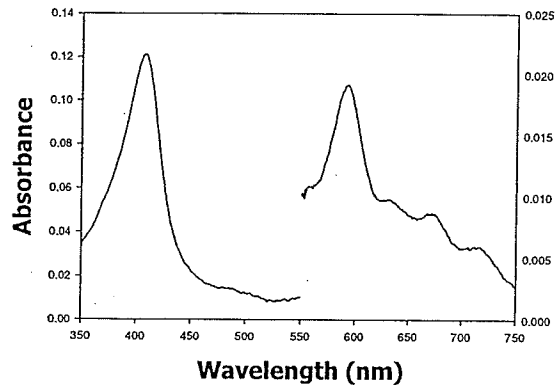


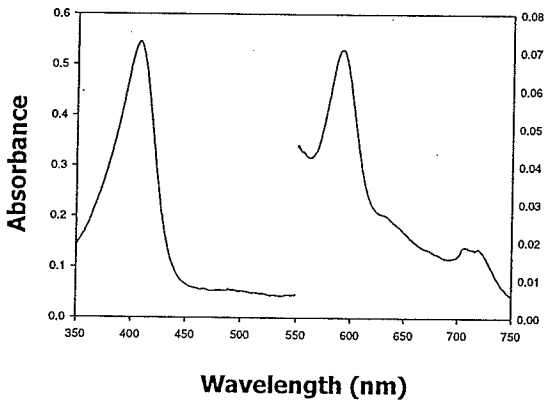
Figure 3.2.1. SDS-polyacrylamide analysis of purified HPII and variant catalases. Approximately 2 μ g of samples were run on an 8% polyacrylamide gel and stained with Coomassie brilliant blue.

Figure 3.2.2. Absorption spectra of wild type HPII and various variants. The left axis is for the range from 350 to 550nm while the right axis is for the range from 550 to 750 nm.

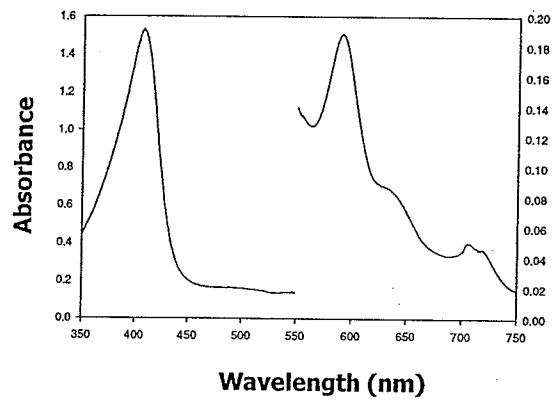
HPII



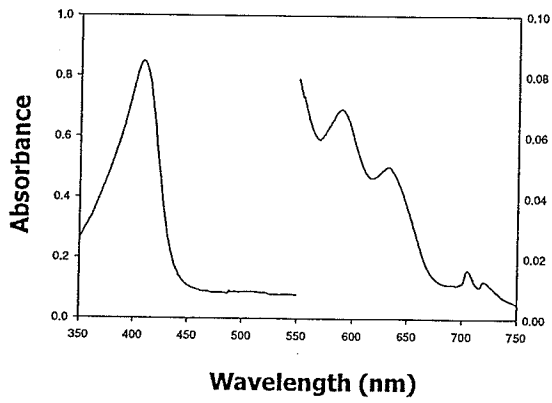
S234A



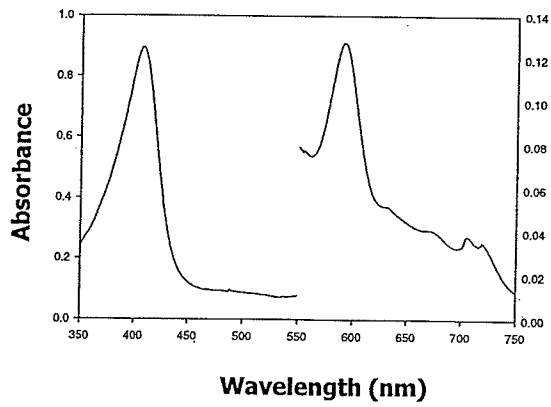
S234D

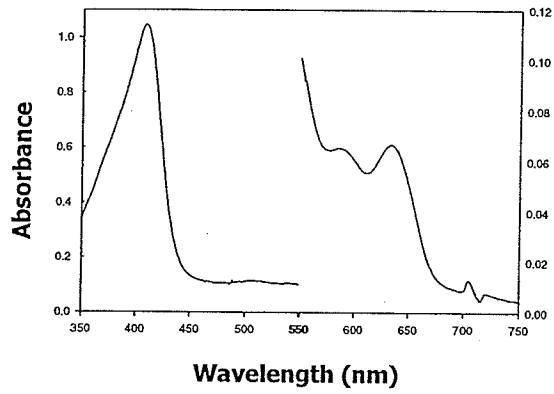
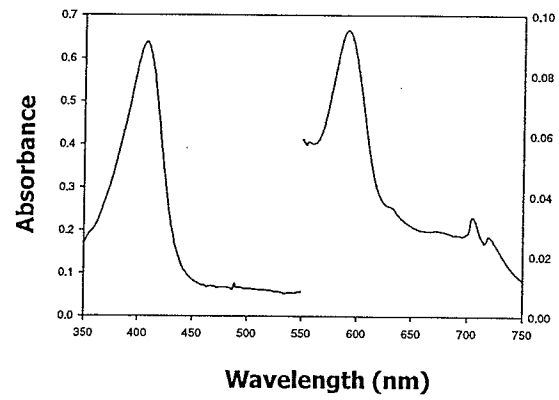
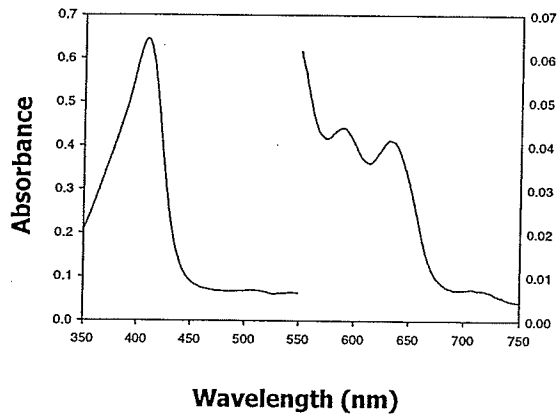
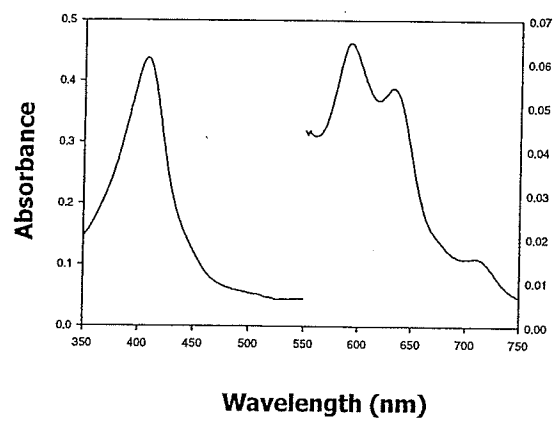


S234I



S234N



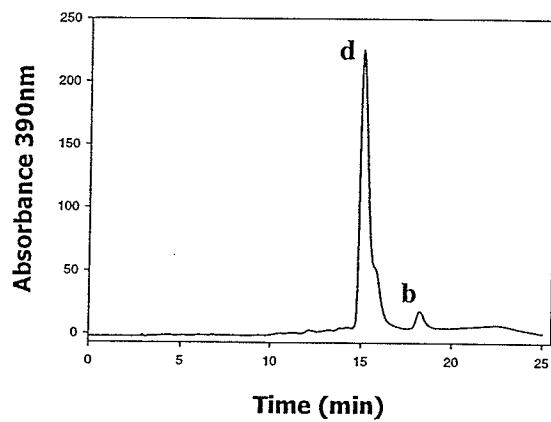
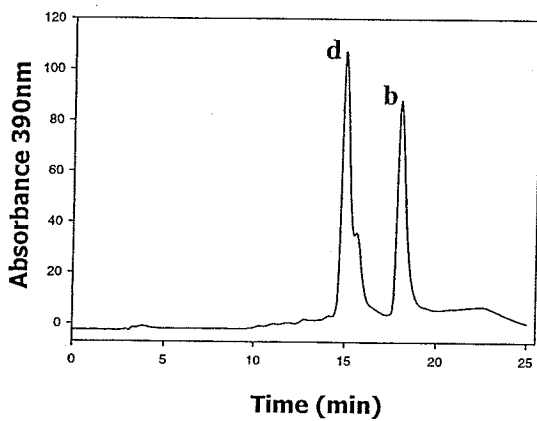
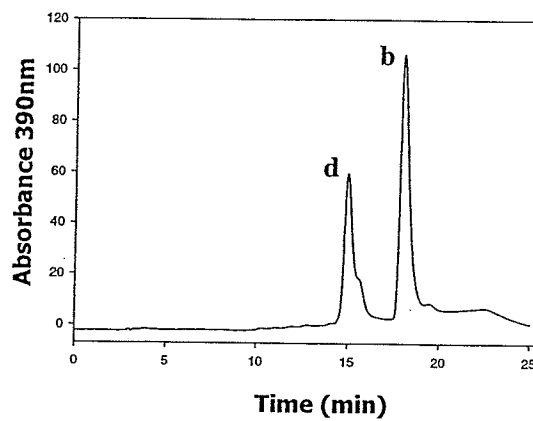
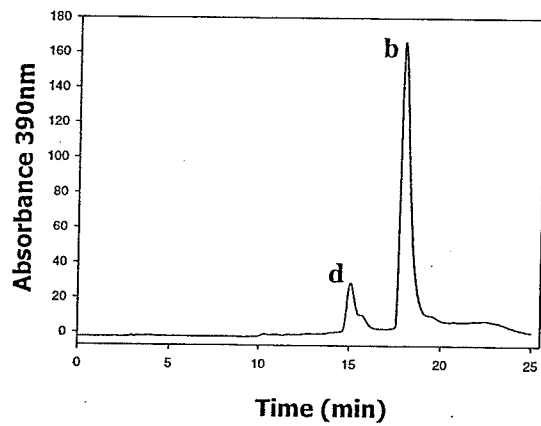
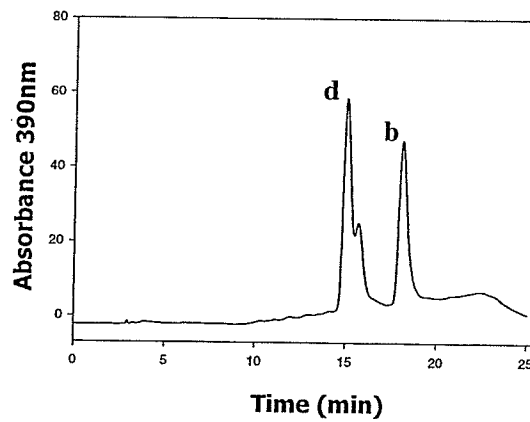
E530A**E530D****E530I****E530Q**

3.2.3. Effect of changes to Glu530 situated 20 Å from heme

In HP11, the side chain of E530 is situated about 4 Å from Ser234 and is hydrogen bonded to waters 8 and 10. The possible importance of this residue was suggested by its interaction with H₂O₂ in the inactive variant H128N (Melik-Adamyian *et al.*, 2001). In fact there is a direct connection between the main channels of the two subunits (A & D related by the molecular R-axis) originating from the E530 (Nicholls *et al.*, 2001). To investigate the role of E530 *katE* was mutated to express E530A, E530D, E530Q and E530I. Purification and characterization of the variants revealed activities that are 40-70% of wild type (Table 3.2.1; Fig. 3.2.1). The kinetic parameters for E530D and E530Q both calculated and observed, were similar to those of the wild type. By contrast the observed and calculated K_m for E530A and E530I were three fold higher than for wild type (Table 3.2.2), while the calculated k_{cat} / K_m value for E530I is lower than the wild type (Fig. 3.2.4).

The heme component of wild type HP11 has been characterized as cis-heme d (Chiu *et al.*, 1989), and the proposal of Timkovich and Bondoc (1990) that heme d arose from hydroxylation of protoheme catalyzed by HP11, was confirmed (Loewen *et al.*, 1993). Poor culture aeration results in HP11 containing predominantly protoheme, presumably because *in situ* H₂O₂ levels are lower. The visible absorption spectra of E530D and E530Q variants revealed predominantly heme d but those of E530A and E530I suggested only partial conversion of protoheme to heme d (Fig. 3.2.2), a fact confirmed by HPLC analysis (Fig. 3.2.3). Since the quantity of protoheme can vary among preparations and the effectiveness of aeration during growth may have determined extent of conversion. Attempts to convert the heme b in variants E530A and E530I to

Figure 3.2.3. Elution profiles of heme extracted from HPII (wild type) and variants analyzed on C18 reverse phase HPLC chromatography. Letters b and d denote heme b and heme d respectively. Samples treated with 100mM ascorbate are labelled as (Ascorbate +).

HPII**S234A****S234D****S234I****S234N**

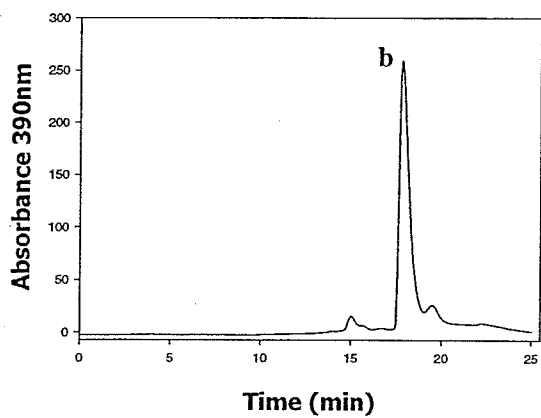
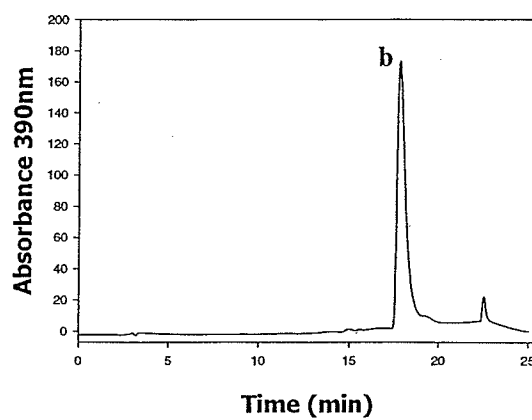
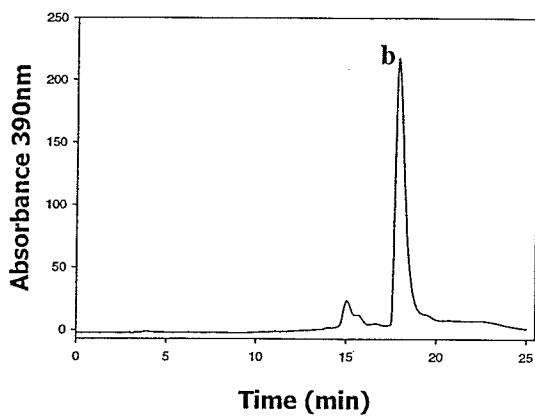
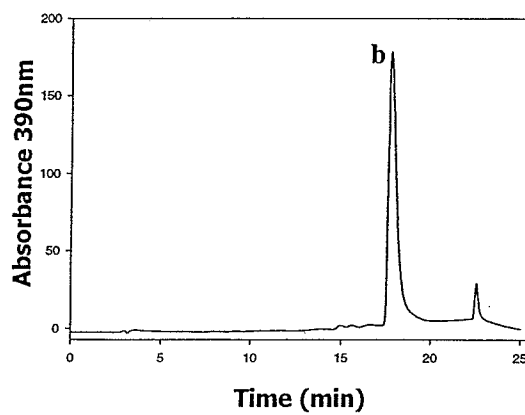
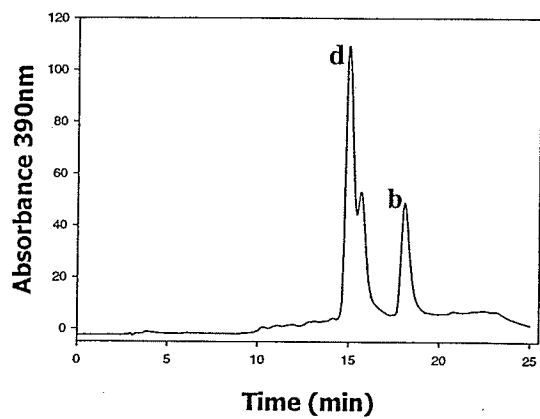
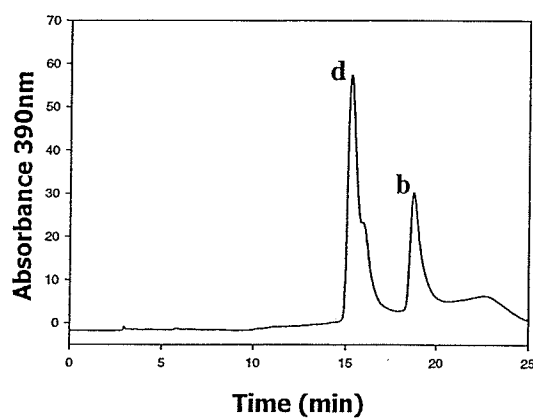
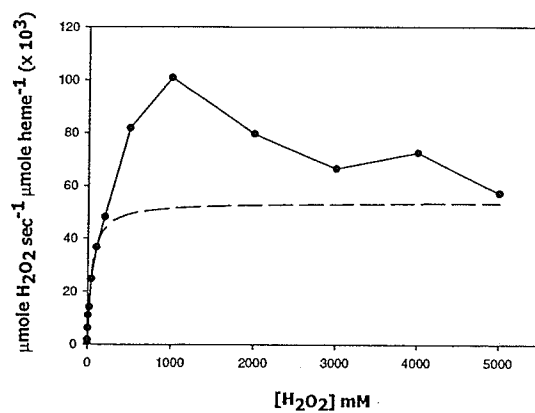
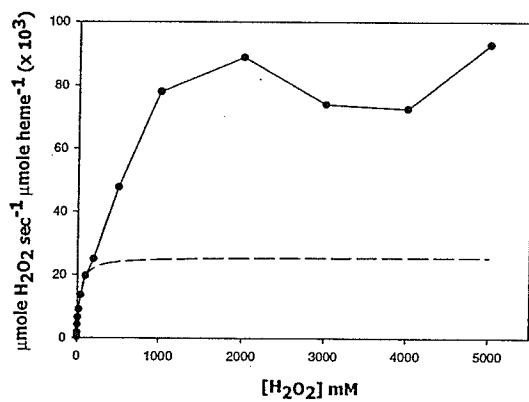
E530A**E530A (Ascorbate +)****E530I****E530I (Ascorbate +)****E530D****E530Q**

Figure 3.2.4. Effect of H_2O_2 concentration on enzyme velocity of HPII and its variants. In all panels the solid line represents the observed data and the dashed line represents the theoretical Michaelis-Menten curve calculated from constants determined at low H_2O_2 concentration (Table 3.1.2). Note the differences in the scales of the velocity axis (i.e. y-axis).

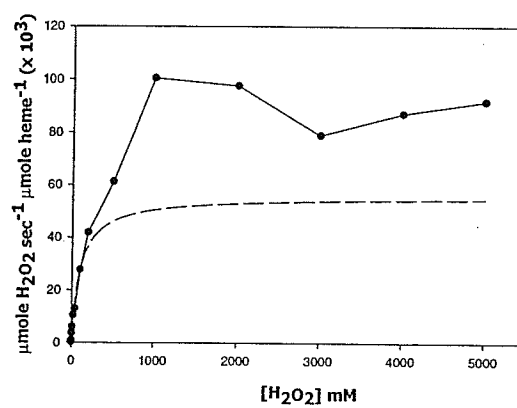
HPII



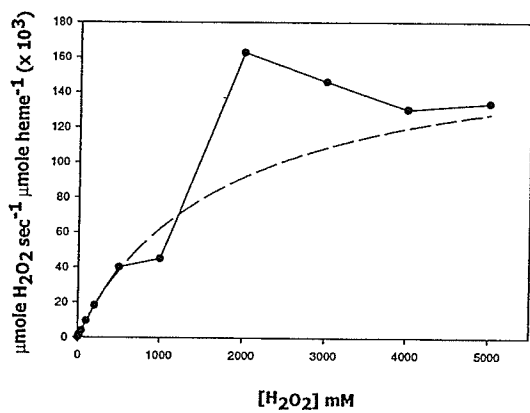
S234A



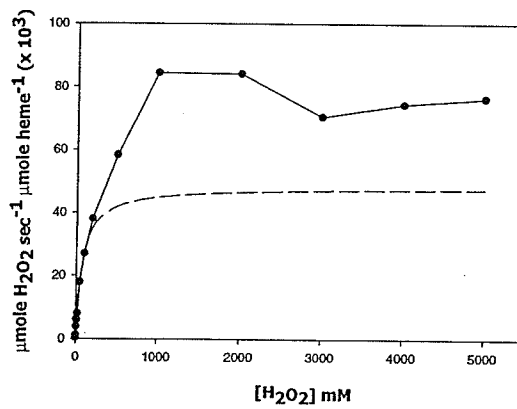
S234D



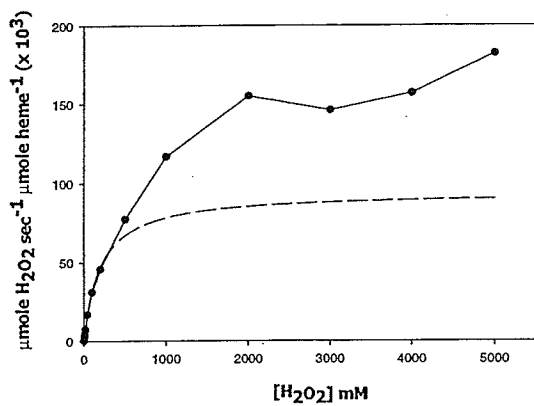
S234I



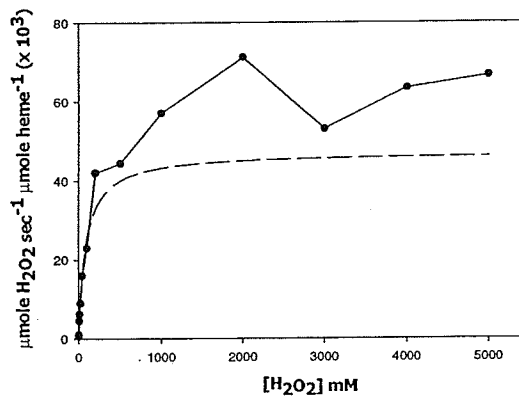
S234N



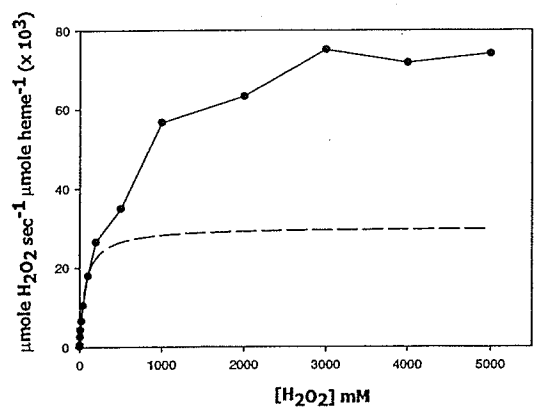
E530A



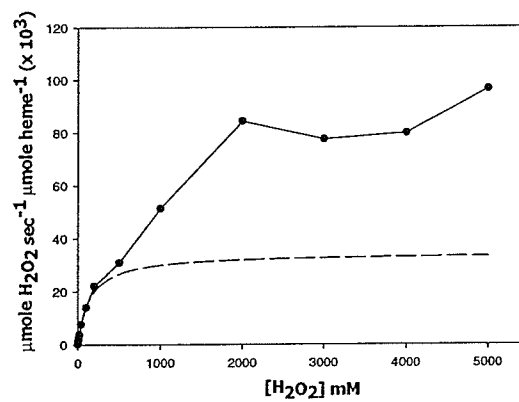
E530D



E530Q



E530I



heme d with ascorbate (100 mM for 60 min at 25°C), the oxidation of which generates low levels of H₂O₂ (Richter and Loewen, 1981) were unsuccessful with HPLC analysis revealing no permanent conversion of the protoheme (Fig. 3.2.3). Promising crystals of E530A and E530D suitable for X-ray diffraction have been obtained to further their characterization (Fig. 3.2.5).

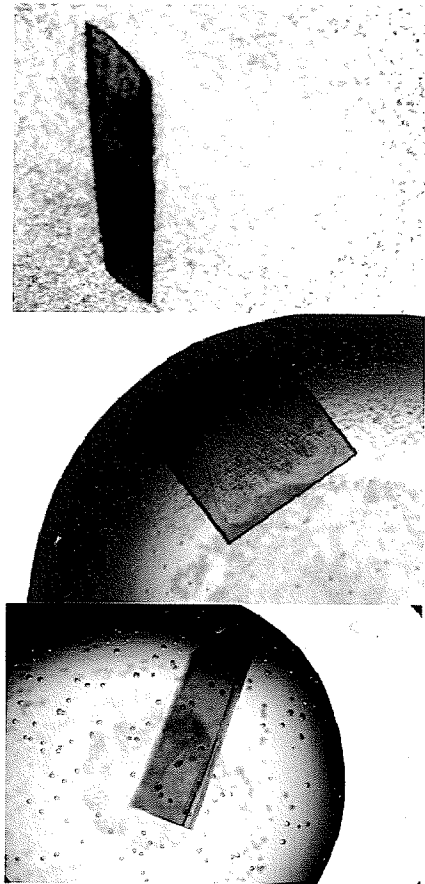


Figure 3.2.5. Crystals of S234I, E530A and E530D variants of HPII.

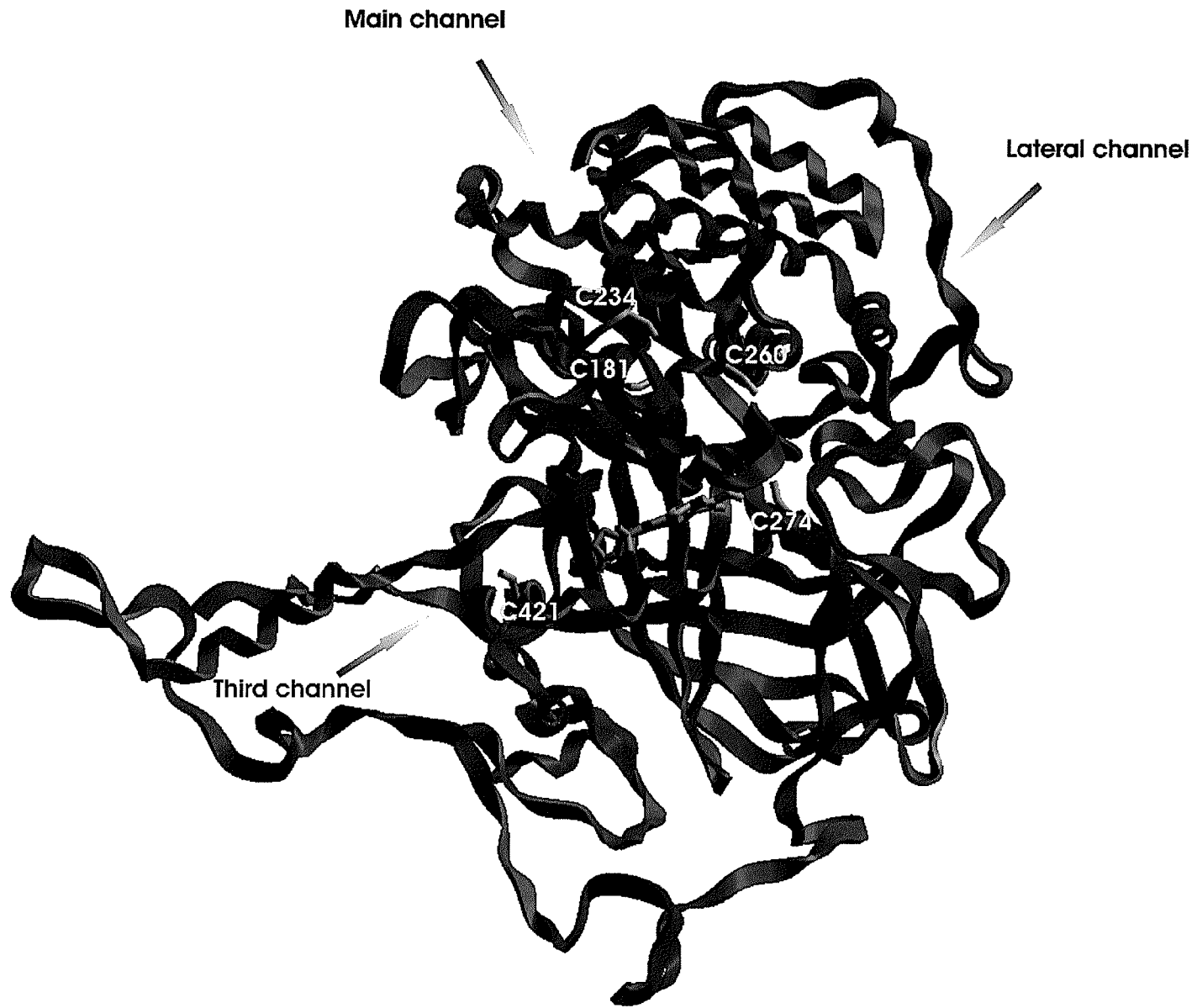
3.3 Construction and characterization of the cysteine variants in the channels of HPII

3.3.1. Introduction

Catalases are one of the most efficient enzymatic systems with turnover rates reaching close to the diffusion limits (Ogura, 1955). The rapid turnover rates require an efficient mechanism to allow H₂O₂ access to, and for the products to be exhausted from, the deeply buried heme containing active site. The existence of more than one channel suggests a directional flow model in which substrate can enter through one channel and products can leave through a second or a third channel. Recent theoretical calculations of solute flow in the enzyme (Kalko *et al.*, 2001; Amara *et al.*, 2001) suggest the main channel to be the primary route for substrate ingress, but do not provide insight about a possible route for substrate exhaust. The importance of channel architecture leading to the active site is illustrated by the 2.5 fold increase in turnover rate in HPII resulting from the single change of Arg260 to Ala located 20 Å from the active site heme in the lateral channel, a possible candidate for the exhaust channel (Sevinc *et al.*, 1999).

Catalases generally have only a small number of cysteine residues. For example, plant catalases have 6-8 Cys/60 kDa subunit, CatF from *Pseudomonas syringae* has no cysteines, and the largest catalase HPII with a subunit size of 84 kDa has only two cysteines (C438 and C669). Only one cysteine, corresponding to Cys438 in HPII, was found to be somewhat conserved (von Ossowski *et al.*, 1994; Klotz *et al.*, 2003), but neither cysteine is in the vicinity of the active site, nor are they important for activity (Sevinc *et al.*, 1994). C438 situated close to the opening of the main channel was

Figure 3.3.1. HPII subunit showing the various cysteine(s). The side chains of C181 and C234 in the main channel; C260 and C274 in the lateral channel; and C421 in the putative third channel are shown in yellow. Arrows represent the entrance of the respective channels. Figure prepared using (SETOR).



found to be modified, but the exact nature of the chemical modification was not determined (Sevinc *et al.*, 1994). In order to elucidate the direction of flow of substrate through the channels in catalase, cysteine mutagenesis of some key channel residues was initiated in HPII (Fig. 3.3.1). To prevent background interference of the native cysteines, the C438A /C669A variant of HPII was used as the starting point. Two cysteines were introduced in the main channel at D181 and S234, two were introduced in the lateral channel at R260 and I274, and one cysteine was introduced in the putative central cavity channel that opens into the center of the molecular tetramer at S241 (Fig. 3.3.1).

3.3.2. Characterization of the cysteine variants

The yields of the variants R260C and S421C were found to be higher at 28°C, while those of D181C, S234C and I274C were higher at 37°C, large-scale cell growth for protein preparations were done at the respective temperature. (Table 3.3.1.). The variant proteins were purified and analyzed by SDS-PAGE, revealing >85% purity for all variants except R260C (Fig 3.3.2). The crude extract activity of R260C variant was only 15% of wild type (Table 3.3.1) which can be attributed to, poor protein accumulation, as determined by SDS-PAGE analysis of the crude extract (data not shown) rather than the enzyme being less active. Attempts to improve protein accumulation by growth at room temperature or under semi-anaerobic conditions were unsuccessful (data not shown). Ultimately, the purity of R260C was improved to ~70%, as indicated by its R_z (A_{407}/A_{280}) value of 0.72 and the specific activity was found to be ~23,000 u/mg, higher than wild type. Interestingly, the R_z value of the other lateral channel cysteine I274C is 0.60, even though SDS-PAGE analysis reveals 85-90% purity (Figure 3.3.2). The calculated and

Table 3.3.1. Catalase activity in crude extracts of cultures of *E. coli* UM255 producing variants of HP11, and specific activity of purified catalase protein.

Variant	Crude extract activity (Units/mg dry cell weight)		Purified enzyme activity (Units/mg)
	28°C ^a	37°C ^a	
Wild type	320 ± 50	440 ± 45	19,100 ± 900
D181C	90 ± 10	110 ± 30	6,070 ± 700
S234C	95 ± 20	145 ± 25	11,090 ± 180
I274C	115 ± 10	110 ± 15	4,560 ± 600
R260C*	40 ± 10	30 ± 10	23,090 ± 1200
S421C*	250 ± 45	210 ± 50	14,900 ± 160
C448A/ C669A	240 ± 30	260 ± 25	14,120 ± 400

^a Denotes the temperatures at which the cultures were grown for 16 - 20 hr prior to catalase assay.

* Large scale cultures for these proteins grown at 28°C.

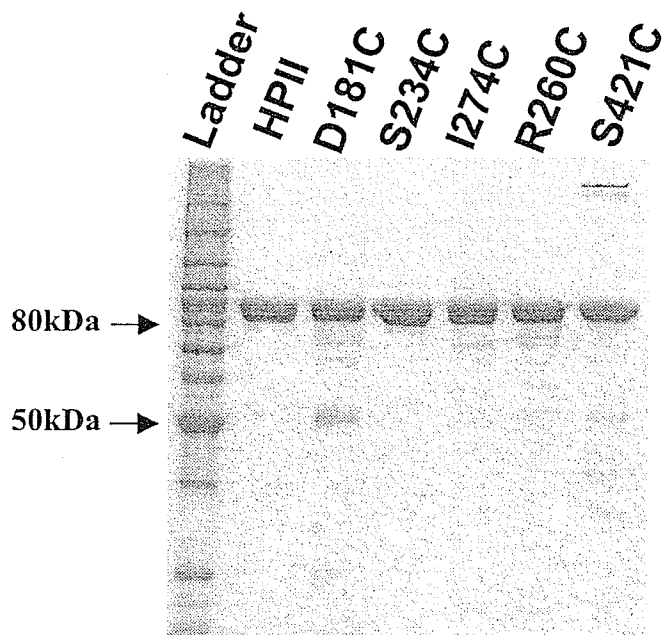


Figure 3.3.2. SDS-polyacrylamide analysis of purified HPII and variant catalases. Approximately 2 μ g of samples were run on an 8% polyacrylamide gel and stained with Coomassie brilliant blue.

Table 3.3.2. Comparison of the calculated and observed kinetic parameters of wild type and HPII variant proteins.

Variant	Observed		Calculated ^a		
	V_{\max}^b	$[\text{H}_2\text{O}_2]@V_{\max}/2, \text{mM}$	V_{\max}^b	$K_m \text{ (mM)}$	$k_{\text{cat}}/K_m \text{ s}^{-1} \text{ M}^{-1}$
Wild Type	100,780	221	54,020	47	1.14×10^6
D181C	37,700	330	21,840	108	2.02×10^5
S234C	52,200	450	27,990	80	3.49×10^5
I274C	9,410	70	8,560	50	1.71×10^5
R260C	314,000	870	47,550	60	0.80×10^6
S421C	50,600	145	37,810	75	5.04×10^5

^a Calculated for $\text{H}_2\text{O}_2 < 100 \text{ mM}$.

^b Units of V_{\max} are $\mu\text{mol H}_2\text{O}_2 \mu\text{mol heme}^{-1} \text{ s}^{-1}$.

Figure 3.3.3. Absorption spectra of wild type HPII and various variants. The left axis is for the range from 350 to 550 nm while the right axis is for the range from 550 to 750 nm.

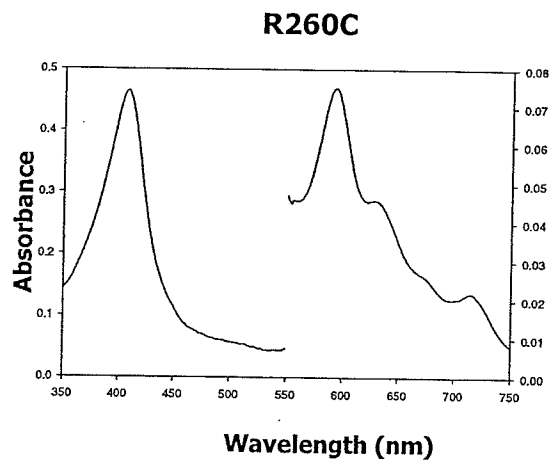
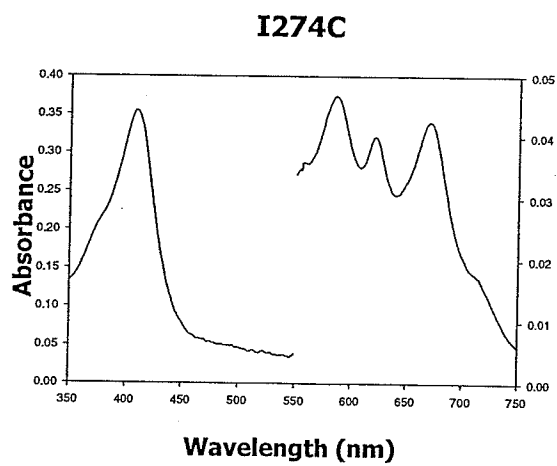
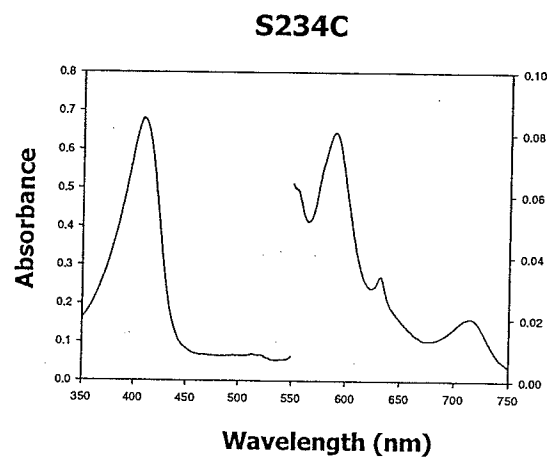
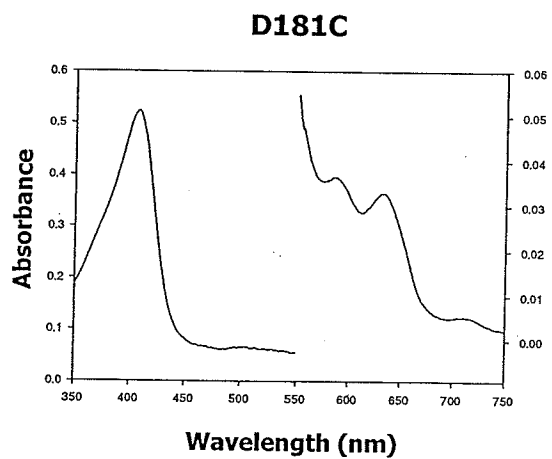
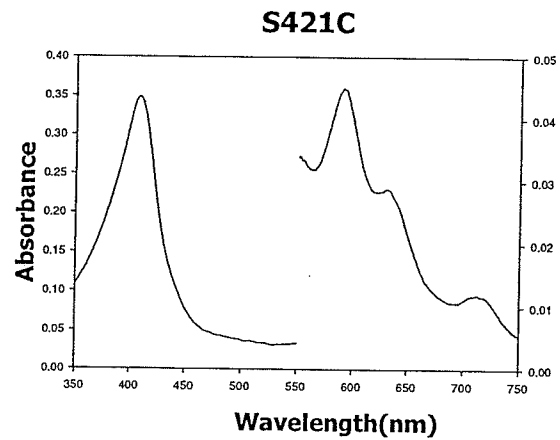
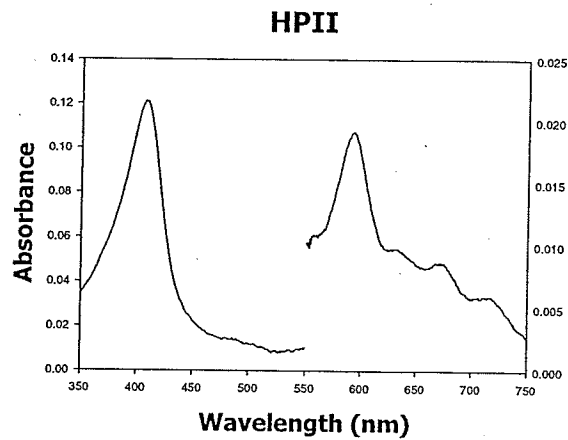


Figure 3.3.4. Elution profiles of heme extracted from HPII (wild type) and variants by C18 reverse phase HPLC chromatography. Letters b and d denote heme b and heme d respectively.

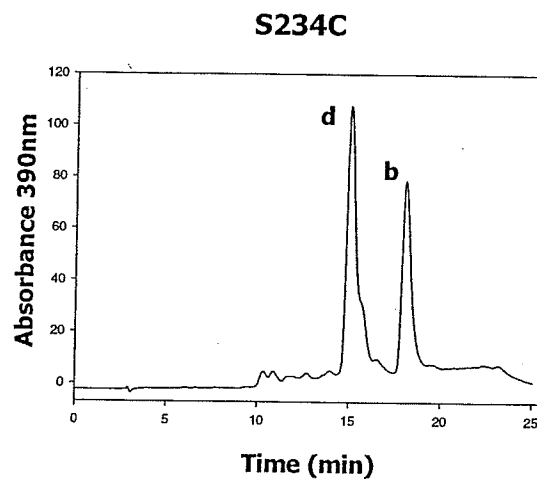
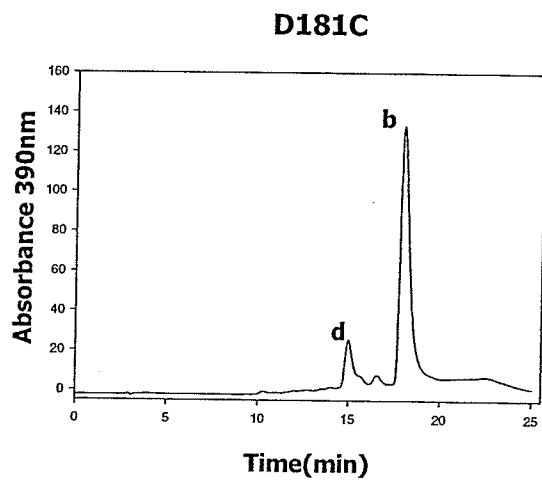
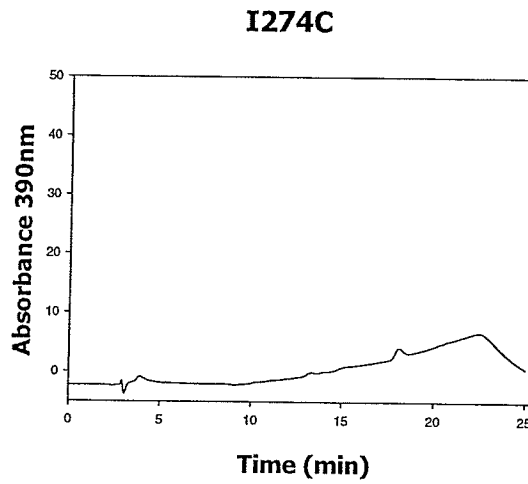
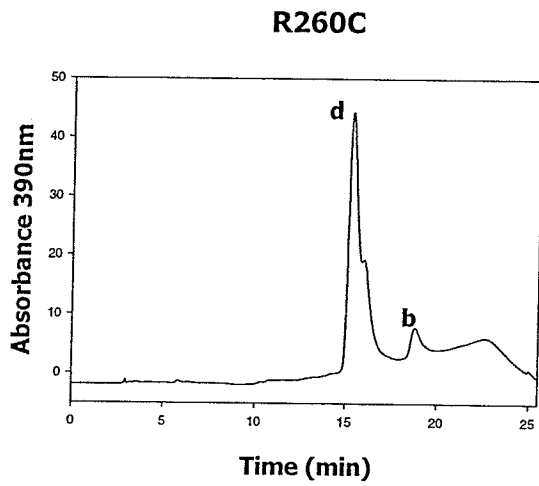
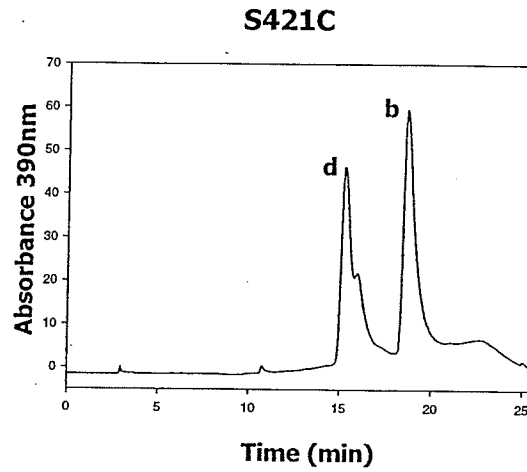
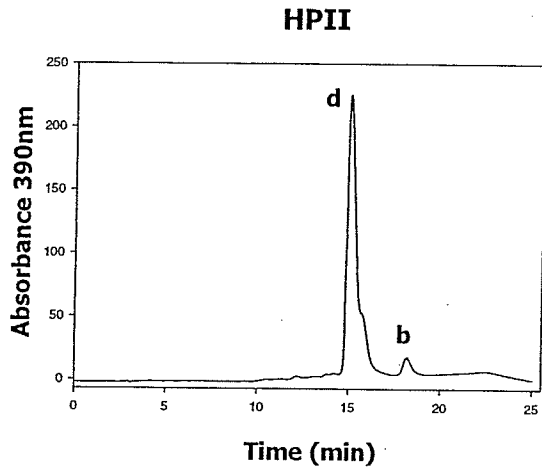
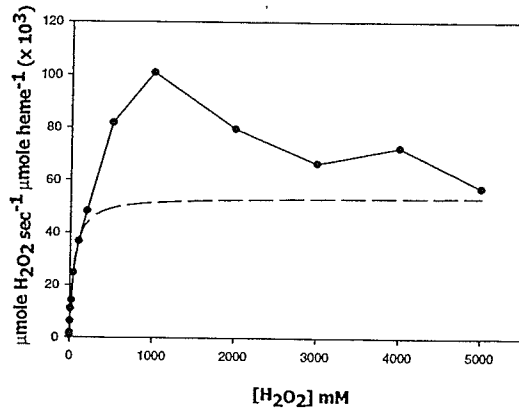
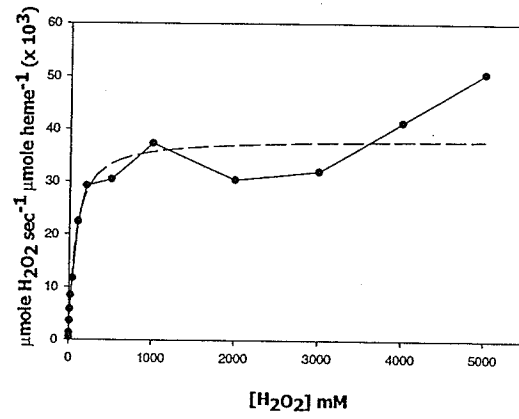


Figure 3.3.5. Effect of H_2O_2 concentration on enzyme velocity of HPII and its variants. In all panels, the solid line represents the observed data and the dashed line represents the theoretical Michaelis-Menten curve calculated from constants determined at low H_2O_2 concentration (Table 3.3.2). Note the differences in the scales of the velocity axis (i.e. y-axis).

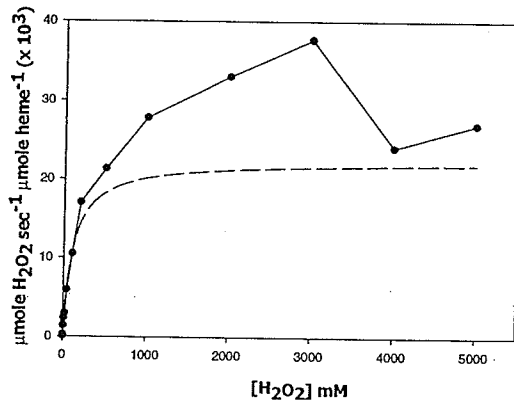
HP11



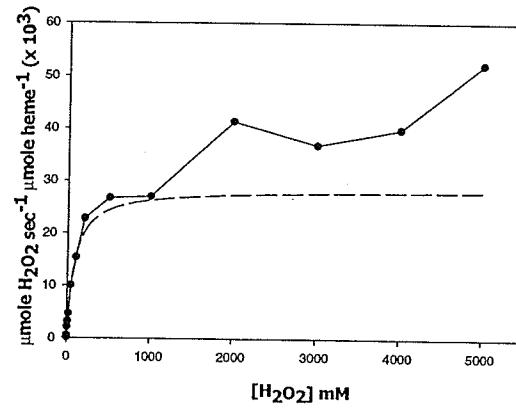
S421C



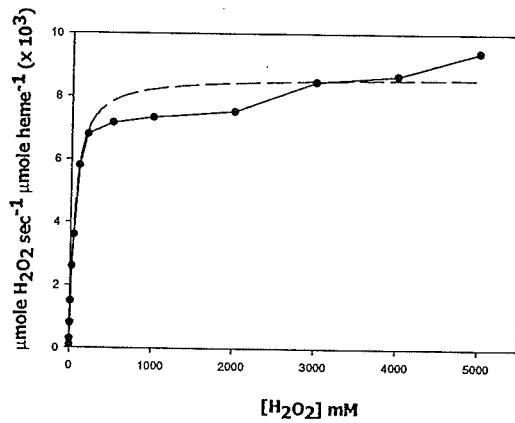
D181C



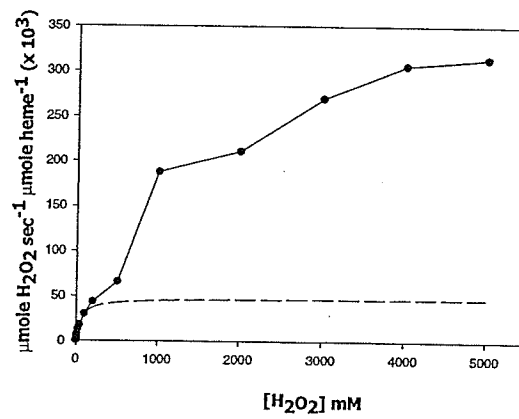
S234C



I274C



R260C



observed kinetic parameters of the cysteine containing variants in the main channel and for I274C were all lower than those of the wild type enzyme by an order of magnitude, (Table 3.3.2). The R260C variant in the lateral channel exhibited three-fold higher observed V_{\max} (Fig. 3.3.5 & Table 3.3.2). The absorption spectra of S234C, R260C and S421C were similar to the spectrum of the wild type enzyme with a Soret band at 407nm and a characteristic heme d peak at 590nm. The spectra of D181C suggested partial conversion (Fig. 3.3.3) and the spectrum of I274C contained a new peak at 670 nm. The HPLC profiles of extracted heme(s) from the variants confirmed the visible spectra analysis except for I274C, where the heme could not be extracted by acetone-HCl treatment (Fig. 3.3.4).

3.3.3. Effect of 2-mercaptoethanol on cysteine variants

Unlike mammalian catalases, HP11 was shown to be unreactive to sulfhydryl agents such as glutathione and dithiothreitol (Takeda *et al.*, 1980; Sevinc *et al.*, 1994) but was sensitive to 2-mercaptoethanol (MSH) (Sevinc *et al.*, 1994). Treatment of HP11 and its cysteine-containing variants with 5 mM MSH for 2 hrs at 37°C caused inactivation of the enzymes to varying degrees (Fig. 3.3.6). For example, the D181C was the least sensitive and S234C was the most sensitive. Extensive overnight dialysis of the enzymes to remove MSH reversed the inactivation.

3.3.4. Quantification of free sulfhydryl groups

The free sulfhydryl groups were quantified in the purified variants using 5,5'-dithiobis-(2-nitrobenzoic acid) (NbS₂). Consistent with the previous data (Sevinc *et al.* 1994), only one free SH was found in wild type HP11, but except for S421C, the cysteine

Table 3.3.3. Quantitation of the free sulfhydryl groups of the cysteines variants with Ellmans reagent [5,5'-dithiobis-(2-nitrobenzoic acid)]*.

Variant	(-SH / subunit)
Wild type	0.81 ± 0.15
D181C	0.16 ± 0.02
S234C	0.12 ± 0.02
I274C	0.03 ± 0.0004
R260C	0.05 ± 0.005
S421C	0.67 ± 0.13
C438A/ C669A	<0.1

* The standard error of three individual assays was shown.

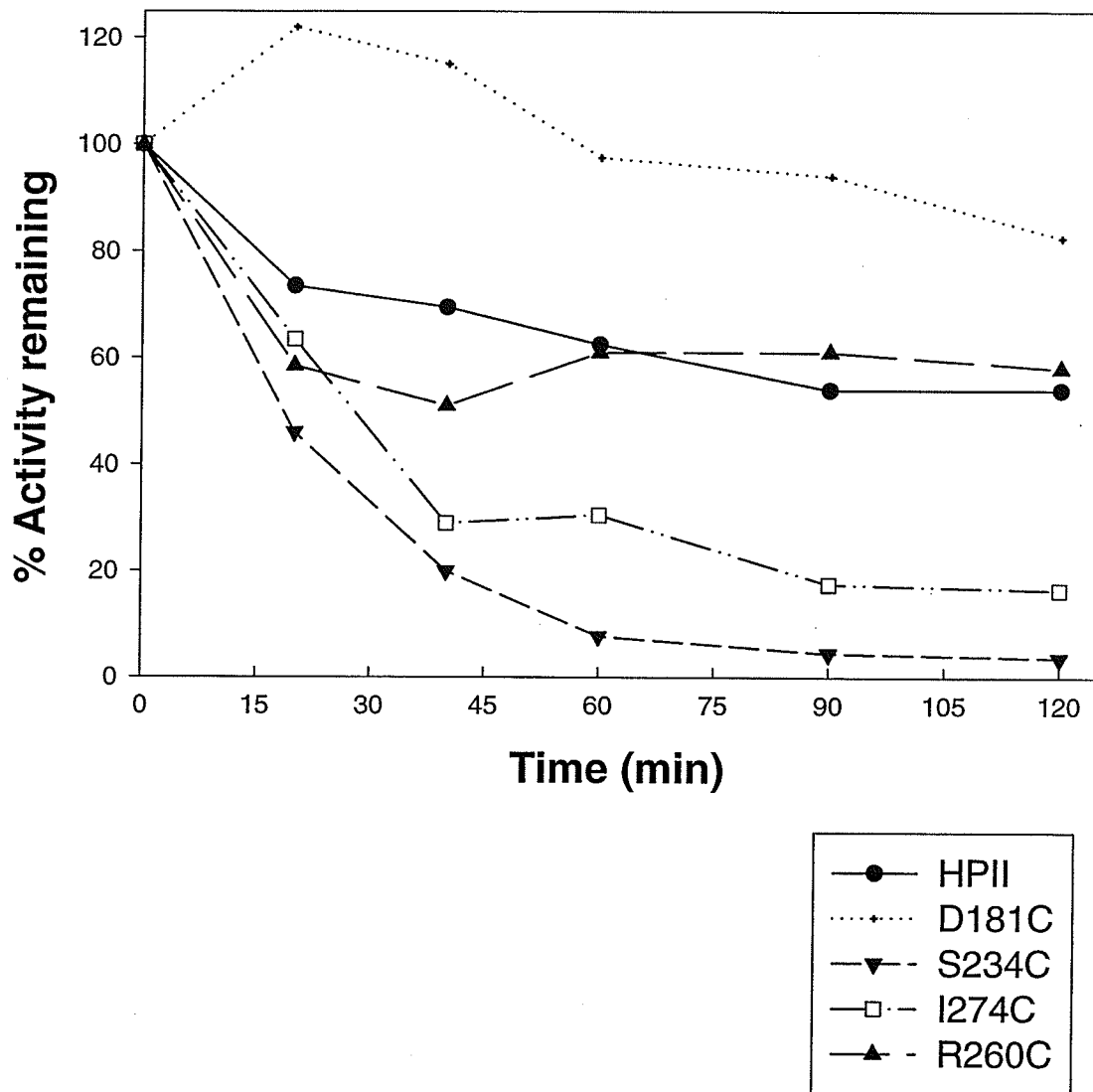


Figure 3.3.6. Comparison of the effects of 2-mercaptoethanol on HPII and its cysteine-containing variants. All assays were repeated in triplicate and the results averaged.

containing variants exhibited less than one free SH, suggesting possible modification of the -SH group. More work is needed to clarify the exact nature of the modification(s).

3.4 HPII exhibits enhanced resistance to proteolytic cleavage compared to other Catalases

3.4.1. Introduction

The most widespread type of catalase is the monofunctional class, examples of which are found in most aerobic organisms. They are typically homotetrameric with, either small subunits (55 to 65kDa) associated with heme b or large subunits (80 to 84 kDa) associated with heme d. The large and small subunit catalases share several highly conserved structural domains, which are supplemented in the large subunit enzyme with an additional 50 residues at the N-terminus and a 150 residue flavodoxin – like domain at the C-terminus. The role of these added domains remains an open question, but HPII exhibits enhanced resistance to thermal denaturation (Switala *et al.*, 1999), which has been attributed in part to the N-terminal extension. Various lengths of the N-terminus, 80 residues in HPII, 30 residues in BLC and 5 in CatF are overlapped by the wrapping domain of an adjacent subunit to form an interwoven structure common to all catalases.

HPII has served as a model for catalases in biochemical and structure function studies investigating the role of active site residues and the catalytic mechanism. The enhanced thermal stability of HPII has been described (Switala *et al.*, 1999), and this work describes the enhanced resistance to proteolysis exhibited by HPII in comparison to other catalases.

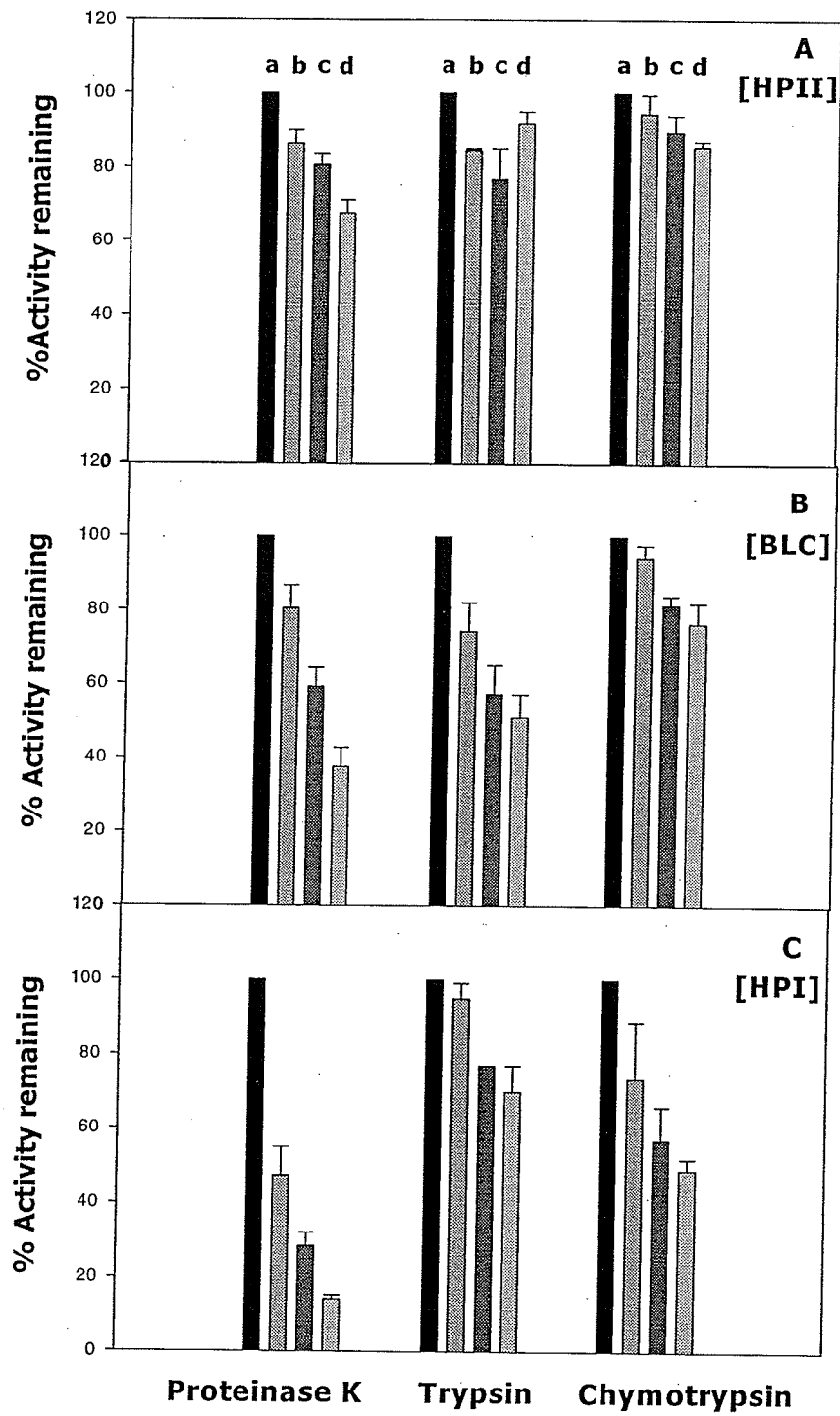
3.4.2. Sensitivity of catalases to proteinase K, trypsin and chymotrypsin

The three catalases, HP11, BLC and HPI, exhibited varying sensitivities to digestion with proteinase K, chymotrypsin and trypsin (Fig 3.4.1) at ratios (w/w) of protease to catalase from 1:100 to 1:20. HP11 (Fig 3.4.1A) was the least sensitive to digestion by all the three proteases, followed in order of increasing sensitivity, by BLC (Fig 3.4.1B), and HPI (Fig 3.4.1C). Of the three proteases, proteinase K was the most effective causing the loss of more than 75% of HPI activity after just one hour incubation with a 1:20 ratio of protease to catalase. This is consistent with the observation that HPI was rapidly proteolyzed to a 35 kDa fragment containing the inactive C-terminal portion (Carpena *et al* 2002).

3.4.3. Time course of digestion of HP11

The time course of digestion of HP11 by a 1:2 ratio (w/w, protease to catalase) was followed by SDS polyacrylamide gel electrophoresis, revealing an initial very rapid cleavage by all three proteases of the 84 kDa subunit via several intermediate sized fragments to a relatively stable 76 kDa fragment (Fig 3.4.2.). Digestion with proteinase K proceeded more quickly producing exclusively the 76 kDa band within one hour (Fig 3.4.2), and longer digestion at a 1:1 ratio, generated a 59 kDa band and, eventually, two bands with apparent masses of 26 kDa and 33 kDa (Fig 3.4.3A). The formation of the 76 kDa fragment was slowest with trypsin (Fig 3.4.2B) compared to chymotrypsin and proteinase K (Figure 3.4.2A,C), and even after 16 hours digestion at a 1:1 ratio, very little smaller material was observed (data not shown). In contrast to HP11, digestion of BLC with any of the proteases did not produce distinguishable partial digest fragments (data

Figure 3.4.1. Effect of treatment with proteinase K, trypsin, and chymotrypsin on the activity of HPII (A), BLC (B), and HPI (C). Mixtures of protease and catalase at 0 (a), 1:100 (b), 1:50 (c), and 1:20 (d) (w/w) were incubated for 1 h at 37 °C and quenched with trypsin inhibitor or PMSF (1 mM). Error bars indicate the standard error of three individual assays.



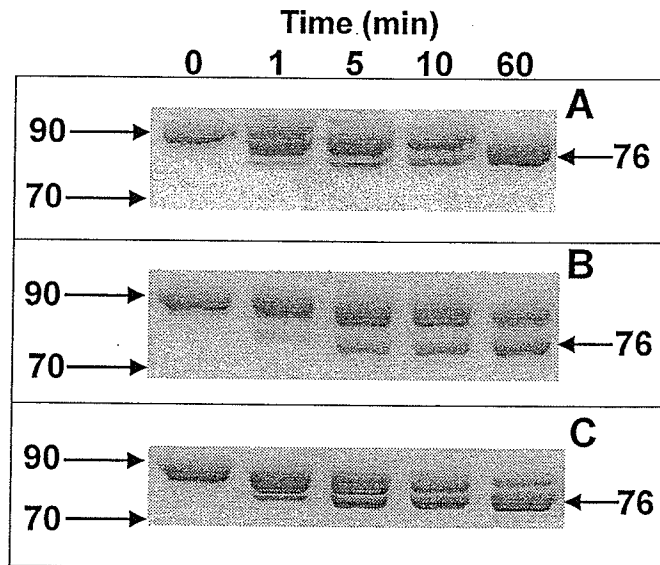
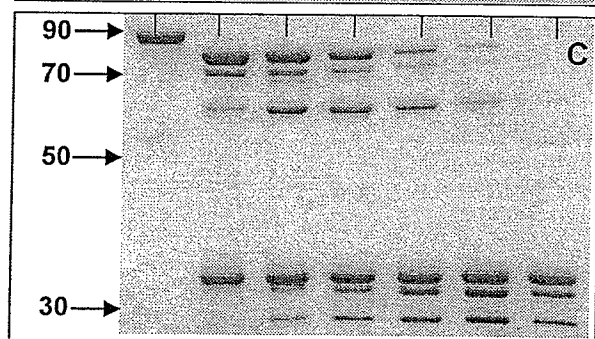
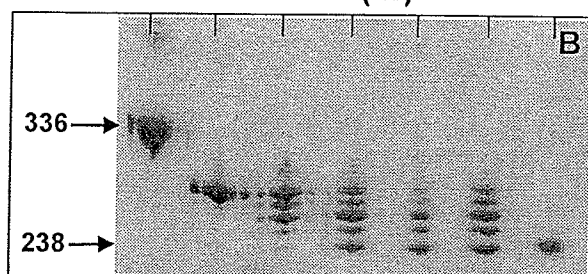
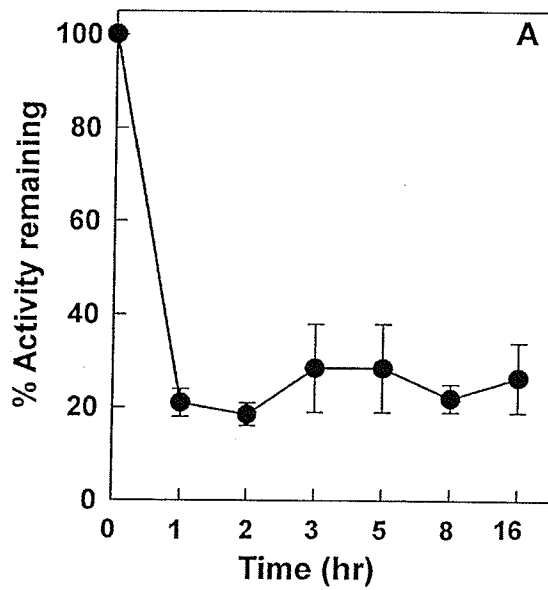


Figure 3.4.2. Products of proteolytic cleavage of HPII by trypsin (A), chymotrypsin (B), and proteinase K (C). HPII and protease (2:1 w/w) were incubated at 37 °C for the times indicated (in minutes), and the mixtures were separated by electrophoresis on 8% SDS polyacrylamide gel. The protein was visualized by staining with Coomassie brilliant blue. Size markers indicated as $\times 10^3$ Da were determined using the GIBCO protein ladder. The 76 kDa product is indicated with the arrow labeled with 76.

Figure 3.4.3. Correlation of product size and activity during proteolytic cleavage of HPII by proteinase K. Samples were incubated in a 1:1 ratio (w/w) with proteinase K at 37 °C for the times indicated. Catalase activities were determined, and the activity remaining is shown in (A). Samples were separated on a nondenaturing 8% gel (B) or a denaturing 8% gel (C), and the protein was visualized by staining with Coomassie brilliant blue. Size markers indicated as $\times 10^3$ Da were determined using HPII (336 kDa), bovine liver catalase (238 kDa), and HPI (160 kDa, not visible) in panel B and the GIBCO protein ladder in panel C.



not shown). Digestion of HPI produced only the expected 35 kDa C-terminal fragment after treatment with a 1 to 100 ratio of the protease to catalase, and higher ratios of protease eliminated even this fragment.

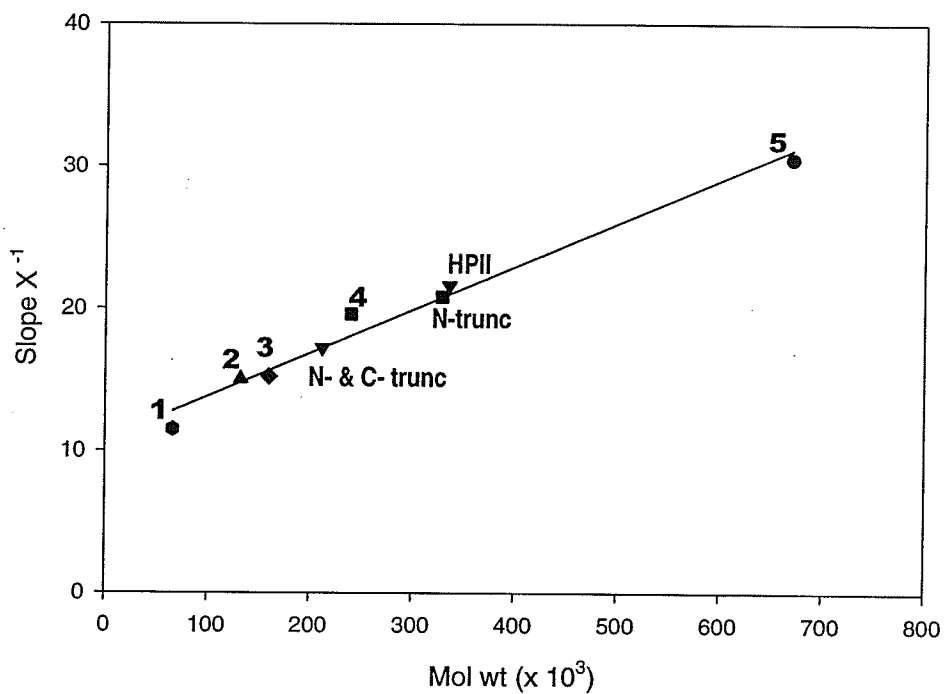
Whereas denaturing gels presented a picture of at least three cleavage sites within HPII resulting in sequential cleavage to 26 and 33 kDa fragments, as much as 20% of the original activity remained suggesting that much of the tertiary and quaternary structure had not been significantly affected. This was confirmed in the time course of cleavage of HPII with proteinase K visualized after electrophoresis on non-denaturing gels (Fig 3.4.3B). There was a rapid conversion of the 336 kDa tetramer to a band of approximately 310 kDa, composed principally of 77 kDa subunits. This was followed by the appearance and disappearance of bands at approximately 290 kDa, 270 kDa and 240 kDa. The subunit sizes associated with these conversions included bands with apparent masses of 76 kDa, 59 kDa, 33 kDa and 26 kDa. All HPII was eventually converted to a band of protein of approximately 220 kDa, containing equal amounts of the 33 kDa and 26 kDa fragments.

3.4.4. N- and C-terminal sequence analysis of protease fragments

In order to identify the sites of cleavage in HPII, the various fragments separated on SDS polyacrylamide gels were subjected to N-terminal sequencing. The 76 kDa fragments generated by all three proteases had very similar cleavage sites (Table 3.4.1), with N-terminal residues at Lys73, Gly74 and Ser75 for chymotrypsin, trypsin and proteinase K, respectively. The unusual cleavage by chymotrypsin is most likely the result of a trypsin contaminant in the chymotrypsin. The 59 kDa fragment generated by proteinase K also had Ser75 at the N-terminus and the shorter size arose from cleavage

Table 3.4.1. Sequences at protease cleavage sites in HP11

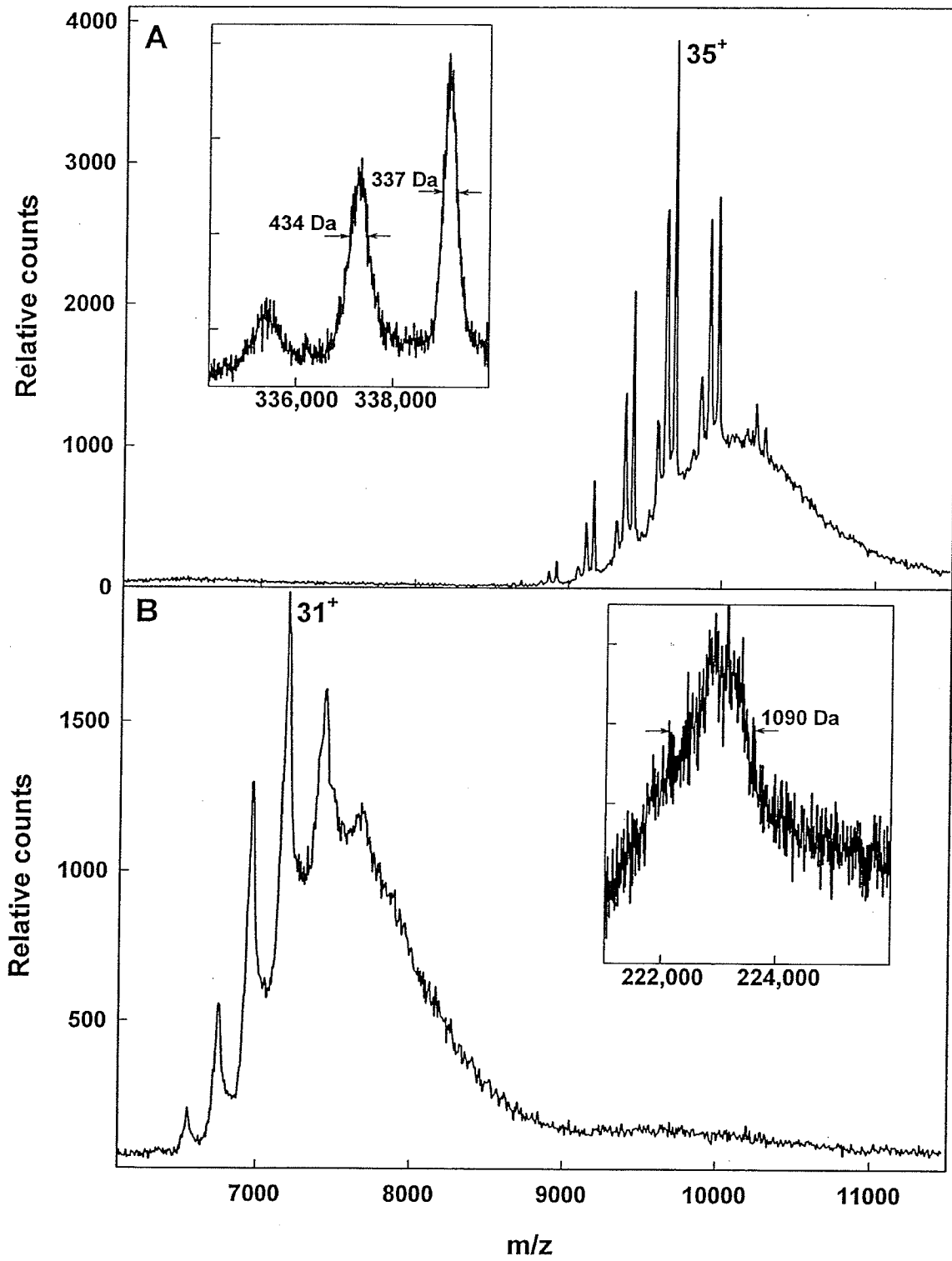
Fragment	Protease	Sequence	Mass (calc)
<i>A. N-terminal sequences</i>			
HP11 sequence		VRKGSSENYALTTNQG 71 72 73 74 75 76 77 78 79 80 81 82 83 84 85	
76 kDa	chymotrypsin	KGSSENYALTTNQG	76,464
76 kDa	trypsin	GSSENYALTTNQG	76,335
76 kDa	proteinase K	SENYALTTNQG	76,279
59 kDa	proteinase K	SENYAL	59,155
26 kDa	proteinase K	SENYALTTNQ	26,512
<i>B. N-terminal sequence at the central site</i>			
HP11 sequence		KLTRDPDFH 309 310 311 312 313 314 315 316 317 318	
33 kDa	proteinase K	KLTR?RD?DFH	32,661
<i>C. C-terminal sequence at C-terminal domain cleavage site</i>			
HP11 sequence		LSLYAIPD 588 589 590 591 592 593 594 595	
59 kDa	proteinase K	LY	59,155

Plot of Mol wt vs Slope X^{-1} 

1	BSA (monomer)	66 kDa
2	BSA (dimer)	132 kDa
3	HPI	160 kDa
4	BLC	240 kDa
5	Thyroglobulin (tetramer)	670 kDa

Figure 3.4.4. Non-denatured molecular weights of N-trunc and N- & C-trunc. Mobility of truncated HPII variants on different percentage acrylamide gels determined from the slopes by the method of Hedrick and Smith (1968). The molecular wt of wild type (HPII) is 336 kDa the N-trunc is 314 ± 14 kDa and the N- & C-trunc is 214 ± 12 kDa

Figure 3.4.5. Mass analysis by nanospray ionization of HPII protein before (A) and after (B) treatment with proteinase K. Deconvolutions of the data from each spectrum are shown as insets with the errors of measurement shown as fwhm. Both spectra were acquired at 200 V with SF6 as the curtain gas. At lower voltage, the ions of the tetramer were not as well resolved. Higher voltage did not change the spectra.



after Tyr591, which removed the C-terminal domain. The 33 kDa and 26 kDa bands had Ser75 and Lys 309 at their N-termini, respectively, revealing a third site of cleavage (Table 3.4.1.).

The multimeric sizes of truncated variants of HP11 were determined by electrophoresis on non-denaturing gels correlating the rate of migration with molecular weights on a series of different percentage gels (Fig 3.4.4.), and by electrospray mass spectrometry (Fig.3.4.5.). The sizes are summarized in Table 3.4.1 along with the calculated sizes of the various fragments. Plotting the location of the three cleavage sites on the tetrameric structure of HP11 reveals that they are located on the surface of the protein (Fig. 3.4.8.).

3.4.5. Thermal stability of the truncated HP11 variants

HP11 is relatively insensitive to thermal denaturation, exhibiting a T_m for loss of activity of 83-84°C (Switala *et al.*, 1999). A thermal denaturation study of the truncated variants of HP11 was undertaken to determine the role, if any, of the N- and C-terminal domains in enhancing the stability of HP11. The 310 kDa multimer, composed of N-terminally truncated 76 kDa subunits, exhibited a T_m for loss of activity of 76°C (Fig 3.4.6.), 8°C lower than that of the native enzyme. The stability of the dimer association was reduced, requiring heating to only 80°C for dissociation (Fig. 3.4.7.). The T_m of the truncated form was independent of the protease used.

By contrast, the 220 kDa multimer, composed of 33 kDa and 26 kDa fragments lacking both the N- and C-termini exhibited a T_m for loss of activity of 60°C (Fig 3.4.6.), 23°C lower than that of the native enzyme. Upon mixing the N- and C-truncated form in SDS-urea loading buffer at room temperature, there was complete dissociation to

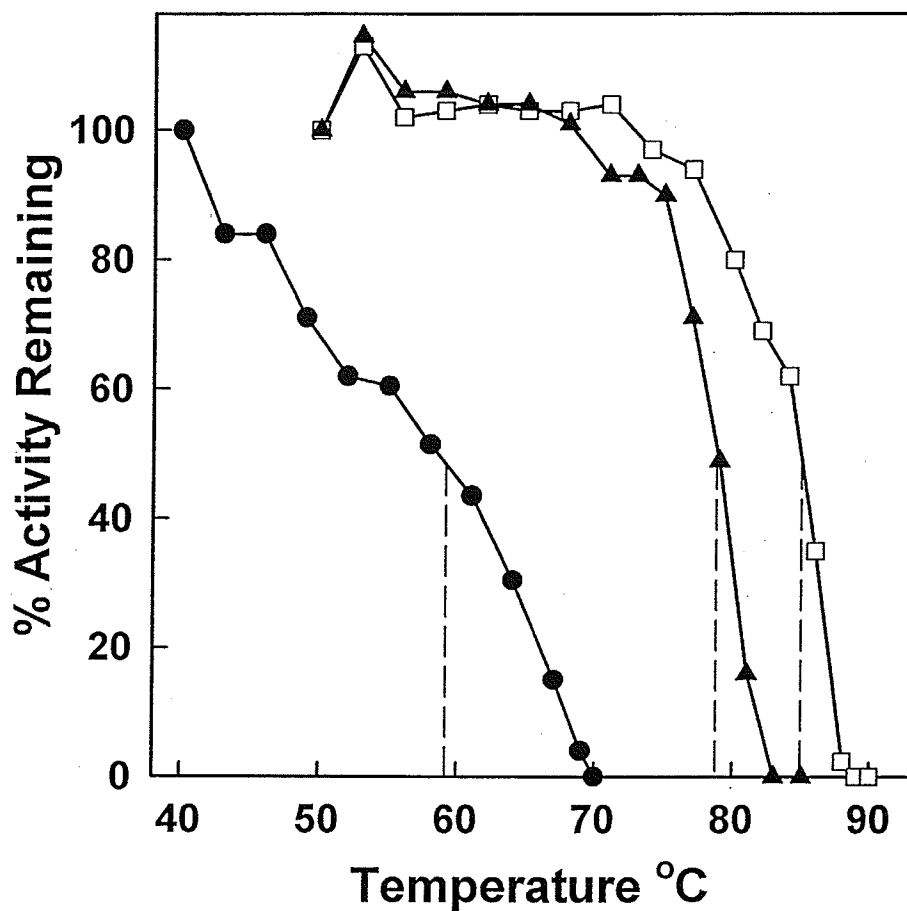


Figure 3.4.6. Activity changes in HPII (open squares) and HPII treated for 1 h (solid triangles) and 16 h (solid squares) at 37 °C with 1:1 (w/w) proteinase K as the temperature is increased at 0.6 °C/min from 40 to 90 °C. The enzymes were in 50 mM potassium phosphate buffer (pH 7). The dashed lines indicate the midpoints or temperatures of 50% inactivation.

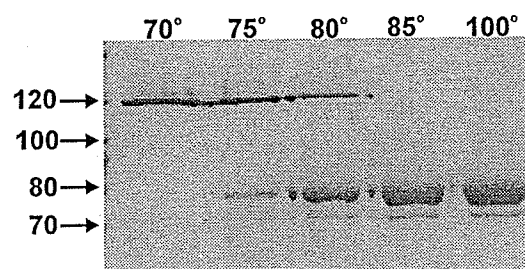


Figure 3.4.7. Conversion of HPII dimers to monomers. HPII was treated with proteinase K in a 1:1 ratio (w/w) for 1 h at 37 °C. Samples were then incubated for 10 min at 70, 75, 80, and 100 °C in 50 mM potassium phosphate buffer (pH 7). The temperatures of incubation are indicated above each lane. Samples were removed, cooled to room temperature, and added to SDS-urea loading buffer. Samples were loaded and run without further heating on an 8% SDS-polyacrylamide gel. Size markers indicated as $\times 10^3$ Da were from the GIBCO protein ladder. The band at 120 kDa is a dimer of two HPII subunits that are resistant to thermal denaturation. As the temperature of incubation is increased, the dimer dissociates into monomers at 76 kDa.

the small fragments indicating that the stability of the dimers was also severely reduced by removal of the C-terminal domain. The T_m and dimer instability of the N- and C-terminally truncated form is similar to those of BLC, which exhibits a T_m of 56°C (Fig 3.4.8.) and dissociates completely in gel loading buffer at room temperature.

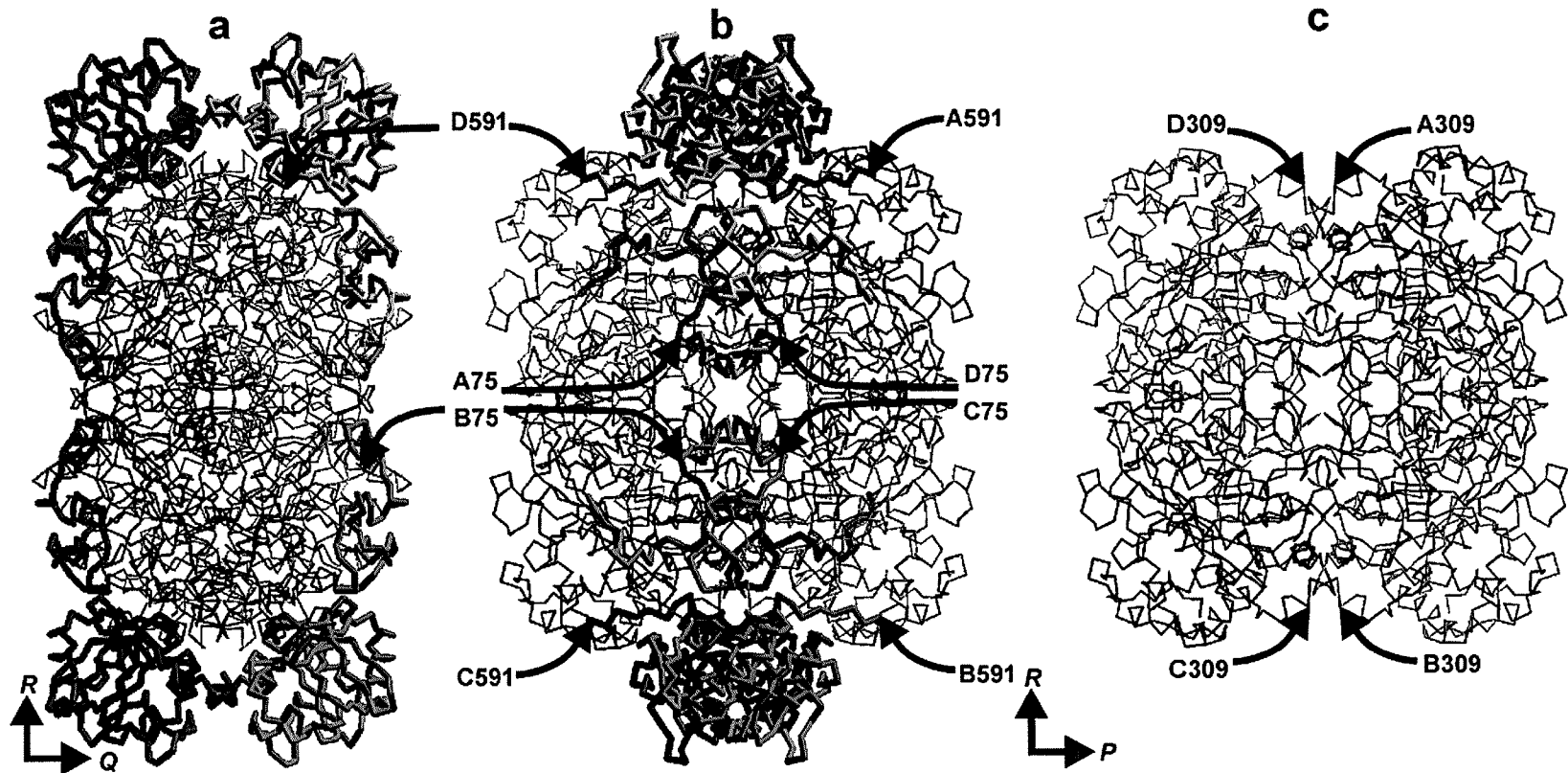


Figure 3.4.8. Location of the three main locations on the HPII tetramer that are sensitive to proteolytic cleavage. HPII is shown in panels a and b rotated 90° around the *R* axis with respect to each other to show the surface locations of the cut sites at residues 75 and 591 in each of subunits A (blue), B (green), C (red), and D (yellow). The N- and C-terminal fragments removed by these cuts are presented as heavier lines in panels a and b and are removed in panel c where the protein has the same orientation as in panel b. The surface locations of the third main cut site at residue 309, exposed by the removal of the excised domains, are evident in panel c. The figure was prepared using SETOR (Evans, 1993).

3.5. Purification and characterization of the truncated variants of HPII

3.5.1. Introduction

The importance of extended domains and the characteristic “interweaving” exhibited by heme catalases has been the subject of intense investigation(s) (Bergdoll *et al* 1997, Sevinc *et al* 1998, Ueda *et al* 2003, Andreoletti *et al* 2003). However, due to the lack of sufficient information on the tetramerization process, no concrete conclusions have been drawn concerning the role of these extended and additional domains. Attempts to address this question by molecular genetic approaches have also been unsuccessful (Sevinc *et al* 1998, Ueda *et al* 2003). In the present study proteolysis has allowed the isolation and characterization of HPII truncated to the size of a small subunit catalase.

3.5.2. Purification of the truncated variants

Limited digestion of HPII with proteinase K in 1:50 ratio (protease: enzyme) at 37°C for 1 hr resulted in the removal of N-terminus (henceforth referred as N-trunc), whereas extensive digestion with proteinase K in 1:2 ratio at 37°C for 16 hr resulted in removal of both the N- and C- termini (N-& C- trunc). Both forms of the truncated enzyme were dialyzed overnight against 50 mM Tris, pH 7.0, 0.1M NaCl buffer (Buffer D). Approximately 5 mg of the above samples were eluted from Superose-12 FPLC column, equilibrated with Buffer D. The protein was eluted using an isocratic flow of buffer D at a rate of 0.2 ml/min. HPII (control) eluted at 9.8 ml, N-trunc at 9.6 ml and N-& C- trunc at 10.5 ml respectively (Fig 3.5.1). In case of the truncated variants (Fig 3.5.1B and 3.5.1C) proteinase K eluted at approximately 15.6 ml. The sizes of the truncated variants were confirmed by SDS-PAGE on an 8.5% gel.

Figure 3.5.1. Elution profiles of truncated variants and wild type HP11 purified by size exclusion chromatography on a Superose-12 FPLC column. Panel (A) represents wild type, (B) N-trunc and (C) N- & C-trunc, respectively. The dashed line indicates the retention volume for the peaks; note the change in retention (elution) volume for the N- & C-trunc variant.

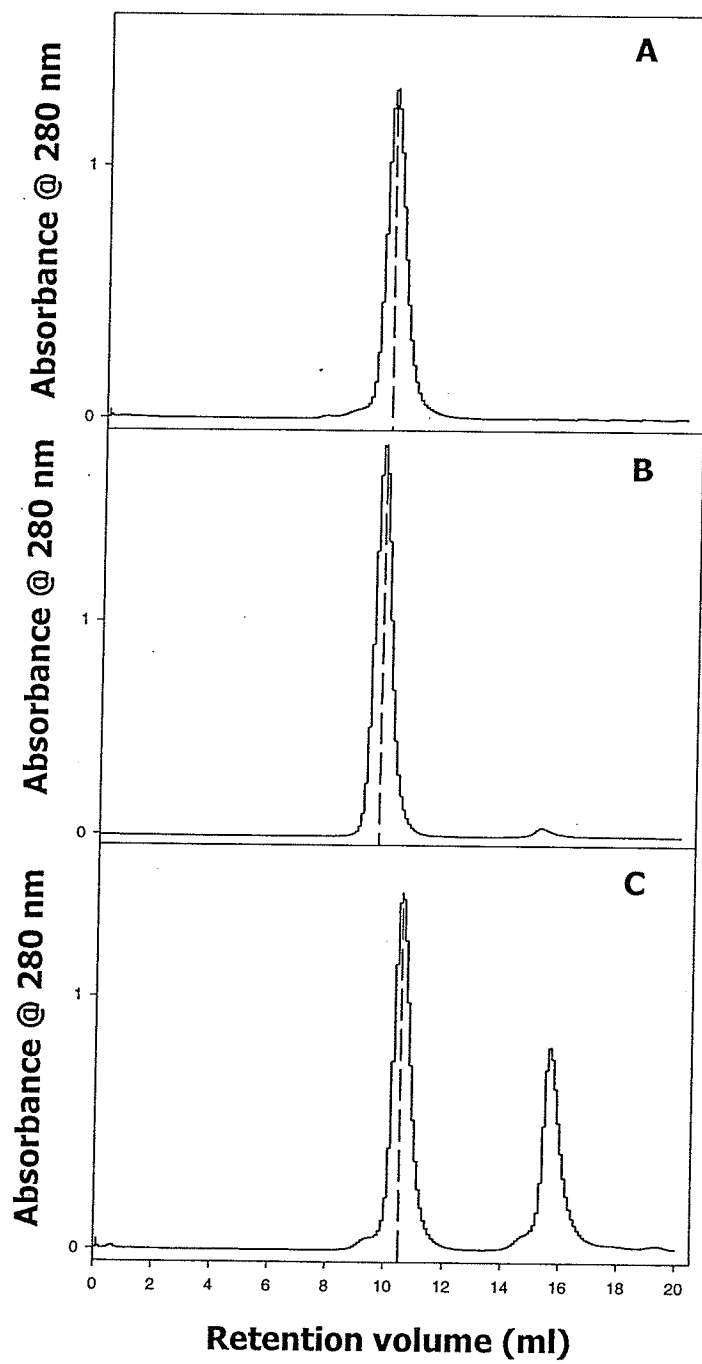


Table 3.5.1. Comparison of the specific activities of wild type HPII and its purified truncated variants.

Protein*	Specific Activity (u/μmole heme)
Wild type	1.43 x 10 ⁶
N-trunc	1.14 x 10 ⁶
N & C trunc	0.77 x 10 ⁶
Hemin (Negative control)	62

*N-trunc corresponds to 310kDa HPII

*N & C trunc corresponds to 220kDa HPII

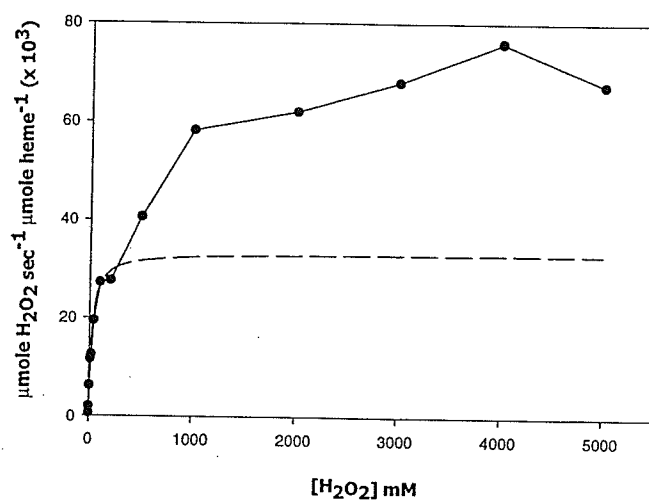
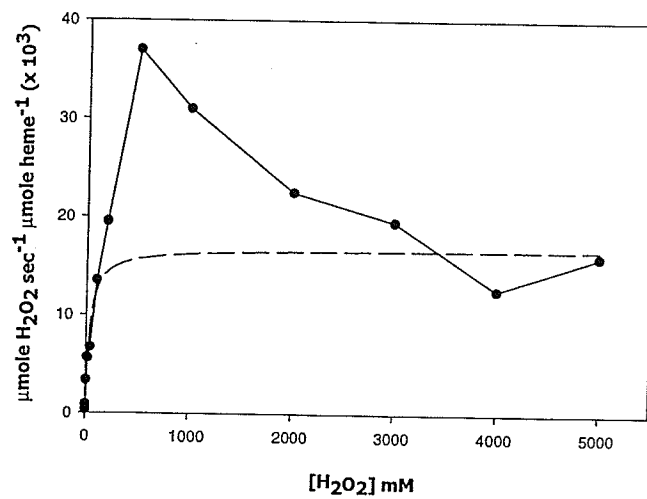
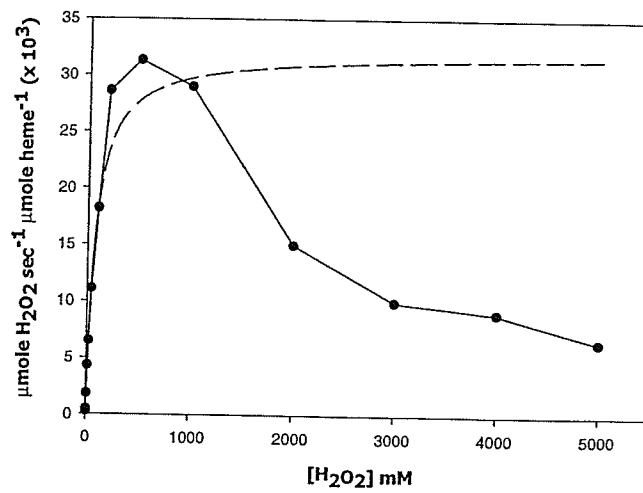
Table 3.5.2. Comparison of the calculated and observed kinetic parameters of wild type and truncated HP11 variant proteins.

Variant	Observed		Calculated ^a		
	V_{\max}^b	$[\text{H}_2\text{O}_2]@V_{\max}/2, \text{mM}$	V_{\max}^b	$K_m \text{ (mM)}$	$k_{\text{cat}}/K_m \text{ s}^{-1} \text{ M}^{-1}$
Wild type	100,780	221	54,020	47	1.14×10^6
N-trunc	37,000	183	16,650	34	4.89×10^5
N-& C-trunc	31,300	78	31,490	74	4.25×10^5

^a Calculated for $\text{H}_2\text{O}_2 < 100 \text{ mM}$.

^b Units of V_{\max} are $\mu\text{mol H}_2\text{O}_2 \mu\text{mol heme}^{-1} \text{ s}^{-1}$.

Figure 3.5.2. Effect of H_2O_2 concentration on enzyme velocity of HPII and its truncated variants. In all panels the solid line represents the observed data and the dashed line represents the theoretical Michaelis-Menten curve calculated from constants determined at low H_2O_2 concentration (Table 3.5.2). Note the differences in the scales of the velocity axis (i.e. y-axis).

HPII**N-trunc****N- & C-trunc**

3.5.3. Catalatic and peroxidatic activities of the truncated variants

Both forms of the truncated enzyme exhibited similar catalatic specific activities of 14800 and 14400 u/mg (compared to 17700 u/mg for the native enzyme), indicating that loss of the N and C-terminal domains had little effect on the function of the deeply buried active site. Therefore, the rapid reduction in activity to an apparent residual 20% (Fig 3.4.3) is most likely an artifact of the high concentration of proteinase K (1:1 w/w) in the mixture interfering with catalase activity. Heme exhibits a negligible 62 units/ μmol compared 1.4×10^6 units/ μmol of heme in HPII (Table 3.5.1), too low a level for the small amount of heme released to have contributed to the residual activity observed. The observed and calculated kinetic parameters of the N-& C-trunc varied were lower than that of the wild type (Table 3.5.2, Fig 3.5.3). Like the wild type enzyme both the truncated variants showed negligible peroxidase activity (< 0.1 u/mg) towards peroxidatic electron donors *o*-dianisidine and ABTS (data not shown), whereas *Burkholderia pseudomallei* KatG (used as a positive control) showed 1.1 u/mg and 3.0 u/mg towards *o*-dianisidine and ABTS, respectively.

3.5.4. Effect of inhibitors on the truncated variants of HPII

The effect of various catalase inhibitors on the truncated variants was investigated. The N-& C- trunc was slightly more sensitive to cyanide than wild type (Fig 3.5.3), and it was significantly more sensitive to azide (Fig 3.5.4 B). The 50% inhibitory concentrations of cyanide and azide are summarized in Table 3.5.3. The inhibitory properties of hydroxylamine and *O*-methyl hydroxylamine were also investigated (Fig 3.5.5 and Table 3.5.3). The truncated variants did not exhibit any changes to inhibition by

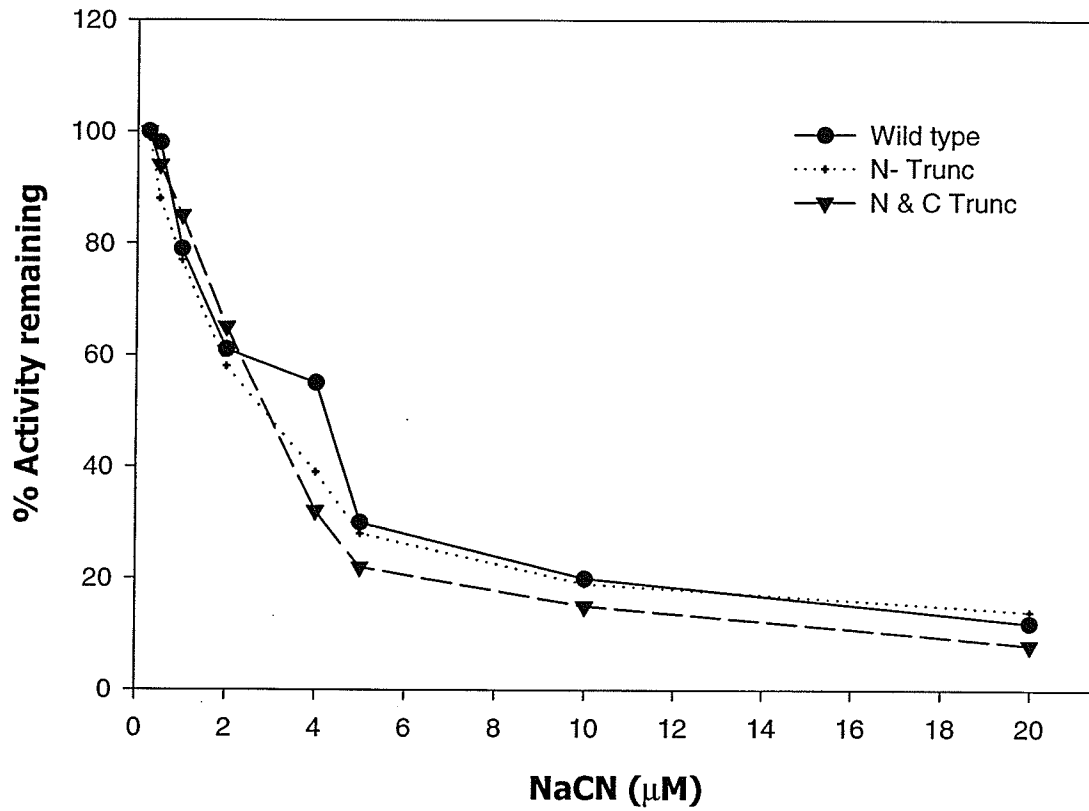


Figure 3.5.3. Comparison of the effects of sodium cyanide (NaCN) on wild type HPII, N-trunc and N- & C-trunc variants respectively. Each enzyme was incubated with the inhibitor for 1 min in 50mM phosphate buffer at 37°C prior to the assay. All assays were repeated in triplicate and the results averaged.

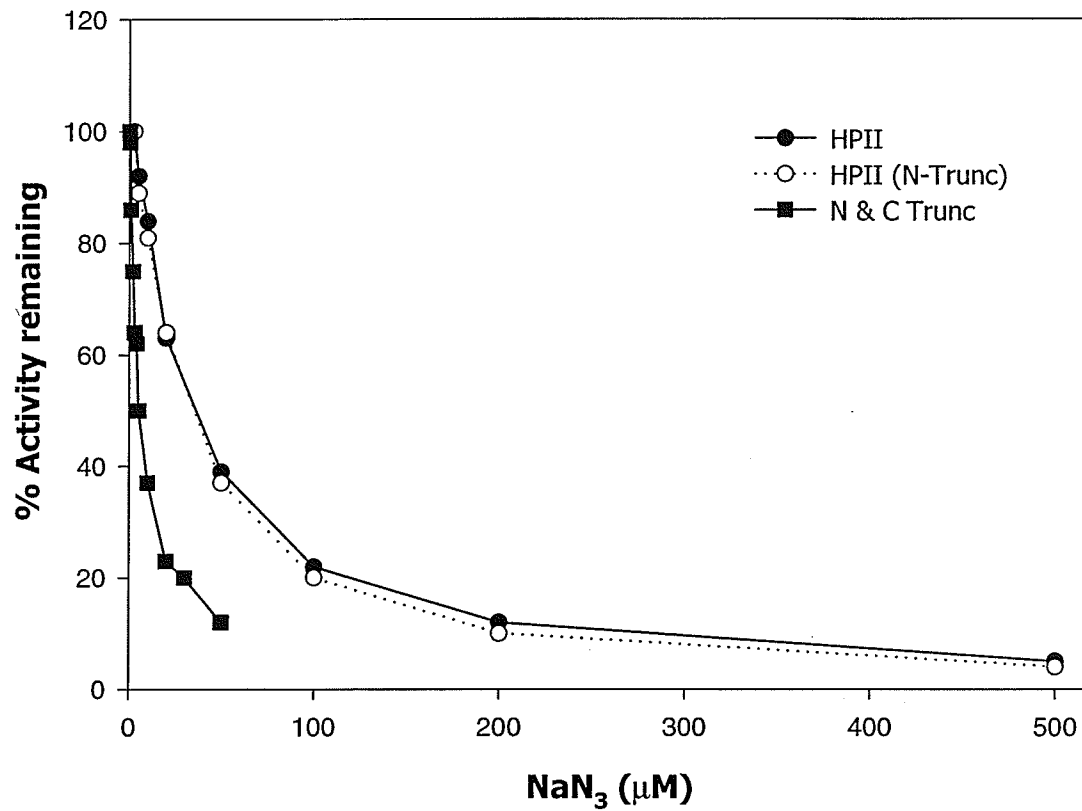


Figure 3.5.4. Comparison of the effects of sodium azide (NaN₃) on wild type HPII, N-trunc and N- & C-trunc variants respectively. Each enzyme was incubated with the inhibitor for 1 min in 50 mM phosphate buffer at 37°C prior to the assay. All assays were repeated in triplicate and the results averaged.

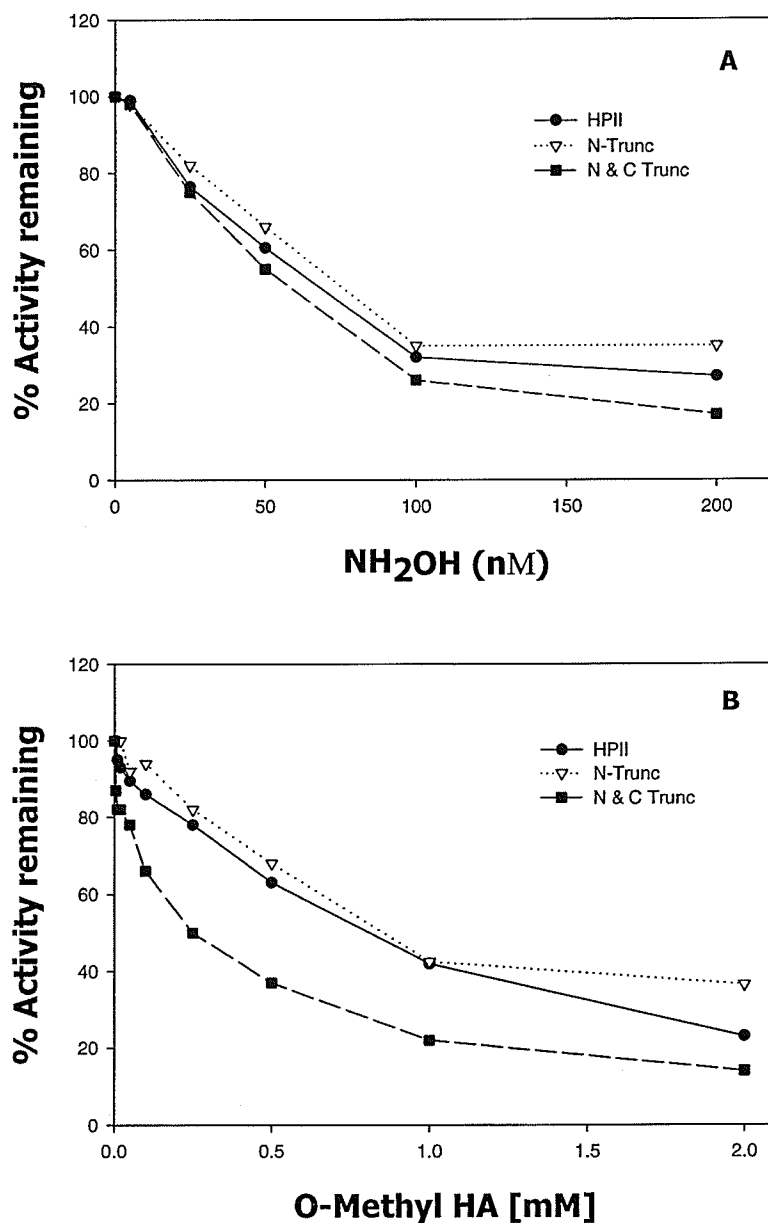


Figure 3.5.5. Comparison of the effects of Hydroxylamine [NH₂OH] (A) and *O*-Methyl hydroxylamine [O-Methyl HA] (B) on wild type HP11, N-trunc and N- & C-trunc variants respectively. Each enzyme was incubated with the inhibitor for 1 min in 50mM phosphate buffer at 37°C prior to the assay. All assays were repeated in triplicate and the results averaged. Note the changes in scale on the x-axis (nM and mM).

Table 3.5.3. Sensitivity of wild type HPII and truncated variants to various inhibitors*

Inhibitor	Concentration (μM) at 50% inhibition		
	Wild type	N-trunc	N & C trunc
Sodium cyanide (NaCN)	5	3	3
Sodium azide (NaN_3)	37	36	0.5
Hydroxylamine (NH_2OH)	0.07	0.08	0.06
<i>O</i> -Methylhydroxylamine (NH_2OCH_3)	560	595	250

*All assays were repeated in triplicate and the results averaged.

hydroxylamine, whereas with *o*-methyl hydroxylamine the N-&C- trunc variant exhibited greater sensitivity than wild type or the N-trunc variant (Table 3.5.3).

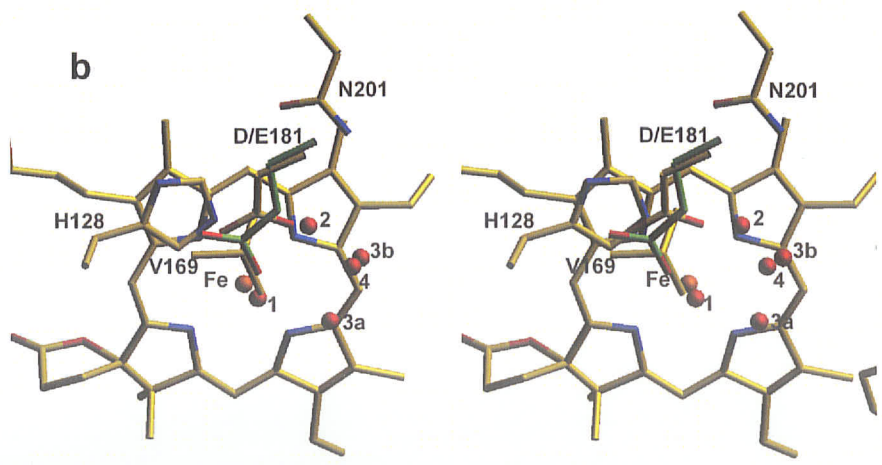
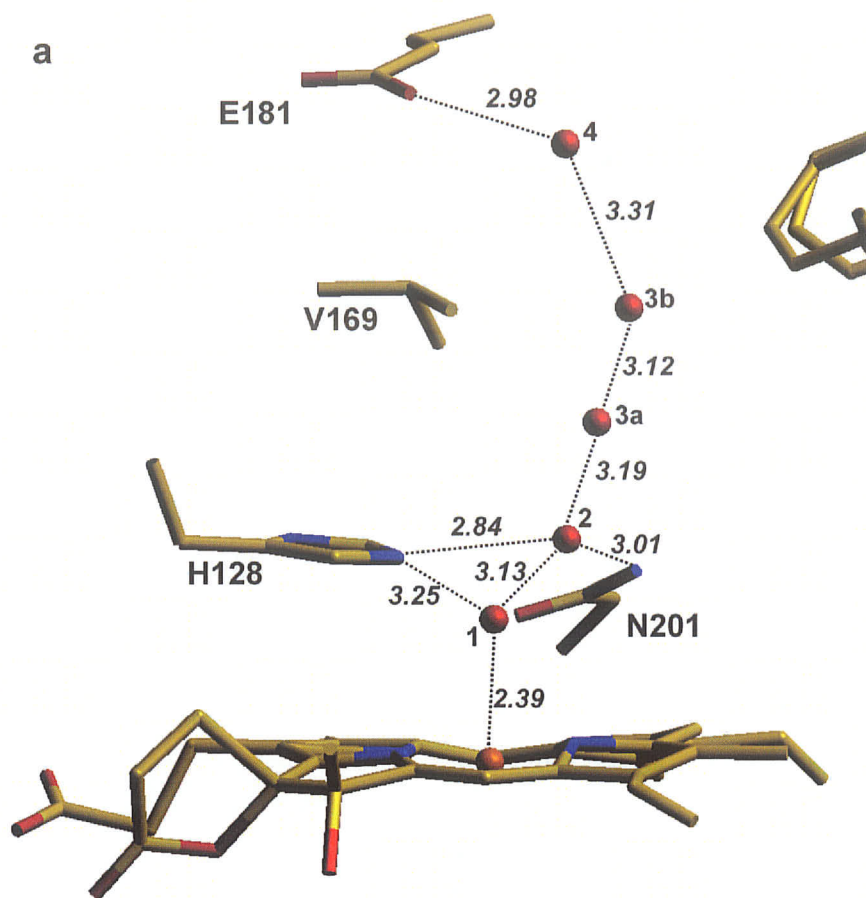
4. DISCUSSION

4.1. Asp181 of HP11 is important for catalysis

A clear understanding of how catalase maintains high selectivity for substrate hydrogen peroxide while at the same time exhibiting turnover rates in excess of 10^6 per second remains elusive. The issue of selectivity can be explained, in part, by the active site heme being deeply buried within the β -barrel core of the subunit, necessitating passage of the substrate through 30 to 50 Å of narrow channels. However, because the narrow channels might conceivably hinder substrate and product movement in and out of the active site, a conceptual problem is created in the light of the high turnover rates. Separate molecular dynamic simulations support the concept of hydrogen peroxide entering the enzyme through the main channel, oriented perpendicular to the plane of the heme, but do not agree on the route of product exhaust. Furthermore, classical molecular interaction potential calculations carried out on CATA suggest that the substrate arrives in the active site properly oriented for interaction with the heme iron, and side chains of the catalytic His and Asn (Kalko *et al.* 2001).

Site directed mutagenesis studies of residue D181 demonstrated that a negatively charged side chain in the main channel of HP11 enhances water occupancy in the access channel, particularly at the sixth ligand position, (Fig 4.1.1a) and, coincidentally, is required for enzyme activity. These observations provide a valuable insight into the mechanism of the catalase reaction.

Figure 4.1.1. (a) Schematic showing the distances among waters in the main channel of the D181E variant. The potential hydrogen bonds are shown as dashed lines and the distances are expressed in Å. The water numbering is as in Fig. 3.1.5 and Table 3.1.3. (b) Stereo view oriented down the main channel towards the heme from D181. The slightly shifted location of the Glu side chain in the D181E variant is indicated in green. The water numbering is as in panel a.



4.2. An Electrical potential in the access channel of catalases enhances catalysis

One obvious explanation for the role of the carboxylate side chain in the main channel lies in the establishment of an electrical potential between it and the positively charged iron of the heme that would act upon any molecule, with an electrical dipole, passing through the channel. Furthermore, given the location of the sixth ligand water in roughly the same position as substrate H_2O_2 , on a direct line between the carboxylate and heme irons (Fig 4.1.1.b), the electrical potential may influence transition state formation.

The hydrogens in H_2O_2 are separated by an angle of about 110° when viewed along the O-O axis resulting in an asymmetric or skewed structure. Orbital interactions present an energy barrier to rotation around the O-O bond of about 2.5 kcal/mol, limiting H_2O_2 to one predominant conformation (Schumb *et al.* 1955). The structure gives rise to an electrical dipole of 2.3 Debye, slightly larger than the 1.9 Debye dipole of water. Consequently, H_2O and H_2O_2 passing D181 in the main channel will be affected by the electrical potential and be forced into an orientation with the oxygens directed towards the heme iron (Fig 4.2.1.). When oxygen O-1 of H_2O_2 becomes associated with the heme iron, spatial constraints in the active site fix H-1 within hydrogen bond distance of the imidazole ring of the active site histidine and O-2 within hydrogen bonding distance of the NH_2 of the active site asparagine. Thus, orientation of the dipole of H_2O_2 in the potential field presents a simple mechanism to explain the prediction arising from molecular dynamic studies that substrate molecules enter the active site in a preferred orientation.

In the hydrophobic portion of the channel between D181 to H128, waters have only other waters to hydrogen bond with and the bond lengths separating waters 2, 3a, 3b

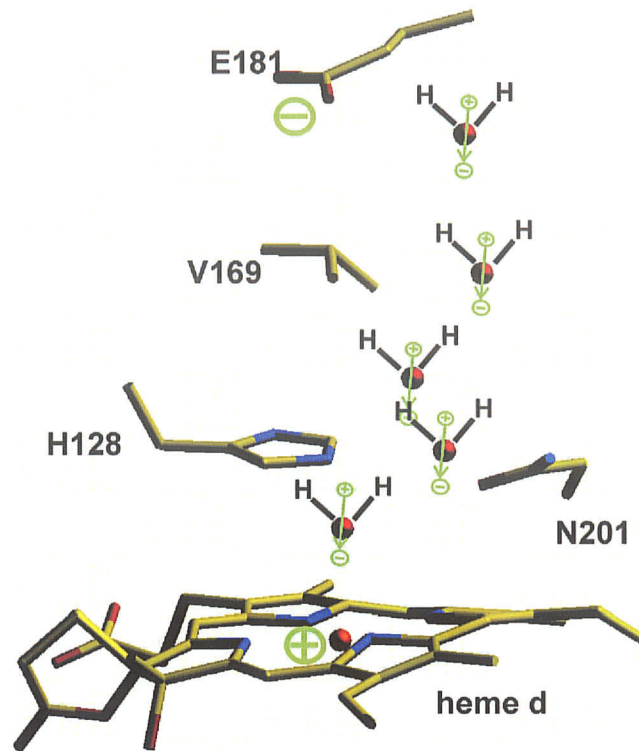


Fig 4.2.1. Schematic of the main channel illustrating the presence of a negative charge (in green) on the side chain of E181 and a positive charge (in green) on the heme iron, and the effect of the electrical potential between these two charges on the electrical dipoles of water in the channel and active site. The orientation of the electrical dipoles is indicated by the green arrow over each H₂O. The location of the water molecules are those in subunit A of variant D181E.

and 4 are longer than optimal for strong hydrogen bonds (Fig 4.1.1a). The favorable orientation of the molecules induced by the electrical potential may be critical in stabilizing the solute matrix in the channel. Similarly, the greater occupancy of water in the channel of the native enzyme and the D181E variant, compared to the other less active D181 variants, can be attributed to the electrical potential acting on the dipoles of the solvent to create a population of waters with common orientation, thereby favoring the formation of a hydrogen bonded matrix. What cannot be satisfactorily explained is the difference in occupancies between the channels of D181E and the native enzyme. One possibility is that it is simply an artifact of the refinement process or may be a result of the extended glutamate side chain facilitating hydrogen bond formation and moving the negative charge slightly closer to the heme iron.

Increased water occupancy in the channel may initially appear to be correlated with higher catalytic activity, but the relationship is not direct, because, while occupancy is clearly higher in the D181E variant, the specific activity is not significantly higher than that of native enzyme. Perhaps more significant is the presence of water in the hydrophobic portion of the channel. It is now clear that water can exist in the hydrophobic portion of the channel, if properly stabilized, suggesting that the simple length of this region does not act as a "molecular ruler" (Putnam *et al.* 2000) preferentially selecting for H_2O_2 over H_2O . The formation of a hydrogen bonded matrix is important for solute accessing the active site, and this is influenced by the total volume or shape of the hydrophobic region. Either an increase or decrease in the volume or shape of the region, caused by modifying the side chain on residue 169, had the same effect of reducing the specific activity of the enzyme. A larger hydrophobic side chain as in the

V169I variant constricts the channel and decreases the volume in which a matrix can form. An analogous phenomenon has recently been reported in superoxide dismutase where the C γ of a valine replacement for a histidine protrudes into the substrate access channel and displaces a water (Hearn *et al.* 2003).

4.3. Importance of hydrophilicity in the upper part of the access channel

The crystal structure of HPII shows the side chains of, Ser234 and Glu530 to be hydrogen bonded to waters in the access channel. However, Ser234 is not a conserved residue and is present only in large subunit enzymes (Klotz and Loewen, 2003). Similarly the position of E530, 20Å from active site heme, differs in small subunit enzymes compared to HPII. The observed K_m ($H_2O_2 @ V_{max}/2$) for the non-polar S234A and S234I variants are 2 to 3 fold higher than wild type showing that these variants have reduced affinity for the substrate, suggesting a need for hydrogen bonding at position 234. The observation that Ser234Ala contains heme d while Ser234Ile contains heme b can be explained by the greater (60% of wild type) activity of S234A compared to S234I (15% of wild type).

The observed and calculated kinetic parameters of the polar variants E530D and E530Q were quite similar to wild type. In contrast, the non-polar variants E530A and E530I were less active and exhibited three fold higher observed K_m ($H_2O_2 @ V_{max}/2$). Consistent with their lower activity, the non-polar variants contained heme b and attempts to convert it “*in vitro*” into heme d were unsuccessful. Timkovich and Bondoc (1990) suggested that protoheme is first bound to HPII apoenzyme and that heme hydroxylation is catalyzed by HPII itself utilizing one of the first H_2O_2 molecules to react catalytically. In this scenario, the interaction of the Glu530 side chain with substrate

H₂O₂ (Melik Adamyan *et al* 2001) supports the notion that it might be influential in selecting hydrophilic molecules (like H₂O and H₂O₂) early in the channel. The longer C-terminal domain extends the channel and may help to exclude larger substrates from accessing the active site. Interestingly all large subunit catalases so far characterized show heme d, or at least a chlorin-like species with a spectrum similar to that of heme d (Hicks *et al.* 1995, Horie *et al.* 1976, Goldberg and Hochman 1989, Peraza and Hansberg, 2002). It becomes tempting to propose that the “flavodoxin like” C-terminal domain has a role in heme conversion, although no flavin nucleotide binding has been noticed in any of the solved crystal structures and a mechanism is not obvious (Bravo *et al* 1999, Reid *et al* 1981). Further work including the determination of the crystal structures of E530 and S234 variants is required.

4.4. I274C: Covalently linked heme prosthetic group in catalases

Isoleucine²⁷⁴ is present in the heme pocket of HP_{II} close to the pyrrol ring I of heme and the I274C substitution should place the thiol group 3-3.5Å from the vinyl CH₂ making a covalent linkage feasible. Several lines of evidence indicate that the prosthetic group in this variant is covalently attached to the protein. (i) The heme is not extractable by acetone-HCl treatment, which normally removes heme from wild type protein (Fig 3.3.4.). (ii) This variant gives no reaction with thiol reactive reagent DTNB (Table 3.3.3). (iii) Preliminary analysis by MALDI-MS of trypsin digested I274C shows no heme in the mass spectrum (Dr. Donald LJ, personal communication). Interestingly, the I274C variant shows no change in the Soret band from 407nm, indicating little effect of the change on the heme coordination sphere and environment. However the intensity of the Soret was 40% lower than wild type giving rise to a lower R_z. (A₄₀₇:A₂₈₀ ratio), suggestive of less

heme in the protein. Given that it is unlikely for HPII to fold in the absence of bound heme, the reduced Soret intensity most likely is the result of a covalent modification.

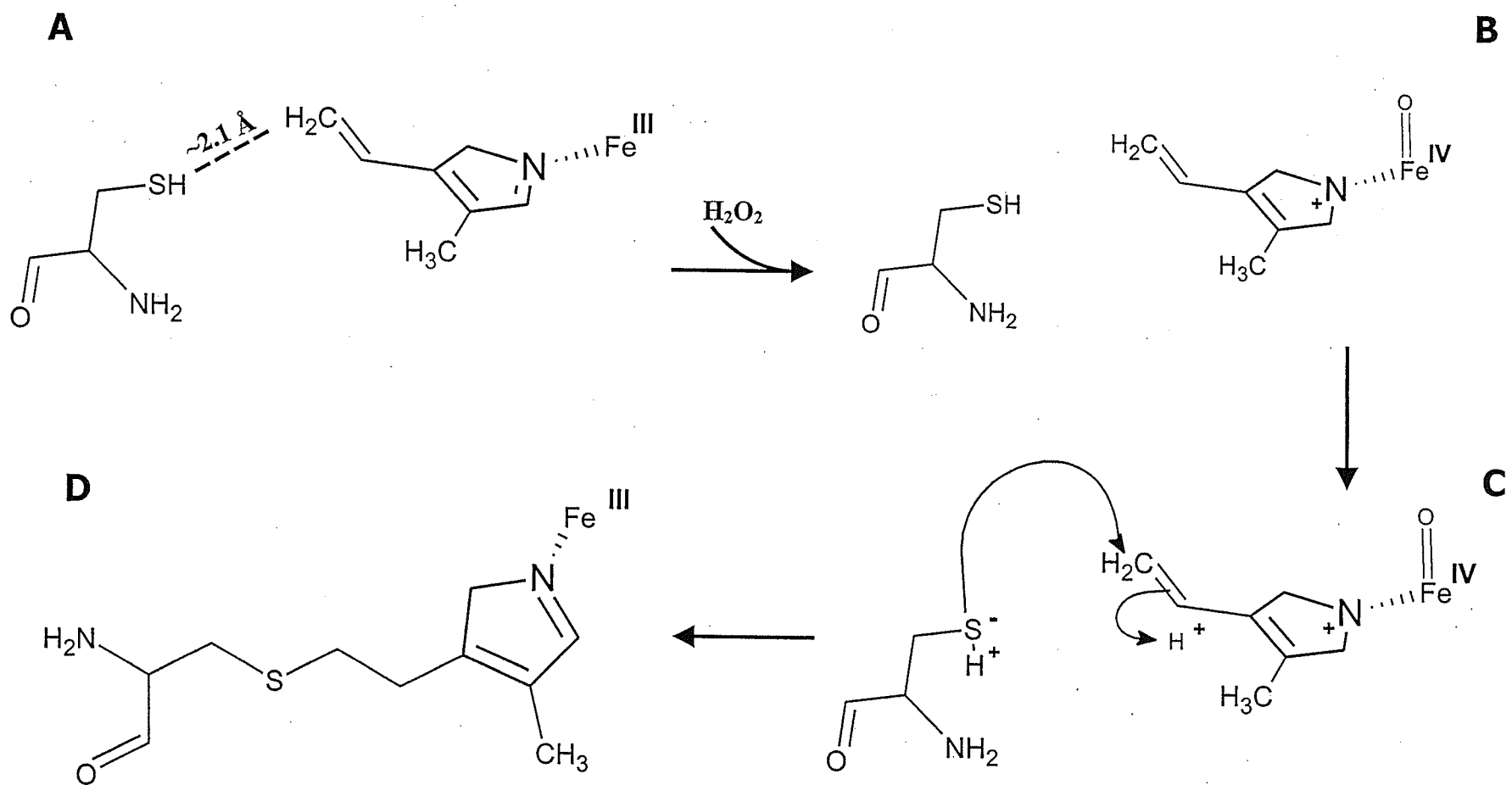
The I274C variant exhibits only ~ 25% of wild type activity. Unfortunately, it is not yet clear whether this is the result of the covalent bond, of conformational changes within the active site, or of low heme content. However, the decrease in Rz value due to the covalent bond formation between protein and heme has a precedent in lactoperoxidase (Colas *et al.*, 2002), for which it has been reported that a D225E mutation caused a 50% decrease in the Rz value accompanied by a 60% decrease in activity. Other hemoproteins showing autocatalytically linked heme prosthetic group include myeloperoxidases (Fiedler *et al.*, 2000), thyroid peroxidases (Fayadat *et al.*, 1999) and eosinophil peroxidase (Oxvig *et al.*, 1999), but the function of the covalent links in these hemoproteins remains to be elucidated. A schematic for the autocatalytic formation of the covalent bond between the protein and heme in HPII is shown in scheme 4.1.

4.4. Cysteine mutagenesis of channel residues

A number of cysteine-containing variants including D181C, S234C, I274C, R260C and S421C have been constructed to study the effect of reactive sulfhydryls and their modification in the channels of HPII. To date only the superficial activities have been determined, and more detailed studies are required.

4.5. HPII exhibits enhanced resistance to proteolysis than other catalases

HPII exhibits unusual resistance not only to sequence specific proteases like trypsin and chymotrypsin, but also to the broad substrate range protease, proteinase K. Globular proteins generally exhibit some level of resistance to proteolysis at least initially



Scheme 4.1. A proposed mechanism to explain the formation of Cys-Heme covalent bond in HPII of *E. coli*. For simplicity, only the pyrrole ring I of heme and heme iron are shown, the distance between the Cys 274 and -CH₂ vinyl on ring I of heme is ~ 2.1 Å (A). The mechanism begins with formation of compound I shown in (B). Compound I is an oxoferryl species formed, along with water in the reaction, of one H₂O₂ with the heme. The iron is in a formal Fe^V oxidation state, but one electron is delocalized from the heme to create the oxo-Fe^{IV}-heme cation, shown as the starting species in (B). The positive charge on heme would favor attack by the Gamma-S⁻ of cysteine leading to the covalent bond shown in (D).

because the tertiary structure of the protein chain imparts sufficient inflexibility that it cannot fit into the protease active site. Such resistance to proteolysis is usually demonstrated under conditions of limited digestion involving substrate to protease ratios of 100 to 1 and lower temperatures around 25°C (Spolaore *et al.* 2001). What makes HPII unusual is its resistance to cleavage even at a very high (1 to 1) ratio of protein to protease at 37°C. This property complements another unusual property of HPII, its enhanced thermal stability (Switala *et al.* 1999).

4.6. Resistance of HPII to proteolytic cleavage provides insights into the enzymes thermal stability

HPII can be considered to be a dimer of dimers in which monomers first associate by forming an interwoven structure with 80 N-terminal residues of each subunit being overlapped by the wrapping domain of the adjacent subunit (subunit A with C, and D with B). Such interweaving was suggested as an explanation for the enhanced stability of the dimers, that dissociate only above 95°C, and for the elevated T_m of inactivation, 83°C (Switala *et al.* 1999). A recent comparison of the properties of 16 different catalases, however, observed that there was no correlation between the length of the N-terminal extension involved in the interweaving and the thermal stability (Switala and Loewen, 2002). The current work supports this conclusion by demonstrating that removal of the N-terminal domain, leaving only seven residues overlapped in the interwoven structure, reduced the T_m by only 6°C, to 77°C. Furthermore, the truncated dimers still required incubation at over 80°C to dissociate. On the other hand, removal of the C-terminal domain caused a significant reduction in the T_m for thermal inactivation to 60°C. Even more striking was the effect on the stability of the dimers, which dissociated on mixing

with gel loading buffer, even without heating, making it impossible to assess the temperature of dissociation.

While the C-terminal domain appears to be a key factor in enhancing the thermal stability of HPII, it was not possible to assess the effect of C-terminal domain removal in the presence of the N-terminal region, because the latter domain was more sensitive to proteolysis and was rapidly removed. Attempts had been made to address this question through the construction of truncated genes, but the truncated variants did not fold correctly and protein did not accumulate (Sevinc *et al* 1998). This conclusion, that the C-terminal domain is more important than subunit interweaving in dimer stability, calls into question the previous surmise that the subunits involved in the stable dimers were interwoven. The alternate possibility is that the interaction of subunits along the R axis (subunit A with D, and B with C) in which the C-terminal domain actually wraps around the beta barrel core of the adjacent subunit may be more important for dimer stability than the interwoven structure.

A clear explanation for the enhanced resistance to proteolysis is more difficult. However, if the common picture of a protein chain having to change conformation to fit into the active site of a protease is accepted, then resistance to proteolysis is a result of greater rigidity in the protein. In the case of HPII, the combination of interweaving and wrapping of domains on adjacent subunits undoubtedly create a structure that is much less flexible than that of small subunit catalases. Consequently, the very same structural features that enhance the thermal stability may be responsible for the enhanced resistance to proteolysis. Are these two usual properties of HPII, enhanced thermal stability and protease resistance, related in some way? This cannot be answered directly. However,

resistance to thermal denaturation is unusual in an enzyme from a bacterium that does not survive exposure to temperatures anywhere near the 83°C required to inactivate the enzyme. What is strange is the retention of thermal stability, when there seems to be no benefit to the host organism. On the other hand, the reason for enhanced resistance to proteolysis in HP_{II} can be easily found in simple bacterial physiology. The expression of *katE* is induced in early stationary phase, and HP_{II} accumulates in stationary phase cells. This is a period of rapid protein turnover as cells adapt to a period of slowed metabolism, and it is here that resistance to proteolysis is important to HP_{II} because it allows the enzyme to survive and function in its role as a protective enzyme. Because both thermal stability and protease resistance may have a common basis in a very stable and rigid structure, the original properties of thermal stability in HP_{II} may have been adapted to the complementary need for protease resistance in the niche of stationary phase metabolism. For comparison, the more protease sensitive HP_I is expressed mainly in log phase where protease resistance would not be as important.

4.7. Truncated variants of HP_{II}

Initial attempts at purifying the truncated variants by ion exchange chromatography and by hydroxyapatite were unsuccessful, but size exclusion chromatography on Superose12 FPLC column offered a good alternative. The truncated variants purified on Superose12 FPLC column, retained nearly 70-80% of wild type activity indicating that loss of the additional domains had little effect on the function of the deeply buried active site. As expected, the active site appears to be more accessible in N-& C-trunc variant than N-trunc and wild type HP_{II}. For example, the double truncation variants is more sensitive to azide and methyl hydroxylamine than wild type or N-trunc,

but equally sensitive to cyanide and hydroxylamine smaller molecules. Ultimately, the crystal structures of the N-trunc and N-& C-trunc are required to define the structural differences.

4.8. Future studies

A number of avenues for further experimentation arise from the work presented here. From my study, a clear picture started emerging regarding the roles of channels in catalases. Although the existence of a substrate inlet channel is supported, both by theoretical and experimental studies, the existence of an exhaust channel remains hypothetical and the importance of residues further up the main channel, require more investigation. For example, the crystal structure(s) of the S234 and E530 variants would provide valuable insights, into the role of channel residues distant from heme. The protein folding mechanism in catalases is poorly understood because of the size and complexity of the protein. Complicating the picture, variants such as D181I, R180A, and R260C were produced in low yield because of aberrant folding, this resulted in the standard purification protocol producing impure protein. The use of protease inhibitors during purification and the introduction of poly-His tag might increase the purity of some preparations. Structural studies of the cysteine variants generated in this work is warranted involving both crystallography and mass spectroscopy. A rational site-directed cysteine mutagenesis study of the lateral and putative third channel should be undertaken, to completely elucidate the “substrate flow” hypothesis in catalases. Finally, the reason(s) for heme conversion in HP11 (and large subunit catalases) still remains enigmatic and a study, involving site directed mutagenesis of aromatic residues in the distal heme pocket should be undertaken.

5. LITERATURE REFERENCES

- Ahern, K. V., Lustig, H. S., Chan, J. & Greenberg, D. A. (1993). Calcium indicators and excitotoxicity in cultured cortical neurons. *Neurosci Lett* 162, 169-172.
- Akanmu, D., Cecchini, R., Aruoma, O. I. & Halliwell, B. (1991). The antioxidant action of ergothioneine. *Arch Biochem Biophys* 288, 10-16.
- Allgood, G. S. & Perry, J. J. (1986). Characterization of a manganese-containing catalase from the obligate thermophile *Thermoleophilum album*. *J Bacteriol* 168, 563-567.
- Almarsson, O., Bruice, T. C., Kerr, J. & Zuckermann, R. N. (1993). Molecular mechanics calculations of the structures of polyamide nucleic acid DNA duplexes and triple helical hybrids. *Proc Natl Acad Sci U S A* 90, 7518-7522.
- Amara, P., Andreoletti, P., Jouve, H. M. & Field, M. J. (2001). Ligand diffusion in the catalase from *Proteus mirabilis*: a molecular dynamics study. *Protein Sci* 10, 1927-1935.
- Amo, T., Atomi, H. & Imanaka, T. (2002). Unique presence of a manganese catalase in a hyperthermophilic archaeon, *Pyrobaculum calidifontis* VA1. *J Bacteriol* 184, 3305-3312.
- Andreoletti, P., Sainz, G., Jaquinod, M., Gagnon, J. & Jouve, H. M. (2003). High-resolution structure and biochemical properties of a recombinant *Proteus mirabilis* catalase depleted in iron. *Proteins* 50, 261-271.
- Antonyuk, S. V., Melik-Adamyanyan, V. R., Popov, A. N., Lamzin, V. S., Hampstead, P. D., Harrison, P. M., et al. (2000) Crystal structure of manganese catalase from *Lactobacillus plantarum*. *Structure* 9, 725-738.
- Aruoma, O. I. & Halliwell, B. (1987). Superoxide-dependent and ascorbate-dependent formation of hydroxyl radicals from hydrogen peroxide in the presence of iron. Are lactoferrin and transferrin promoters of hydroxyl-radical generation? *Biochem J* 241, 273-278.
- Aslund, F., Zheng, M., Beckwith, J. & Storz, G. (1999). Regulation of the OxyR transcription factor by hydrogen peroxide and the cellular thiol-disulfide status. *Proc Natl Acad Sci U S A* 96, 6161-6165.
- Asmus, K. D., Bensasson, R. V., Bernier, J. L., Houssin, R. & Land, E. J. (1996). One-electron oxidation of ergothioneine and analogues investigated by pulse radiolysis: redox reaction involving ergothioneine and vitamin C. *Biochem J* 315 (Pt 2), 625-629.

- Ausubel, F.M., Brent, R., Kingston, R.E., Moore, D.D., Seidman, J.G., Smith, J.A., & Struhl, K. (1989) *Current Protocols in Molecular Biology*. Green Publishing- Wiley Interscience. New York.
- Bagyan, I., Casillas-Martinez, L. & Setlow, P. (1998). The katX gene, which codes for the catalase in spores of *Bacillus subtilis*, is a forespore-specific gene controlled by sigmaF, and KatX is essential for hydrogen peroxide resistance of the germinating spore. *J Bacteriol* 180, 2057-2062.
- Ballou, D., Palmer, G. & Massey, V. (1969). Direct demonstration of superoxide anion production during the oxidation of reduced flavin and of its catalytic decomposition by erythrocyte cytochrome c. *Biochem Biophys Res Commun* 36, 898-904.
- Barynin, V. V., Whittaker, M. M., Antonyuk, S. V., Lamzin, V. S., Harrison, P. M., Artymiuk, P. J. & Whittaker, J. W. (2001). Crystal structure of manganese catalase from *Lactobacillus plantarum*. *Structure (Camb)* 9, 725-38.
- Becker, G., Klauck, E. & Hengge-Aronis, R. (2000). The response regulator RssB, a recognition factor for sigmaS proteolysis in *Escherichia coli*, can act like an anti-sigmaS factor. *Mol Microbiol* 35, 657-666.
- Bendich, A. (1996). Antioxidant vitamins and human immune responses. *Vitam Horm* 52, 35-62.
- Berthet, S., Nykyri, L. M., Bravo, J., Mate, M. J., Berthet-Colominas, C., Alzari, P. M., Koller, F. & Fita, I. (1997). Crystallization and preliminary structural analysis of catalase A from *Saccharomyces cerevisiae*. *Protein Sci* 6, 481-483.
- Beyer, R. E. (1990). The participation of coenzyme Q in free radical production and antioxidation. *Free Radic Biol Med* 8, 545-565.
- Bishai, W. R., Smith, H. O. & Barcak, G. J. (1994). A peroxide/ascorbate-inducible catalase from *Haemophilus influenzae* is homologous to the *Escherichia coli* katE gene product. *J Bacteriol* 176, 2914-2921.
- Bordes, P., Conter, A., Morales, V., Bouvier, J., Kolb, A. & Gutierrez, C. (2003). DNA supercoiling contributes to disconnect sigmaS accumulation from sigmaS-dependent transcription in *Escherichia coli*. *Mol Microbiol* 48, 561-571.
- Bravo, J., Mate, M. J., Schneider, T., Switala, J., Wilson, K., Loewen, P. C. & Fita, I. (1999). Structure of catalase HPII from *Escherichia coli* at 1.9 Å resolution. *Proteins* 34, 155-166.
- Bravo, J., Verdaguer, N., Tormo, J., Betzel, C., Switala, J., Loewen, P. C. & Fita, I. (1995). Crystal structure of catalase HPII from *Escherichia coli*. *Structure* 3, 491-502.

- Britton, G.** (1995). Structure and properties of carotenoids in relation to function. *Faseb J* 9, 1551-1558.
- Bsat, N., Herbig, A., Casillas-Martinez, L., Setlow, P. & Helmann, J. D.** (1998). *Bacillus subtilis* contains multiple Fur homologues: identification of the iron uptake (Fur) and peroxide regulon (PerR) repressors. *Mol Microbiol* 29, 189-198.
- Bult, C. J., White, O., Olsen, G. J., Zhou, L., Fleischmann, R. D., Sutton, G. G., Blake, J. A., FitzGerald, L. M., Clayton, R. A., Gocayne, J. D., Kerlavage, A. R., Dougherty, B. A., Tomb, J. F., Adams, M. D., Reich, C. I., Overbeek, R., Kirkness, E. F., Weinstock, K. G., Merrick, J. M., Glodek, A., Scott, J. L., Geoghagen, N. S. & Venter, J. C.** (1996). Complete genome sequence of the methanogenic archaeon, *Methanococcus jannaschii*. *Science* 273, 1058-1073.
- Bunkelmann, J. R. & Trelease, R. N.** (1996). Ascorbate peroxidase. A prominent membrane protein in oilseed glyoxysomes. *Plant Physiol* 110, 589-598.
- Burton, G. W. & Ingold, K. U.** (1981) Autoxidation of biological molecules. 1. The antioxidant activity of vitamin E and related chain-breaking phenolic antioxidants in vitro. *Journal of the American Chemical Society* 103, 6472-6477.
- Calcutt, M. J., Becker-Hapak, M., Gaut, M., Hoerter, J. & Eisenstark, A.** (1998). The rpoS gene of *Erwinia carotovora*: gene organization and functional expression in *E. coli*. *FEMS Microbiol Lett* 159, 275-281.
- Carmel-Harel, O. & Storz, G.** (2000). Roles of the glutathione- and thioredoxin-dependent reduction systems in the *Escherichia coli* and *Saccharomyces cerevisiae* responses to oxidative stress. *Annu Rev Microbiol* 54, 439-461.
- Carpena, X., Guarne, A., Ferrer, J. C., Alzari, P. M., Fita, I. & Loewen, P. C.** (2002). Crystallization and preliminary X-ray analysis of the hydroperoxidase I C-terminal domain from *Escherichia coli*. *Acta Crystallogr D Biol Crystallogr* 58, 853-855.
- Carpena, X., Loprasert, S., Mongkolsuk, S., Switala, J., Loewen, P. C. & Fita, I.** (2003). Catalase-peroxidase KatG of *Burkholderia pseudomallei* at 1.7 Å resolution. *J Mol Biol* 327, 475-489.
- Carpena, X., Perez, R., Ochoa, W. F., Verdaguer, N., Klotz, M. G., Switala, J., Melik-Adamyanyan, W., Fita, I. & Loewen, P. C.** (2001). Crystallization and preliminary X-ray analysis of clade I catalases from *Pseudomonas syringae* and *Listeria seeligeri*. *Acta Crystallogr D Biol Crystallogr* 57, 1184-1186.
- Carpena, X., Soriano, M., Klotz, M. G., Duckworth, H. W., Donald, L. J., Melik-Adamyanyan, W., Fita, I. & Loewen, P. C.** (2003). Structure of the Clade 1 catalase, CatF of *Pseudomonas syringae*, at 1.8 Å resolution. *Proteins* 50, 423-436.

- Carpena, X., Switala, J., Loprasert, S., Mongkolsuk, S., Fita, I. & Loewen, P. C.** (2002). Crystallization and preliminary X-ray analysis of the catalase-peroxidase KatG from *Burkholderia pseudomallei*. *Acta Crystallogr D Biol Crystallogr* 58, 2184-2186.
- Chaudiere, J. & Ferrari-Iliou, R.** (1999). Intracellular antioxidants: from chemical to biochemical mechanisms. *Food Chem Toxicol* 37, 949-962.
- Cho, Y. H., Lee, E. J. & Roe, J. H.** (2000). A developmentally regulated catalase required for proper differentiation and osmoprotection of *Streptomyces coelicolor*. *Mol Microbiol* 35, 150-160.
- Choi, H., Kim, S., Mukhopadhyay, P., Cho, S., Woo, J., Storz, G. & Ryu, S.** (2001). Structural basis of the redox switch in the OxyR transcription factor. *Cell* 105, 103-113.
- Christman, M. F., Morgan, R. W., Jacobson, F. S. & Ames, B. N.** (1985). Positive control of a regulon for defenses against oxidative stress and some heat-shock proteins in *Salmonella typhimurium*. *Cell* 41, 753-762.
- Chung, C. T., Niemela, S. L. & Miller, R. H.** (1989). One-step preparation of competent *Escherichia coli*: transformation and storage of bacterial cells in the same solution. *Proc Natl Acad Sci U S A* 86, 2172-2175.
- Chiu, J. T., Loewen, P. C., Switala, J., Gennis, R. B. & Timkovich, R.** (1989). Proposed structure for the prosthetic group of the catalase HPII from *Escherichia coli* J. *Am. Chem. Soc.* 111, 7046-7050
- Claiborne, A., Malinowski, D. P. & Fridovich, I.** (1979). Purification and characterization of hydroperoxidase II of *Escherichia coli* B. *J Biol Chem* 254, 11664-11668.
- Clare, D. A., Duong, M. N., Darr, D., Archibald, F. & Fridovich, I.** (1984). Effects of molecular oxygen on detection of superoxide radical with nitroblue tetrazolium and on activity stains for catalase. *Anal Biochem* 140, 532-537.
- Clark, P. & Walsh, R. J.** (1960). Haem synthesis in vitro. Studies with mammalian and avian erythrocytes. *Aust J Exp Biol Med Sci* 38, 135-145.
- Cohen, A., Mizanin, J. & Schwartz, E.** (1985). Treatment of iron overload in Cooley's anemia. *Ann N Y Acad Sci* 445, 274-281.
- Davis, B. J.** (1964). Disc Electrophoresis. II. Method and Application to Human Serum Proteins. *Ann N Y Acad Sci* 121, 404-427.
- Donald, L. J., Krokhin, O. V., Duckworth, H. W., Wiseman, B., Deemagarn, T., Singh, R., Switala, J., Carpena, X., Fita, I. & Loewen, P. C.** (2003). Characterization

of the catalase-peroxidase KatG from *Burkholderia pseudomallei* by mass spectrometry. *J Biol Chem* 278, 35687-35692.

Ellman, G. L. (1959). Tissue sulfhydryl groups. *Arch Biochem Biophys* 82, 70-77.

Engelmann, S., Lindner, C. & Hecker, M. (1995). Cloning, nucleotide sequence, and regulation of katE encoding a sigma B-dependent catalase in *Bacillus subtilis*. *J Bacteriol* 177, 5598-5605.

Escolar, L., Perez-Martin, J. & de Lorenzo, V. (1999). Opening the iron box: transcriptional metalloregulation by the Fur protein. *J Bacteriol* 181, 6223-9.

Faguy, D. M. & Doolittle, W. F. (2000). Horizontal transfer of catalase-peroxidase genes between archaea and pathogenic bacteria. *Trends Genet* 16, 196-197.

Fang, F. C., DeGroot, M. A., Foster, J. W., Baumler, A. J., Ochsner, U., Testerman, T., Bearson, S., Giard, J. C., Xu, Y., Campbell, G. & Laessig, T. (1999). Virulent *Salmonella typhimurium* has two periplasmic Cu, Zn-superoxide dismutases. *Proc Natl Acad Sci U S A* 96, 7502-7507.

Fang, F. C., Libby, S. J., Buchmeier, N. A., Loewen, P. C., Switala, J., Harwood, J. & Guiney, D. G. (1992). The alternative sigma factor katF (rpoS) regulates *Salmonella* virulence. *Proc Natl Acad Sci U S A* 89, 11978-11982.

Farr, S. B. & Kogoma, T. (1991). Oxidative stress responses in *Escherichia coli* and *Salmonella typhimurium*. *Microbiol Rev* 55, 561-585.

Fita, I. & Rossmann, M. G. (1985). The active center of catalase. *J Mol Biol* 185, 21-37.

Fita, I. & Rossmann, M. G. (1985). The NADPH binding site on beef liver catalase. *Proc Natl Acad Sci U S A* 82, 1604-1608.

Fondren, L. M., Sloan, G. L., LeBlanc, P. A. & Heath, H. E. (1994). Plasmid-encoded catalase of *Staphylococcus simulans* biovar staphylolyticus. *FEMS Microbiol Lett* 117, 231-235.

Fridovich, I. (1978). The biology of oxygen radicals. *Science* 201, 875-880.

Fridovich, I. (1995). Superoxide radical and superoxide dismutases. *Annu Rev Biochem* 64, 97-112.

Fuangthong, M. & Helmann, J. D. (2003). Recognition of DNA by Three Ferric Uptake Regulator (Fur) Homologs in *Bacillus subtilis*. *J Bacteriol* 185, 6348-6357.

- Fuangthong, M., Herbig, A. F., Bsat, N. & Helmann, J. D.** (2002). Regulation of the *Bacillus subtilis* fur and perR genes by PerR: not all members of the PerR regulon are peroxide inducible. *J Bacteriol* 184, 3276-3286.
- Flohe L., Gunzler W. A. and Schock H. H.** (1973) Glutathione peroxidase: a selenoenzyme. *FEBS Letters* 32, 132-134.
- Flohe L.** (1989) The selenoprotein glutathione peroxidase. In *Glutathione: Chemical, Biochemical and Medical Aspects, Part A*, ed. D. Dolphin, O. Avramovic and R. Poulson, pp. 643-31. John Wiley & Sons.
- Gaballa, A. & Helmann, J. D.** (1998). Identification of a zinc-specific metalloregulatory protein, Zur, controlling zinc transport operons in *Bacillus subtilis*. *J Bacteriol* 180, 5815-5821.
- Gaballa, A., Wang, T., Ye, R. W. & Helmann, J. D.** (2002). Functional analysis of the *Bacillus subtilis* Zur regulon. *J Bacteriol* 184, 6508-6514.
- Gerard-Monnier, D. & Chaudiere, J.** (1996). [Metabolism and antioxidant function of glutathione]. *Pathol Biol (Paris)* 44, 77-85.
- Gilbert, D. L.** (2000). Fifty years of radical ideas. *Ann N Y Acad Sci* 899, 1-14.
- Gonzalez-Flecha, B. & Demple, B.** (1997). Transcriptional regulation of the *Escherichia coli* oxyR gene as a function of cell growth. *J Bacteriol* 179, 6181-6186.
- Gouet, P., Jouve, H. M. & Dideberg, O.** (1995). Crystal structure of *Proteus mirabilis* PR catalase with and without bound NADPH. *J Mol Biol* 249, 933-954.
- Grant, C. M.** (2001). Role of the glutathione/glutaredoxin and thioredoxin systems in yeast growth and response to stress conditions. *Mol Microbiol* 39, 533-541.
- Haber, F. & Weiss, J.** (1934) The catalytic decomposition of hydrogen peroxide by iron salts. *Proc. Roy. Soc. Lond. Ser A.* 147, 332-336.
- Hagensee, M. E. & Moses, R. E.** (1989). Multiple pathways for repair of hydrogen peroxide-induced DNA damage in *Escherichia coli*. *J Bacteriol* 171, 991-995.
- Hahn, J. S., Oh, S. Y., Chater, K. F., Cho, Y. H. & Roe, J. H.** (2000). H₂O₂-sensitive fur-like repressor CatR regulating the major catalase gene in *Streptomyces coelicolor*. *J Biol Chem* 275, 38254-38260.
- Hahn, J. S., Oh, S. Y. & Roe, J. H.** (2000). Regulation of the furA and catC operon, encoding a ferric uptake regulator homologue and catalase-peroxidase, respectively, in *Streptomyces coelicolor* A3(2). *J Bacteriol* 182, 3767-3774.

- Halliwell, B. (1999). Antioxidant defence mechanisms: from the beginning to the end (of the beginning). *Free Radic Res* 31, 261-272.
- Halliwell, B. & Chirico, S. (1993). Lipid peroxidation: its mechanism, measurement, and significance. *Am J Clin Nutr* 57, 715S-724S.
- Hartman, P. E. (1990). Ergothioneine as antioxidant. *Methods Enzymol* 186, 310-318.
- Hassett, D. J., Sokol, P. A., Howell, M. L., Ma, J. F., Schweizer, H. T., Ochsner, U. & Vasil, M. L. (1996). Ferric uptake regulator (Fur) mutants of *Pseudomonas aeruginosa* demonstrate defective siderophore-mediated iron uptake, altered aerobic growth, and decreased superoxide dismutase and catalase activities. *J Bacteriol* 178, 3996-4003.
- Hedrick, J. L. & Smith, A. J. (1968). Size and charge isomer separation and estimation of molecular weights of proteins by disc gel electrophoresis. *Arch Biochem Biophys* 126, 155-164.
- Helmann, J. D., Wu, M. F., Gaballa, A., Kobel, P. A., Morshedi, M. M., Fawcett, P. & Paddon, C. (2003). The global transcriptional response of *Bacillus subtilis* to peroxide stress is coordinated by three transcription factors. *J Bacteriol* 185, 243-253.
- Hengge-Aronis, R. (2002). Stationary phase gene regulation: what makes an *Escherichia coli* promoter sigmaS-selective? *Curr Opin Microbiol* 5, 591-595.
- Herbig, A. F. & Helmann, J. D. (2001). Roles of metal ions and hydrogen peroxide in modulating the interaction of the *Bacillus subtilis* PerR peroxide regulon repressor with operator DNA. *Mol Microbiol* 41, 849-859.
- Herouart, D., Sigaud, S., Moreau, S., Frendo, P., Touati, D. & Puppo, A. (1996). Cloning and characterization of the katA gene of *Rhizobium meliloti* encoding a hydrogen peroxide-inducible catalase. *J Bacteriol* 178, 6802-6809.
- Hicks, D. B. (1995). Purification of three catalase isozymes from facultatively alkaliphilic *Bacillus firmus* OF4. *Biochim Biophys Acta* 1229, 347-355.
- Hillar, A. & Nicholls, P. (1992). A mechanism for NADPH inhibition of catalase compound II formation. *FEBS Lett* 314, 179-182.
- Hillar, A., Nicholls, P., Switala, J. & Loewen, P. C. (1994). NADPH binding and control of catalase compound II formation: comparison of bovine, yeast, and *Escherichia coli* enzymes. *Biochem J* 300 (Pt 2), 531-539.
- Hillar, A., Peters, B., Pauls, R., Loboda, A., Zhang, H., Mauk, A. G. & Loewen, P. C. (2000). Modulation of the activities of catalase-peroxidase HPI of *Escherichia coli* by site-directed mutagenesis. *Biochemistry* 39, 5868-5875.

- Horsburgh, M. J., Ingham, E. & Foster, S. J. (2001). In *Staphylococcus aureus*, fur is an interactive regulator with PerR, contributes to virulence, and Is necessary for oxidative stress resistance through positive regulation of catalase and iron homeostasis. *J Bacteriol* 183, 468-475.
- Horsburgh, M. J., Wharton, S. J., Karavolos, M. & Foster, S. J. (2002). Manganese: elemental defence for a life with oxygen. *Trends Microbiol* 10, 496-501.
- Huckerby, T. N., Sanderson, P. N. & Nieduszynski, I. A. (1985). N.m.r. studies of the disulphated disaccharide obtained by degradation of bovine lung heparin with nitrous acid. *Carbohydr Res* 138, 199-206.
- Imlay, K. R. & Imlay, J. A. (1996). Cloning and analysis of sodC, encoding the copper-zinc superoxide dismutase of *Escherichia coli*. *J Bacteriol* 178, 2564-2571.
- Jakopitsch, C., Auer, M., Ivancich, A., Ruker, F., Furtmuller, P. G. & Obinger, C. (2003). Total conversion of bifunctional catalase-peroxidase (KatG) to monofunctional peroxidase by exchange of a conserved distal side tyrosine. *J Biol Chem* 278, 20185-20191.
- Jenney, F. E., Jr., Verhagen, M. F., Cui, X. & Adams, M. W. (1999). Anaerobic microbes: oxygen detoxification without superoxide dismutase. *Science* 286, 306-309.
- Jung, G., Breitmaier, E. & Voelter, W. (1972). [Dissociation equilibrium of glutathione. A Fourier transform-¹³C-NMR spectroscopic study of pH-dependence and of charge densities]. *Eur J Biochem* 24, 438-445.
- Jung, I. L. & Kim, I. G. (2003). Transcription of *ahpC*, *katG*, and *katE* genes in *Escherichia coli* is regulated by polyamines: polyamine-deficient mutant sensitive to H₂O₂-induced oxidative damage. *Biochem Biophys Res Commun* 301, 915-922.
- Kagan, V. E., Serbinova, E. A., Stoyanovsky, D. A., Khwaja, S. & Packer, L. (1994). Assay of ubiquinones and ubiquinol as antioxidants. *Methods Enzymol* 234, 343-354.
- Kalko, S. G., Gelpi, J. L., Fita, I. & Orozco, M. (2001). Theoretical study of the mechanisms of substrate recognition by catalase. *J Am Chem Soc* 123, 9665-72.
- Kao, S. M. & Hassan, H. M. (1985). Biochemical characterization of a paraquat-tolerant mutant of *Escherichia coli*. *J Biol Chem* 260, 10478-10481.
- Katsuwon, J. & Anderson, A. J. (1989) Response of plant-colonizing pseudomonads to hydrogen peroxide. *Appl Environ Microbiol* 55: 986-989.
- Kawarabayasi, Y., Sawada, M., Horikawa, H., Haikawa, Y., Hino, Y., Yamamoto, S., Sekine, M., Baba, S., Kosugi, H., Hosoyama, A., Nagai, Y., Sakai, M., Ogura, K., Otsuka, R., Nakazawa, H., Takamiya, M., Ohfuku, Y., Funahashi, T., Tanaka, T.,

- Kudoh, Y., Yamazaki, J., Kushida, N., Oguchi, A., Aoki, K. & Kikuchi, H.** (1998). Complete sequence and gene organization of the genome of a hyper-thermophilic archaeobacterium, *Pyrococcus horikoshii* OT3. *DNA Res* 5, 55-76.
- Kawasaki, L. & Aguirre, J.** (2001). Multiple catalase genes are differentially regulated in *Aspergillus nidulans*. *J Bacteriol* 183, 1434-1440.
- Kawasaki, L., Wysong, D., Diamond, R. & Aguirre, J.** (1997). Two divergent catalase genes are differentially regulated during *Aspergillus nidulans* development and oxidative stress. *J Bacteriol* 179, 3284-3292.
- Khosla, C. & Bailey, J. E.** (1989). Evidence for partial export of *Vitreoscilla* hemoglobin into the periplasmic space in *Escherichia coli*. Implications for protein function. *J Mol Biol* 210, 79-89.
- Kim, J. A. & Mayfield, J.** (2000). Identification of *Brucella abortus* OxyR and its role in control of catalase expression. *J Bacteriol* 182, 5631-5633.
- Kim, S. O., Merchant, K., Nudelman, R., Beyer, W. F., Jr., Keng, T., DeAngelo, J., Hausladen, A. & Stamler, J. S.** (2002). OxyR: a molecular code for redox-related signaling. *Cell* 109, 383-396.
- Kirkman, H. N. & Gaetani, G. F.** (1984). Catalase: a tetrameric enzyme with four tightly bound molecules of NADPH. *Proc Natl Acad Sci U S A* 81, 4343-4347.
- Kirkman, H. N., Rolfo, M., Ferraris, A. M. & Gaetani, G. F.** (1999). Mechanisms of protection of catalase by NADPH. Kinetics and stoichiometry. *J Biol Chem* 274, 13908-13914.
- Klenk, H. P., Clayton, R. A., Tomb, J. F., White, O., Nelson, K. E., Ketchum, K. A., Dodson, R. J., Gwinn, M., Hickey, E. K., Peterson, J. D., Richardson, D. L., Kerlavage, A. R., Graham, D. E., Kyrpides, N. C., Fleischmann, R. D., Quackenbush, J., Lee, N. H., Sutton, G. G., Gill, S., Kirkness, E. F., Dougherty, B. A., McKenney, K., Adams, M. D., Loftus, B., Venter, J. C. & et al.** (1997). The complete genome sequence of the hyperthermophilic, sulphate-reducing archaeon *Archaeoglobus fulgidus*. *Nature* 390, 364-370.
- Klotz, M. G. & Hutcheson, S. W.** (1992). Multiple periplasmic catalases in phytopathogenic strains of *Pseudomonas syringae*. *Appl Environ Microbiol* 58, 2468-2473.
- Klotz, M. G., Klassen, G. R. & Loewen, P. C.** (1997). Phylogenetic relationships among prokaryotic and eukaryotic catalases. *Mol Biol Evol* 14, 951-958.

- Klotz, M. G. & Loewen, P. C.** (2003). The molecular evolution of catalatic hydroperoxidases: evidence for multiple lateral transfer of genes between prokaryota and from bacteria into eukaryota. *Mol Biol Evol* 20, 1098-1012.
- Kono, Y. & Fridovich, I.** (1983). Isolation and characterization of the pseudocatalase of *Lactobacillus plantarum*. *J Biol Chem* 258, 6015-6019.
- Krinsky, N. I., Sladdin, D. G., Levine, P. H., Taub, I. A. & Simic, M. G.** (1981). Modification of platelet function by radical species produced during irradiation of oxygenated water. *Thromb Haemost* 45, 116-120.
- Kunkel, T. A., Roberts, J. D. & Zakour, R. A.** (1987). Rapid and efficient site-specific mutagenesis without phenotypic selection. *Methods Enzymol* 154, 367-382.
- Layne, E.** (1957) Spectrophotometric and turbidimetric methods for measuring proteins, *Methods Enzymol.* 3, 447-454.
- Lee B. J., Park S. I., Park J. M., Chittum H. S. & Hatfield D. L.** (1996) Molecular biology of selenium and its role in human health. *Molecular Cells* 6, 509-520.
- Loew, O.** (1900) U.S. Dept of Agri. Repts. 65,5.
- Loewen, P. C. & Switala, J.** (1986). Purification and characterization of catalase HPII from *Escherichia coli* K12. *Biochem Cell Biol* 64, 638-646.
- Loewen, P. C., Switala, J. & Triggs-Raine, B. L.** (1985). Catalases HPI and HPII in *Escherichia coli* are induced independently. *Arch Biochem Biophys* 243, 144-149.
- Loewen, P. C., Switala, J., von Ossowski, I., Hillar, A., Christie, A., Tattrie, B. & Nicholls, P.** (1993). Catalase HPII of *Escherichia coli* catalyzes the conversion of protoheme to cis-heme d. *Biochemistry* 32, 10159-10164.
- Loewen, P. C., Triggs, B. L., George, C. S. & Hrabarchuk, B. E.** (1985). Genetic mapping of katG, a locus that affects synthesis of the bifunctional catalase-peroxidase hydroperoxidase I in *Escherichia coli*. *J Bacteriol* 162, 661-667.
- Ma, J. F., Ochsner, U. A., Klotz, M. G., Nanayakkara, V. K., Howell, M. L., Johnson, Z., Posey, J. E., Vasil, M. L., Monaco, J. J. & Hassett, D. J.** (1999). Bacterioferritin A modulates catalase A (KatA) activity and resistance to hydrogen peroxide in *Pseudomonas aeruginosa*. *J Bacteriol* 181, 3730-3742.
- Maeda, Y., Trautwein, A., Gonser, U., Yoshida, K., Kikuchi-Torii, K., Homma, T. & Ogura, Y.** (1973). Mossbauer effect in bacterial catalase. *Biochim Biophys Acta* 303, 230-236.

- Mate, M. J., Sevinc, M. S., Hu, B., Bujons, J., Bravo, J., Switala, J., Ens, W., Loewen, P. C. & Fita, I.** (1999). Mutants that alter the covalent structure of catalase hydroperoxidase II from *Escherichia coli*. *J Biol Chem* 274, 27717-27725.
- Mate, M. J., Zamocky, M., Nykyri, L. M., Herzog, C., Alzari, P. M., Betzel, C., Koller, F. & Fita, I.** (1999). Structure of catalase-A from *Saccharomyces cerevisiae*. *J Mol Biol* 286, 135-149.
- Mathews M. C., Summers C. B. & Felton G. W.** (1997) Ascorbate peroxidase: A novel antioxidant enzyme in insects. *Archives of Insect Biochemistry and Physiology* 34, 57-68.
- McCord, J. M. & Day, E. D., Jr.** (1978). Superoxide-dependent production of hydroxyl radical catalyzed by iron-EDTA complex. *FEBS Lett* 86, 139-142.
- McCord, J. M. & Fridovich, I.** (1969). The utility of superoxide dismutase in studying free radical reactions. I. Radicals generated by the interaction of sulfite, dimethyl sulfoxide, and oxygen. *J Biol Chem* 244, 6056-6063.
- Mead, D. A., Skorupa, E. S. & Kemper, B.** (1985). Single stranded DNA SP6 promoter plasmids for engineering mutant RNAs and proteins: synthesis of a 'stretched' preproparathyroid hormone. *Nucleic Acids Res* 13, 1103-1118.
- Meister, A.** (1988). On the discovery of glutathione. *Trends Biochem Sci* 13, 185-188.
- Melik-Adamyany, W., Bravo, J., Carpena, X., Switala, J., Mate, M. J., Fita, I. & Loewen, P. C.** (2001). Substrate flow in catalases deduced from the crystal structures of active site variants of HPII from *Escherichia coli*. *Proteins* 44, 270-281.
- Misra, H. P. & Fridovich, I.** (1971). The generation of superoxide radical during the autoxidation of ferredoxins. *J Biol Chem* 246, 6886-6890.
- Misra, H. P. & Fridovich, I.** (1972). The univalent reduction of oxygen by reduced flavins and quinones. *J Biol Chem* 247, 188-192.
- Mongkolsuk, S. & Helmann, J. D.** (2002). Regulation of inducible peroxide stress responses. *Mol Microbiol* 45, 9-15.
- Mongkolsuk, S., Loprasert, S., Vattanaviboon, P., Chanvanichayachai, C., Chamnongpol, S. & Supsamran, N.** (1996). Heterologous growth phase- and temperature-dependent expression and H₂O₂ toxicity protection of a superoxide-inducible monofunctional catalase gene from *Xanthomonas oryzae* pv. *oryzae*. *J Bacteriol* 178, 3578-3584.

- Mulvey, M. R., Sorby, P. A., Triggs-Raine, B. L. & Loewen, P. C. (1988). Cloning and physical characterization of katE and katF required for catalase HPII expression in *Escherichia coli*. *Gene* 73, 337-345.
- Murshudov, G. N., Grebenko, A. I., Barynin, V., Dauter, Z., Wilson, K. S., Vainshtein, B. K., Melik-Adamyanyan, W., Bravo, J., Ferran, J. M., Ferrer, J. C., Switala, J., Loewen, P. C. & Fita, I. (1996). Structure of the heme d of *Penicillium vitale* and *Escherichia coli* catalases. *J Biol Chem* 271, 8863-8868.
- Murshudov, G. N., Melik-Adamyanyan, W. R., Grebenko, A. I., Barynin, V. V., Vagin, A. A., Vainshtein, B. K., Dauter, Z. & Wilson, K. S. (1992). Three-dimensional structure of catalase from *Micrococcus lysodeikticus* at 1.5 Å resolution. *FEBS Lett* 312, 127-131.
- Murthy, M. R., Reid, T. J., 3rd, Sicignano, A., Tanaka, N. & Rossmann, M. G. (1981). Structure of beef liver catalase. *J Mol Biol* 152, 465-499.
- Nakjarung, K., Mongkolsuk, S. & Vattanaviboon, P. (2003). The oxyR from *Agrobacterium tumefaciens*: evaluation of its role in the regulation of catalase and peroxide responses. *Biochem Biophys Res Commun* 304, 41-47.
- Naqui, A., Chance, B. & Cadenas, E. (1986). Reactive oxygen intermediates in biochemistry. *Annu Rev Biochem* 55, 137-166.
- Navarro, R. E. & Aguirre, J. (1998). Posttranscriptional control mediates cell type-specific localization of catalase A during *Aspergillus nidulans* development. *J Bacteriol* 180, 5733-5738.
- Nelson, K. E., Clayton, R. A., Gill, S. R., Gwinn, M. L., Dodson, R. J., Haft, D. H., Hickey, E. K., Peterson, J. D., Nelson, W. C., Ketchum, K. A., McDonald, L., Utterback, T. R., Malek, J. A., Linher, K. D., Garrett, M. M., Stewart, A. M., Cotton, M. D., Pratt, M. S., Phillips, C. A., Richardson, D., Heidelberg, J., Sutton, G. G., Fleischmann, R. D., Eisen, J. A., Fraser, C. M. & et al. (1999). Evidence for lateral gene transfer between Archaea and bacteria from genome sequence of *Thermotoga maritima*. *Nature* 399, 323-329.
- Nicholls, P., Fita, I., & Loewen, P. C. (2001) Enzymology and structure of catalases, *Adv. Inorg. Chem.* 51, 51-106.
- Ochsner, U. A., Vasil, M. L., Alsabbagh, E., Parvatiyar, K. & Hassett, D. J. (2000). Role of the *Pseudomonas aeruginosa* oxyR-recG operon in oxidative stress defense and DNA repair: OxyR-dependent regulation of katB-ankB, ahpB, and ahpC-ahpF. *J Bacteriol* 182, 4533-4544.

- Odenbreit, S., Wieland, B. & Haas, R. (1996). Cloning and genetic characterization of *Helicobacter pylori* catalase and construction of a catalase-deficient mutant strain. *J Bacteriol* 178, 6960-6967.
- Ogura, Y. (1955) Catalase activity at high concentration of hydrogen peroxide. *Archives of Biochemistry and Biophysics* 57, 288-300.
- Ohwada, T., Shirakawa, Y., Kusumoto, M., Masuda, H. & Sato, T. (1999). Susceptibility to hydrogen peroxide and catalase activity of root nodule bacteria. *Biosci Biotechnol Biochem* 63, 457-462.
- Olson, L. P. & Bruice, T. C. (1995). Electron tunneling and ab initio calculations related to the one-electron oxidation of NAD(P)H bound to catalase. *Biochemistry* 34, 7335-7347.
- Oxvig, C., Thomsen, A. R., Overgaard, M. T., Sorensen, E. S., Hojrup, P., Bjerrum, M. J., Gleich, G. J. & Sottrup-Jensen, L. (1999). Biochemical evidence for heme linkage through esters with Asp-93 and Glu-241 in human eosinophil peroxidase. The ester with Asp-93 is only partially formed in vivo. *J Biol Chem* 274, 16953-16958.
- Palozza, P. & Krinsky, N. I. (1992). Antioxidant effects of carotenoids in vivo and in vitro: an overview. *Methods Enzymol* 213, 403-420.
- Peraza, L. & Hansberg, W. (2002). *Neurospora crassa* catalases, singlet oxygen and cell differentiation. *Biol Chem* 383, 569-575.
- Prinz, W. A., Aslund, F., Holmgren, A. & Beckwith, J. (1997). The role of the thioredoxin and glutaredoxin pathways in reducing protein disulfide bonds in the *Escherichia coli* cytoplasm. *J Biol Chem* 272, 15661-15667.
- Putnam, C. D., Arvai, A. S., Bourne, Y. & Tainer, J. A. (2000). Active and inhibited human catalase structures: ligand and NADPH binding and catalytic mechanism. *J Mol Biol* 296, 295-309.
- Pym, A. S., Domenech, P., Honore, N., Song, J., Deretic, V. & Cole, S. T. (2001). Regulation of catalase-peroxidase (KatG) expression, isoniazid sensitivity and virulence by furA of *Mycobacterium tuberculosis*. *Mol Microbiol* 40, 879-889.
- Regelsberger, G., Jakopitsch, C., Furtmuller, P. G., Rueker, F., Switala, J., Loewen, P. C. & Obinger, C. (2001). The role of distal tryptophan in the bifunctional activity of catalase-peroxidases. *Biochem Soc Trans* 29, 99-105.
- Regelsberger, G., Jakopitsch, C., Ruker, F., Krois, D., Peschek, G. A. & Obinger, C. (2000). Effect of distal cavity mutations on the formation of compound I in catalase-peroxidases. *J Biol Chem* 275, 22854-22861.

- Rice-Evans, C. A., Sampson, J., Bramley, P. M. & Holloway, D. E. (1997). Why do we expect carotenoids to be antioxidants in vivo? *Free Radic Res* 26, 381-398.
- Richter, H. E. & Loewen, P. C. (1981). Induction of catalase in *Escherichia coli* by ascorbic acid involves hydrogen peroxide. *Biochem Biophys Res Commun* 100, 1039-1046.
- Robbe-Saule, V., Coynault, C., Ibanez-Ruiz, M., Hermant, D. & Norel, F. (2001). Identification of a non-haem catalase in *Salmonella* and its regulation by RpoS (σ S). *Mol Microbiol* 39, 1533-1545.
- Rocha, E. R., Owens, G., Jr. & Smith, C. J. (2000). The redox-sensitive transcriptional activator OxyR regulates the peroxide response regulon in the obligate anaerobe *Bacteroides fragilis*. *J Bacteriol* 182, 5059-5069.
- Rorth, M. & Jensen, P. K. (1967). Determination of catalase activity by means of the Clark oxygen electrode. *Biochim Biophys Acta* 139, 171-173.
- Rossi, F., Della Bianca, V. & de Togni, P. (1985). Mechanisms and functions of the oxygen radicals producing respiration of phagocytes. *Comp Immunol Microbiol Infect Dis* 8, 187-204.
- Rougee, M., Bensasson, R. V., Land, E. J. & Pariente, R. (1988). Deactivation of singlet molecular oxygen by thiols and related compounds, possible protectors against skin photosensitivity. *Photochem Photobiol* 47, 485-489.
- Sanger, F., Nicklen, S. & Coulson, A. R. (1977). DNA sequencing with chain-terminating inhibitors. *Proc Natl Acad Sci U S A* 74, 5463-5467.
- Sambrook, J., Fritsch, E.F., & Maniatis, T. (1989) *Molecular cloning: A Laboratory Manual*, Cold Spring Harbor Laboratory, New York.
- Saraste, M. & Castresana, J. (1994). Cytochrome oxidase evolved by tinkering with denitrification enzymes. *FEBS Lett* 341, 1-4.
- Scherer, M., Wei, H., Liese, R. & Fischer, R. (2002). *Aspergillus nidulans* catalase-peroxidase gene (*cpeA*) is transcriptionally induced during sexual development through the transcription factor StuA. *Eukaryot Cell* 1, 725-735.
- Schumb, W. C., Satterfield, C. N., & Wentworth, R. L. (1955) *Hydrogen Peroxide*. *American Chemical Society Monograph Series*. No 128. Reinhold, New York, NY
- Seaver, L. C. & Imlay, J. A. (2001). Hydrogen peroxide fluxes and compartmentalization inside growing *Escherichia coli*. *J Bacteriol* 183, 7182-7189.

- Sevinc, M. S., Mate, M. J., Switala, J., Fita, I. & Loewen, P. C. (1999). Role of the lateral channel in catalase HP_{II} of *Escherichia coli*. *Protein Sci* 8, 490-498.
- Sevinc, M. S., Switala, J., Bravo, J., Fita, I. & Loewen, P. C. (1998). Truncation and heme pocket mutations reduce production of functional catalase HP_{II} in *Escherichia coli*. *Protein Eng* 11, 549-555.
- Sevinc, M. S., Ens, W., & Loewen, P. C. (1995) The cysteines of catalase HP_{II} of *Escherichia coli*, including Cys438 which is blocked, do not have a catalytic role. *Eur J Biochem.* 230:127-132.
- Sigaud, S., Becquet, V., Frendo, P., Puppo, A. & Herouart, D. (1999). Differential regulation of two divergent *Sinorhizobium meliloti* genes for HP_{II}-like catalases during free-living growth and protective role of both catalases during symbiosis. *J Bacteriol* 181, 2634-2639.
- Smirnoff, N. & Pallanca, J. E. (1996). Ascorbate metabolism in relation to oxidative stress. *Biochem Soc Trans* 24, 472-478.
- Sohal, R. S. (2002). Oxidative stress hypothesis of aging. *Free Radic Biol Med* 33, 573-574.
- Spolaore, B., Bermejo, R., Zambonin, M., & Fontana A. (2001) Protein interactions leading to conformational changes monitored by limited proteolysis: apo form and fragments of horse cytochrome c. *Biochemistry.* 40, 9460-9468.
- Stadtman, T. C. (1991). Biosynthesis and function of selenocysteine-containing enzymes. *J Biol Chem* 266, 16257-16260.
- Steinman, H. M. (1982). Copper-zinc superoxide dismutase from *Caulobacter crescentus* CB15. A novel bacteriocuprein form of the enzyme. *J Biol Chem* 257, 10283-10293.
- Storz, G. & Imlay, J. A. (1999). Oxidative stress. *Curr Opin Microbiol* 2, 188-194.
- Storz, G. & Tartaglia, L. A. (1992). OxyR: a regulator of antioxidant genes. *J Nutr* 122, 627-630.
- Sundquist, A. R., Briviba, K. & Sies, H. (1994). Singlet oxygen quenching by carotenoids. *Methods Enzymol* 234, 384-388.
- Switala, J. & Loewen, P. C. (2002). Diversity of properties among catalases. *Arch Biochem Biophys* 401, 145-154.
- Switala, J., O'Neil, J. O. & Loewen, P. C. (1999). Catalase HP_{II} from *Escherichia coli* exhibits enhanced resistance to denaturation. *Biochemistry* 38, 3895-3901.

- Takeda, A., Miyahara, T., Hachimori, A. & Samejima, T. (1980). The interactions of thiol compounds with porcine erythrocyte catalase. *J Biochem (Tokyo)* 87, 429-439.
- Tkachenko, A., Nesterova, L. & Pshenichnov, M. (2001). The role of the natural polyamine putrescine in defense against oxidative stress in *Escherichia coli*. *Arch Microbiol* 176, 155-157.
- Triggs-Raine, B. L., Doble, B. W., Mulvey, M. R., Sorby, P. A. & Loewen, P. C. (1988). Nucleotide sequence of katG, encoding catalase HPI of *Escherichia coli*. *J Bacteriol* 170, 4415-4419.
- Tseng, H. J., McEwan, A. G., Apicella, M. A. & Jennings, M. P. (2003). OxyR acts as a repressor of catalase expression in *Neisseria gonorrhoeae*. *Infect Immun* 71, 550-556.
- Tsuchiya, M., Kagan, V. E., Freisleben, H. J., Manabe, M. & Packer, L. (1994). Antioxidant activity of alpha-tocopherol, beta-carotene, and ubiquinol in membranes: cis-parinaric acid-incorporated liposomes. *Methods Enzymol* 234, 371-383.
- Ueda, M., Kinoshita, H., Maeda, S. I., Zou, W. & Tanaka, A. (2003). Structure-function study of the amino-terminal stretch of the catalase subunit molecule in oligomerization, heme binding, and activity expression. *Appl Microbiol Biotechnol* 61, 488-494.
- Uden, G., Becker, S., Bongaerts, J., Holighaus, G., Schirawski, J. & Six, S. (1995). O₂-sensing and O₂-dependent gene regulation in facultatively anaerobic bacteria. *Arch Microbiol* 164, 81-90.
- Ursini, F., Maiorino, M., Brigelius-Flohe, R., Aumann, K. D., Roveri, A., Schomburg, D. & Flohe, L. (1995). Diversity of glutathione peroxidases. *Methods Enzymol* 252, 38-53.
- Vainshtein, B. K., Melik-Adamyan, W. R., Barynin, V. V., Vagin, A. A. & Grebenko, A. I. (1981). Three-dimensional structure of the enzyme catalase. *Nature* 293, 411-412.
- Vainshtein, B. K., Melik-Adamyan, W. R., Barynin, V. V., Vagin, A. A., Grebenko, A. I., Borisov, V. V., Bartels, K. S., Fita, I. & Rossmann, M. G. (1986). Three-dimensional structure of catalase from *Penicillium vitale* at 2.0 Å resolution. *J Mol Biol* 188, 49-61.
- Vargas Mdel, C., Encarnacion, S., Davalos, A., Reyes-Perez, A., Mora, Y., Garcia-de los Santos, A., Brom, S. & Mora, J. (2003). Only one catalase, katG, is detectable in *Rhizobium etli*, and is encoded along with the regulator OxyR on a plasmid replicon. *Microbiology* 149, 1165-1176.

- Vattanaviboon, P. & Mongkolsuk, S.** (2000). Expression analysis and characterization of the mutant of a growth-phase- and starvation-regulated monofunctional catalase gene from *Xanthomonas campestris* pv. phaseoli. *Gene* 241, 259-265.
- Vieira, J. & Messing, J.** (1987). Production of single-stranded plasmid DNA. *Methods Enzymol* 153, 3-11.
- Visick, K. L. & Ruby, E. G.** (1998). The periplasmic, group III catalase of *Vibrio fischeri* is required for normal symbiotic competence and is induced both by oxidative stress and by approach to stationary phase. *J Bacteriol* 180, 2087-2092.
- Von Ossowski, I., Hausner, G. & Loewen, P. C.** (1993). Molecular evolutionary analysis based on the amino acid sequence of catalase. *J Mol Evol* 37, 71-76.
- Von Ossowski, I., Mulvey, M. R., Leco, P. A., Borys, A. & Loewen, P. C.** (1991). Nucleotide sequence of *Escherichia coli* katE, which encodes catalase HPII. *J Bacteriol* 173, 514-520.
- Wada, K., Tada, T., Nakamura, Y., Kinoshita, T., Tamoi, M., Shigeoka, S. & Nishimura, K.** (2002). Crystallization and preliminary X-ray diffraction studies of catalase-peroxidase from *Synechococcus* PCC 7942. *Acta Crystallogr D Biol Crystallogr* 58, 157-159.
- Wang, P. & Schellhorn, H. E.** (1995). Induction of resistance to hydrogen peroxide and radiation in *Deinococcus radiodurans*. *Can J Microbiol* 41, 170-176.
- Wardell, J. L.** (1974) Preparation of thiols, in *The Chemistry of the thiol group*. (Patio, S., ed) pp 164-258, John Wiley and Sons, London
- Weber, K., Pringle, J.R., & Osborn, M.** (1972) Measurement of molecular weights by electrophoresis on SDS-acrylamide gels. *Methods Enzymol.* 26: 3-27.
- Welinder, K. G.** (1991). Bacterial catalase-peroxidases are gene duplicated members of the plant peroxidase superfamily. *Biochim Biophys Acta* 1080, 215-220.
- Wittenberg, J. B. & Wittenberg, B. A.** (1990). Mechanisms of cytoplasmic hemoglobin and myoglobin function. *Annu Rev Biophys Biophys Chem* 19, 217-241.
- Witteveen, F. B., van de Vondervoort, P. J., van den Broeck, H. C., van Engelenburg, A. C., de Graaff, L. H., Hillebrand, M. H., Schaap, P. J. & Visser, J.** (1993). Induction of glucose oxidase, catalase, and lactonase in *Aspergillus niger*. *Curr Genet* 24, 408-416.
- Wood, P. M.** (1988). The potential diagram for oxygen at pH7. *Biochem.J* 253, 287-289.

- Yamada, Y., Fujiwara, T., Sato, T., Igarashi, N. & Tanaka, N.** (2002). The 2.0 Å crystal structure of catalase-peroxidase from *Haloarcula marismortui*. *Nat Struct Biol* 9, 691-695.
- Yamada, Y., Saijo, S., Sato, T., Igarashi, N., Usui, H., Fujiwara, T. & Tanaka, N.** (2001). Crystallization and preliminary X-ray analysis of catalase-peroxidase from the halophilic archaeon *Haloarcula marismortui*. *Acta Crystallogr D Biol Crystallogr* 57, 1157-1158.
- Yanisch-Perron, C., Vieira, J. & Messing, J.** (1985). Improved M13 phage cloning vectors and host strains: nucleotide sequences of the M13mp18 and pUC19 vectors. *Gene* 33, 103-119.
- Yonei, S., Yokota, R. & Sato, Y.** (1987). The distinct role of catalase and DNA repair systems in protection against hydrogen peroxide in *Escherichia coli*. *Biochem Biophys Res Commun* 143, 638-644.
- Zahrt, T. C., Song, J., Siple, J. & Deretic, V.** (2001). Mycobacterial FurA is a negative regulator of catalase-peroxidase gene katG. *Mol Microbiol* 39, 1174-1185.
- Zamocky, M., Herzog, C., Nykyri, L. M. & Koller, F.** (1995). Site-directed mutagenesis of the lower parts of the major substrate channel of yeast catalase A leads to highly increased peroxidatic activity. *FEBS Lett* 367, 241-245.
- Zhang, Y., Heym, B., Allen, B., Young, D. & Cole, S.** (1992). The catalase-peroxidase gene and isoniazid resistance of *Mycobacterium tuberculosis*. *Nature* 358, 591-593.
- Zheng, M., Wang, X., Templeton, L. J., Smulski, D. R., LaRossa, R. A. & Storz G.** (2001) DNA microarray-mediated transcriptional profiling of the *Escherichia coli* response to hydrogen peroxide. *J Bacteriol* 183, 4562-4570.
- Zhou, Y., Gottesman, S., Hoskins, J. R., Maurizi, M. R. & Wickner, S.** (2001). The RssB response regulator directly targets sigma(S) for degradation by ClpXP. *Genes Dev* 15, 627-637.
- Zou, P., Borovok, I., Ortiz de Orue Lucana, D., Muller, D. & Schrempf, H.** (1999). The mycelium-associated *Streptomyces reticuli* catalase-peroxidase, its gene and regulation by FurS. *Microbiology* 145, 549-559.